University of Tennessee Health Science Center
UTHSC Digital Commons

Theses and Dissertations (ETD) College of Graduate Health Sciences

12-2023

Understanding the Host Cellular Response to Astrovirus Infection

Theresa Mary Taggart Bub
University of Tennessee Health Science Center

Follow this and additional works at: https://dc.uthsc.edu/dissertations

 Part of the Medicine and Health Sciences Commons

Recommended Citation

Bub, Theresa Mary Taggart (0000-0002-7330-9872), "Understanding the Host Cellular Response to Astrovirus Infection" (2023). *Theses and Dissertations (ETD).* Paper 657. http://dx.doi.org/10.21007/etd.cghs.2023.0641.

This Dissertation is brought to you for free and open access by the College of Graduate Health Sciences at UTHSC Digital Commons. It has been accepted for inclusion in Theses and Dissertations (ETD) by an authorized administrator of UTHSC Digital Commons. For more information, please contact jwelch30@uthsc.edu.

Understanding the Host Cellular Response to Astrovirus Infection

Abstract

Astrovirus is a non-enveloped positive-sense single-stranded RNA virus that infects the small intestine and causes gastrointestinal disease in most hosts. However, in immunocompromised patients, astrovirus can infect the brain, causing encephalitis and death. Here, we characterize astrovirus induction of replication organelles and dysregulation of cellular processes. It is known that autophagy can play a key role in the viral lifecycle, from entry to egress, and can be either pro-virus or pro-host depending on the virus. RNA viruses often exploit autophagy machinery to create double membrane vesicles (DMVs) as sites of replication and to protect viral RNAs from detection by innate immune sensors. In these studies, we provide the first evidence that astrovirus exploits some, but not all autophagy machinery to assist in viral replication at DMVs. Astrovirus replication and DMV formation relies upon induction of PI3KC3 machinery, but not LC3 conjugation machinery. Astrovirus also disrupts lysosomal enzyme expression. These are the first studies describing astrovirus replication mechanism, and we have shown that the machinery involved may span species infected with astrovirus. We have also shown that astrovirus DMV formation likely originates from the endoplasmic reticulum (ER) and may affect ER stress pathways involved in normal cellular function. These results relate DMV formation to autophagosome biogenesis and suggest that ER stress could play a role in DMV biogenesis. Finally, we have shown that astrovirus replication results in cell cycle arrest during G1 phase of the cell cycle. This is beneficial to the viral life cycle, because G1 phase may provide an environment of growth for the replicating virus. In all, our studies have significantly grown the understanding of astrovirus replication mechanism and disruption of host cellular machinery. This has resulted in relating astrovirus to other positive strand RNA viruses and potentially finding common therapeutics for these viral infections.

Document Type

Dissertation

Degree Name

Doctor of Philosophy (PhD)

Program

Biomedical Sciences

Research Advisor

Stacey Schultz-Cherry, PhD

Keywords

Astrovirus;Autophagy;Cell Cycle;Endoplasmic Reticulum;Infectious Disease;Viral Replication

Subject Categories

Medicine and Health Sciences

This dissertation is available at UTHSC Digital Commons: https://dc.uthsc.edu/dissertations/657

UNIVERSITY OF TENNESSEE HEALTH SCIENCE CENTER

DOCTORAL DISSERTATION

Understanding the Host Cellular Response to Astrovirus Infection

---

Author:
Theresa Mary Taggart Bub

Advisor:
Stacey Schultz-Cherry, Ph.D.

A Dissertation Presented for The Graduate Studies Council of
The University of Tennessee Health Science Center
in Partial Fulfillment of Requirements for the Doctor of Philosophy degree from
The University of Tennessee

in

Biomedical Sciences: Microbiology, Immunology, and Biochemistry
College of Graduate Health Sciences

October 2023

Appendix A © 2023 by American Society for Microbiology.
All other material © 2023 by Theresa Mary Taggart Bub.
All rights reserved.

Modified with permission
Masters/Doctoral Thesis LaTeX Template
Version 2.5 (8/27/2017)
http://www.LaTeXTemplates.com
Creative Commons License CC BY-NC-SA 3.0

This work is dedicated to my grandmother, Mary Lou Curro, PhD in educational psychology. You had four children, raised them, and then pursued your education. When I didn't understand what educational psychology was as a little girl, you told me it was "the study of helping people to reach their best potential." I wish you were here to see this. Thank you for inspiring me to reach a potential I didn't know I had.

Acknowledgements

I would like to thank my mentor, Dr. Stacey Schultz-Cherry. Taking on a graduate student is a huge responsibility. Taking on a graduate student who has switched labs comes with its own unique challenges. From day one in the lab, Stacey treated me with respect and believed in my ideas. She encouraged me to rediscover my confidence as a scientist and be excited about my work. Being in her lab allowed me opportunities to travel, meet incredible scientists around the world, and truly enjoy the scientific process.

I would also like to thank Dr. Mondira Kundu and her entire lab for teaching me everything I know about autophagy. That knowledge set the stage for all I have accomplished in the Schultz-Cherry lab. A special thank you to Amber, who was an incredible mentor and supportive friend throughout my graduate school career.

My committee members, Dr. Jason Rosch, Dr. Elaine Tuomanen, Dr. Mike Whitt, and Dr. Joanne Murphy-Ullrich, were instrumental in my success as a graduate student. This committee was excited about my ideas, encouraged me to pursue the project I was passionate about, and helped me to believe in my abilities to meet my goals and work hard throughout my years in the Schultz-Cherry lab. The St. Jude Infectious Disease department as a whole was incredibly supportive of my project and so much fun to work with.

A very special thank you to the St. Jude Core Facilities, including the electron microscopy core, the confocal microscopy core, and the Hartwell Center. I need to specifically thank George Campbell, who taught me how to use each confocal microscope I needed, but also went above and beyond to give me insights and advice on my project. Nathan Kurtz is responsible for each beautiful electron microscopy image in my thesis. He is an excellent researcher and was just as excited as I was about this work.

Thank you to UTHSC for giving me an incredible education in biomedical sciences, even in the midst of a global pandemic. I have such positive memories of our courses, including Dr. Nelson's evolutionary biochemistry lectures, Dr. Cox's paper discussions, and Dr. Fitzpatrick's journal clubs. Dr. Fitzpatrick, thank you for facilitating my track switch into Microbiology, Immunology, and Biochemistry as soon as I discovered my passion for it. Dr. Cox, thank you for the laughs and the constructive criticism that I believe truly shaped me into a critical thinker. Dr. Nelson, thank you for warmly inviting your students over for Darwin parties and Cinco de Mayo celebrations.

To the Schultz-Cherry lab, you have made my experience in graduate school so enjoyable. Thank you to Pam, who quickly became my lab mom and continues to encourage me even after moving away. Thank you to Ginna, Bridgett, Victoria, and Pam B for being excellent mentors and teaching me what I needed to know to be a successful scientist in this lab. Thank you to Shaoyuan for all the laughs, Teams calls, and every single cell RNA sequencing analysis. Thank you to Lauren L for being potentially the most thoughtful, fun, and helpful coworker I have ever had and for being such a great friend over these years.

My favorite surprise of graduate school was the lifelong friendships I made along the way. Ana, you are a huge role model for me in science and in life. You remind me to keep working hard but also take care of myself and others. Maria, my defense buddy, you are the best listener and audience for all of the jokes I make. If I don't laugh at my own jokes, I know you will. Traveling to Glasgow and London with both of you was the highlight of graduate school for me.

McKenna, Madison, and Taylor, my "grad school girls," I remember the minute I met each of you. You have not ceased to inspire me since that day. I know we have said this a million times, but it is unbelievable that we were lucky enough to find each other, become friends, and witness each other's lives over these years. I cannot wait to see what each of you do in life as scientists and as the unique people you are. I'll be cheering you on and screaming Taylor Swift songs with you for as long as you'll let me. Long live the walls we crashed through, how the kingdom lights shined just for me and you.

To my Mullins family, I don't have sufficient words to describe what you have done for Andrew and I over these years in Memphis. From Harriet's warm welcome to parties at the Williams and Lyons households to every minute I've gotten to laugh and sing with your kiddos, I will cherish each memory for the rest of my life. You have become my home away from home.

To my family- both the family I married into and the family I have always known, thank you. You have made each break from school full of love and reminded me of who I am throughout this journey. Mom, thank you for being my original "Woman in Science" inspiration. Dad, thank you for every time I needed to cry or laugh. You are the most encouraging and light-filled person I've ever known. Mom and Dad, your insistence on making me do my homework as soon as I got home and your ability to make me think taking 10 books home from the library wasn't enough is what got me here today. Sarah, you are a huge role model to me, and I'm blessed to call you my sister. Mike, you're the best older brother I could've asked for. Thanks for reminding me I can do difficult things. Katie, my twin sister and my inspiration in life, thank you for everything you are to me. My cheerleader, my phone call at the end of the day, my best friend. I could never have done this without you. Tonight I'm gonna dance for all that we've been through. But I don't wanna dance if I'm not dancing with you.

Finally, thank you to my husband, Andrew - the best thing that's ever been mine. Since the day I met you, I have wanted to be a better person. To dream bigger, work harder, be kinder, and show more love to everyone I know. That is because you demonstrate these things to me every day. You didn't hesitate when I asked you to move across the country so I could follow my dreams. You made me dinner, hyped me up through marathon training, and cheered me on in the lowest moments and in the best moments. I love you so much. Hopefully this is the last time you'll have to ask me, "Do you believe in yourself yet?" I do, because of you. I can't wait to see what this life with you looks like next.

Preface

The body Chapters of this dissertation are organized in a way that introduces readers to astrovirus and the host cellular response to viral infection through literature review, followed by research aims and hypotheses. The research and methods utilized are presented, followed by analysis and discussion of our findings. The concluding chapter discusses the research and its impact on the field, as well as future directions and significance of this work.

For readers to have immediate access to the full presentation of our previously published research study, the article is presented in **Appendix A**. This mode of presentation allows for **Chapter 3**, which uses it as its basis, to focus more narrowly on a summary and discussion of the article in Appendix A, and to show specifically how it relates to the dissertation's larger goals and objectives. References in the chapters to relevant sections, tables, or figures in **Appendix A** look like the following example. A chapter callout to **Figure A.1** refers to Figure 1 in **Appendix A**. The blue highlight links back to the appendix figure.

NOTE ON PDF NAVIGATION: Document navigation is greatly facilitated by using Adobe Acrobat "Previous view" and "Next view" functions. For "Previous view," use quick keys Alt/Ctrl+Left Arrow on PC or Command+Left Arrow on Mac. For "Next view," use Alt/Ctrl+Right Arrow on PC or Command+Right Arrow on Mac. Using these quick keys in tandem allows the reader to toggle between document locations. Since every scroll represents a new view; depending on how much scrolling is done for a specific view destination, more than one press of the back or forward arrows may be needed. For additional navigational tips, click View at the top of the PDF, then Page Navigation. These Adobe Acrobat functions are not functional for other PDF readers or for PDFs opened in web browsers.

Abstract

Theresa Mary Taggart Bub

Understanding the Host Cellular Response to Astrovirus Infection

Astrovirus is a non-enveloped positive-sense single-stranded RNA virus that infects the small intestine and causes gastrointestinal disease in most hosts. However, in immunocompromised patients, astrovirus can infect the brain, causing encephalitis and death. Here, we characterize astrovirus induction of replication organelles and dysregulation of cellular processes.

It is known that autophagy can play a key role in the viral lifecycle, from entry to egress, and can be either pro-virus or pro-host depending on the virus. RNA viruses often exploit autophagy machinery to create double membrane vesicles (DMVs) as sites of replication and to protect viral RNAs from detection by innate immune sensors.

In these studies, we provide the first evidence that astrovirus exploits some, but not all autophagy machinery to assist in viral replication at DMVs. Astrovirus replication and DMV formation relies upon induction of phosphatidylinositol 3-kinase (PI3KC3) machinery, but not LC3 conjugation machinery. Astrovirus also disrupts lysosomal enzyme expression. These are the first studies describing astrovirus replication mechanism, and we have shown that the machinery involved may span species infected with astrovirus.

We have also shown that astrovirus DMV formation likely originates from the endoplasmic reticulum (ER) and may affect ER stress pathways involved in normal cellular function. These results relate DMV formation to autophagosome biogenesis and suggest that ER stress could play a role in DMV biogenesis.

Finally, we have shown that astrovirus replication results in cell cycle arrest during Gap 1 (G1) phase of the cell cycle. This is beneficial to the viral life cycle, because G1 phase may provide an environment of growth for the replicating virus.

In all, our studies have significantly grown the understanding of astrovirus replication mechanism and disruption of host cellular machinery. This has resulted in relating astrovirus to other positive strand RNA viruses and potentially finding common therapeutics for these viral infections.

Contents

List of Figures

List of Abbreviations

+ssRNA	Positive Sense Single Stranded RNA
AAstV	Avastrovirus
AMBRA1	Activating Molecule in Beclin 1-Regulated Autophagy
AMPK	Adenosine Monophosphate-Activated Protein Kinase
AstV	Astrovirus
AstV-ND	Astrovirus Neurological Disease
ATF6	Activating Transcription Factor 6
ATG	Autophagy Protein
ATP	Adenosine Triphosphate
BDV	Bovine Diarrhea Virus
BHK	Baby Hamster Kidney Cells
BiP	ER Chapterone Immunoglobulin Heavy-Chain Binding Protein
BoAstV	Bovine Astrovirus
C1q	Complement Component 1q
Caco-2	Cancer coli (colon cancer) cells
CDK	Cyclin-Dependent Kinase
CHIKV	Chikungunya Virus
CHOP	C/EBP Homologous Protein
CIRV	Carnation Italian Ringspot Virus
CNS	Central Nervous System
CP	Coat Protein
CSF	Cerebrospinal Fluid
CTSB	Cathepsin B
CTSD	Cathepsin D
CVB3	Coxsackievirus B3
DENV	Dengue Virus
DMV	Double Membrane Vesicle
DNA	Deoxyribonucleic Acid
dsRNA	Double Stranded RNA
EBNA1	EBV Nuclear Antigen 1
EBV	Epstein-Barr Virus
eIF2α	Eukaryotic Translation Initiation Factor 2A
ELISA	Enzyme Linked Immunosorbent Assay
EM	Electron Microscopy

EMT	Epithelial to Mesenchymal Transition
ER	Endoplasmic Reticulum
ERGIC	ER-Golgi Intermediate Compartment
ERK1/2	Extracellular Signal-Regulated Protein Kinase 1 and 2
ERSE	ER Stress-Response Elements
FcRn	Neonatal Fc Receptor
FFU	Focus-Forming Unit
FFZE	Free-Flow Zonal Electrophoresis
FIP200	PTK/FAK Family-Interacting Protein of 200kDa
FMDV	Foot and Mouth Disease Virus
G1	Gap 1
G2	Gap 2
GI	Gastrointestinal
GPCR	G-Protein-Coupled Receptor
gRNA	Genomic RNA
HAstV	Human Astrovirus
HCMV	Human Cytomegalovirus
HCV	Hepatitis C Virus
HIE	Human Intestinal Enteroids
HIV-1	Human Immunodeficiency Virus Type 1
HK2	Hexokinase 2
HMO	Human-Mink-Ovine
HPIV3	Human Parainfluenza Virus 3
HPV1	Human Papillomavirus
HSV	Herpes Simplex Virus
HTC	Human Colorectal Carcinoma Epithelial Cells
IAV	Influenza A Virus
IBD	Inflammatory Bowel Disease
IBV	Infectious Bronchitis Virus
IDO1	Indoleamine 2,3-Dioxygenase 1
IFN	Interferon
IFNaR	Interferon-α/β Receptor
IRE1	Inositol-Requiring Enzyme 1
ISG	Interferon-Stimulated Gene
IVIG	Intravenous Immunoglobulin
JEV	Japanese Encephalitis Virus
KSHV	Kaposi's Sarcoma-Associated Herpesvirus
LAMP1	Lysosomal Associated Membrane Protein 1
LC3	Microtubule-Associated Protein Light Chain 3
M	Mitosis
Mab PL-2	HAstV-2-Neutralizing Monoclonal Antibody PL-2
MAstV	Mamastrovirus

MBL	Mannose-Binding Lectin
MFI	Mean Fluorescence Intensity
MLB	Melbourne Astrovirus
mNGS	Metagenomic Next Generation Sequencing
MOI	Multiplicity Of Infection
mTOR	Mammalian Target of Rapamycin
MuAstV	Murine Astrovirus
Na/K-ATPase	Sodium/Potassium Adenosine Triphosphatase
NGS	Normal Goat Serum
NPF	Nucleation Promoting Factor
nsp	Non-structural Protein
ORF	Open Reading Frame
OvAstV	Ovine Astrovirus
p53	Tumor Protein 53
p62	Sequestosome-1
PAMP	Pathogen-Associated Molecular Pattern
PARKIN	Phosphatase and Tensin Homologue-Induced Kinase 1
PBS	Phosphate Buffered Saline
PE	Phosphatidylethanolamine
PERK	PKR-like Endoplasmid Reticulum Kinase
PFA	Paraformaldehyde
PI3K	Phosphoinositide 3-Kinase
PI3KC1	PI3K Complex 1
PI3KC2	PI3K Complex 2
PI3KC3	Phosphatidylinositol 3-Kinase, or PtdIns3K Complex 3
PI3P	Phosphatidylinositol 3-Phosphate
PI4K	Phosphatidylinositol 4 Kinase
PI4KIIIβ	Phosphatidylinositol 4-Phosphate β
PI4P	Phosphatidylinositol 4-Phosphate
PIK-III	PI3KC3-specific Inhibitor
PINK1	PTEN-Induced Kinase 1
PKR	Protein Kinase R
PPM1D	Protein Phosphatase Magnesium-Dependent 1 Delta
pRb	Phosphorylated Rb Protein
PRR	Pattern Recognition Receptor
PtdIns3K	Phosphatidylinositol 3-Kinase
PtdIns3P	Phosphatidylinositol 3-Phosphate
PV	Poliovirus
PVDF	Polyvinylidene Fluoride
Rab	Ras-Associated Binding Protein
Rb1	Retinoblastoma Protein 1
RdRp	RNA-dependent RNA Polymerase

RIPA	Radioimmunoprecipitation Assay
RIPK3	Receptor-Interacting Protein Kinase 3
RNA	Ribonucleic Acid
RO	Replication Organelle
RSS	Runting-Stunting Syndrome
RSV	Respiratory Syncytial Virus
RT-PCR	Reverse Transcription Polymerase Chain Reaction
S	Synthesis
SARS-CoV-2	Severe Acute Respiratory Syndrome Coronavirus 2
scRNA-seq	Single Cell RNA Sequencing
sgRNA	Subgenomic RNA
siRNA	Small Interfering RNA
SJCRH	St. Jude Children's Research Hospital
SNARE	SNAP Receptor
Spike-2-CDC-Spain	HAstV-2-Spain Capsid Spike Domain
Spike-2-Oxford	HAstV-2-Oxford Capsid Spike Domain
SQSTM1	Sequestosome-1
ssRNA	Single Stranded RNA
STAT1	Signal Transducer and Activator of Transcription 1
SV	Sindbis Virus
TAstV	Turkey Astrovirus
TBSV	Tomato Bushy Stunt Virus
TGF-β	Transforming Growth Factor β
TGN38	Trans-Golgi Network Protein 38
TRIM31	Tripartite Motif Containing 31
ULK1	Unc51-Like Autophagy Activating Kinase 1
UPR	Unfolded Protein Response
UTHSC	University of Tennessee Health Science Center
UTR	Untranslated Region
UVRAG	UV Radiation Resistance-Associated Gene Protein
VA	Virginia Astrovirus
VP90	Viral Protein of 90 kDa
VPg	Viral Genome-Linked Protein
VPS34	Phosphatidylinositol 3-Kinase
VSV	Vesicular Stomatitis Virus
WHAMM	WASP Homolog Associated with Actin, Golgi Membranes, and Microtubules
WIPI	WD-Repeat Protein Interacting with Phosphoinositides
WT	Wildtype
XBP1	X-box-Binding Protein 1
XP	Viroporin

Yuc8	Another name for HAstV-8

Chapter 1

Astrovirus

Astroviridae is an understudied family of positive sense, single stranded RNA (ssRNA) viruses first discovered in 1975. These non-enveloped viruses infect a wide range of mammals, including humans. In humans, astrovirus (AstV) infection causes gastrointestinal (GI) illness and can lead to stomach pain, nausea, diarrhea, and other symptoms. Infection with astrovirus typically results in short-lasting and mild symptoms. However, a new attention has been brought to astrovirus infection as it can enter the brain through an unknown mechanism. This typically occurs in at-risk populations such as the immunocompromised and has been associated in clinical studies with encephalitis and death. Although astrovirus is becoming more commonly recognized as a potential cause of serious disease, it remains critically under researched. This chapter reviews the known information of astrovirus classification, structure, replication cycle, and host response to infection, as well as epidemiology and current treatment and prevention options.

1.1 Classification

The family Astroviridae has similarities to other families of positive sense ssRNA viruses such as Picornaviridae and Caliciviridae (Donato and Vijaykrishna, 2017; Guix, Bosch, and Pintó, 2013; Moser and Schultz-Cherry, 2008a). It was not until 1993 that Astroviridae was reclassified as its own family due to the differences in some elements of the genome from other families of viruses (Monroe et al., 1993). For instance, astroviruses do not express a helicase, have different capsid proteins, and have subgenomic RNA (sgRNA) (Cortez, V. A. Meliopoulos, et al., 2017; Donato and Vijaykrishna, 2017; Guix, Bosch, and Pintó, 2013; Moser and Schultz-Cherry, 2008a). Generally, both deoxyribonucleic acid (DNA) and ribonucleic acid (RNA) viruses encode their own helicases in order to aid in the genome replication process, making the lack of a helicase-encoding region in the astrovirus genome unique.

There are two genera within the astrovirus family, Mamastrovirus (MAstVs) and Avastrovirus (AAstVs) for mammalian and avian species respectively (Donato and Vijaykrishna, 2017; Guix, Bosch, and Pintó, 2013; Moser and Schultz-Cherry, 2008a). Within the genus of MAstVs at least 30 species are known to be infected, including humans, cats, mice,

cattle, sheep, pigs, mink, camels, and sea lions. Within the AAstV genus at least 14 species are infected, including chickens, pigeons, ducks, and turkeys (Cortez, V. A. Meliopoulos, et al., 2017) (**Figure** 1.1).

Human Astrovirus Classification Human astroviruses (HAstVs) can be split into three separate clades. The first clade includes HAstV-1-8, where HAstV-1 is the most prevalent detected serotype. After detection of these viruses, additional clades were discovered in Melbourne (MLBs) and Virginia (VAs), which relate more closely to other mammalian clades than they do to the HAstV clade. The VA clade is also known as HMO, or Human-Mink-Ovine for its close relationship to mink and ovine clades. Although astroviruses have been historically classified based on species infected, it is now clear with sequencing that some astrovirus strains are closely related regardless of species infected. Among these human strains, HAstV-1 is most prevalent worldwide (Donato and Vijaykrishna, 2017; Guix, Bosch, and Pintó, 2013; Moser and Schultz-Cherry, 2008a). However, with recent studies utilizing reverse transcription polymerase chain reaction (RT-PCR) methodology which can detect VA and MLB strains, increased prevalence of these HAstVs has been recorded. In multiple studies, MLB1 has now been recorded at an equal to or higher prevalence than HAstV-1 (Khamrin et al., 2016; Niendorf et al., 2022; Okitsu et al., 2023).

1.2 Astrovirus Genome

The astrovirus genome is relatively small, measuring between 6.2 and 7.7 kilobase (kb) (Cortez, V. A. Meliopoulos, et al., 2017). With three open reading frames (ORFs), ORF1 encodes a viral protease, a viral genome-linked protein (VPg), and an RNA-dependent RNA polymerase (RdRp); alternative ORFx encodes a viroporin (XP), and ORF2 encodes a viral capsid. There is no 5′ cap. Instead, the genome begins with a 5′ untranslated region (UTR), followed by ORF1 (Cortez, V. A. Meliopoulos, et al., 2017; Donato and Vijaykrishna, 2017; Guix, Bosch, and Pintó, 2013; Monroe et al., 1993; Moser and Schultz-Cherry, 2008a). Translation of the RdRp depends on a ribosomal frameshifting mechanism. There have been five nonstructural proteins (nsps) characterized thus far, but others and their functions have not yet been described. Within ORF2, the genome includes an alternative frame ORFX, encoding XP, followed by capsid, a 3′ UTR, and a 3′ poly(A) tail. ORF2 is also preceded by a subgenomic RNA (sgRNA) promoter which may be longer than previously described (Lulla and Firth, 2020) (**Figure** 1.2).

1.3 Astrovirus Structure

The gene for astrovirus capsid encodes a 90 kDa protein termed VP90 (Geigenmüller et al., 2002; Méndez, Aguirre-Crespo, et al., 2007). This precursor is cleaved to VP70 within the host cell, and upon exit from the cell is further cleaved by extracellular proteases. The capsid is composed of 180 VP70 subunits (Del Rocío Banos-Lara and Méndez, 2010; Méndez, Fernández-Luna, et al., 2002; Méndez, Salas-Ocampo, and Arias, 2004). Mature virions

Figure 1.1: Astrovirus Phylogenetic Tree. Phylogenetic tree generated using neighbor-joining analysis in MEGA11 based on astrovirus capsid protein sequences.

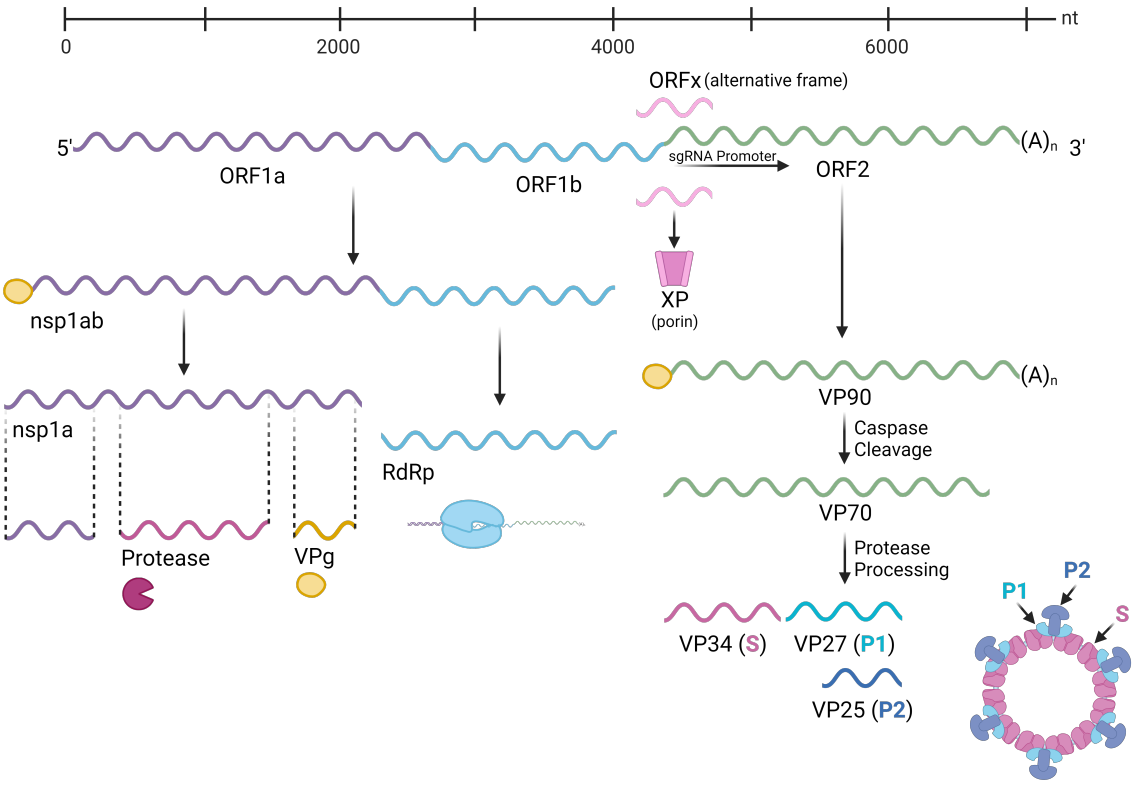

Figure 1.2: Astrovirus Genome. Representation of astrovirus genome organization. The genome consists of three open reading frames (ORFs). ORF1 encodes the astrovirus protease, viral genome-linked protein (VPg), and RNA-dependent RNA polymerase (RdRp). ORF2 encodes the capsid protein, consisting of precursor VP90, which is subsequently cleaved to VP70, then VP34, VP27, and VP25. An alternative frame encodes the viral porin (XP).

must be cleaved from VP70 to VP34, VP27, and VP25 in order to facilitate further infection of cells. Without this cleavage step, the virion is not infectious. It should be noted that this is not the case for the VA-1 strain of astrovirus, which does not require trypsin activation for replication in cell culture. VP34, VP27, and VP25 are the inner core and spike domains of the capsid (Méndez, Fernández-Luna, et al., 2002). Once fully cleaved, the astrovirus virion appears star-shaped, with T=3 icosahedral symmetry. The virion is about 43 nm wide (Arias and DuBois, 2017).

Viroporin ORFX is unique to human astroviruses and some mammalian astrovirus genomes. It encodes XP, a viroporin. Generally, viroporins form hydrophilic pores that modulate calcium signaling and membrane permeability, as well as aid in formation and release of virions. While the function of the XP viroporin is not yet known, knocking out ORFX attenuates the virus. The replication defect associated with XP knockout is related to later stages of infection, and the authors suggest an association of XP with plasma and trans Golgi membranes. Further, ORFX mutants pseudo-revert, restoring ORFX function with passaging, suggesting that ORFX is necessary to the viral life cycle in these specific hosts (Lulla and Firth, 2020). The XP protein is most likely important for viral assembly, and it is possible that it resembles other viroporins necessary for passage of viral RNA through replication organelle (RO) membranes. The question stands as to why all strains of astrovirus would not contain ORFX. In astrovirus strains without a predicted ORFX, the authors show a predicted ORFY potentially encoding another viroporin, the function of which could be similar to ORFX but evolved independently from ORFX in other strains. It is possible that for these strains of astrovirus, there is a different viral assembly mechanism that does not require the same XP.

1.4 Viral Life Cycle

1.4.1 Viral entry

While a receptor for astrovirus has yet to be identified, one study suggests a role for the neonatal Fc Receptor (FcRn) in viral entry (Haga et al., 2022). In vivo, host tryptophan catabolizing enzyme indoleamine 2,3-dioxygenase 1 (IDO1) is necessary for epithelial cell maturation and permissivity to astrovirus infection. Murine astrovirus (MuAstV) infection is also limited to cell types in the small intestine, where mucus-secreting goblet cells are most susceptible to infection. Knowing this may help to narrow in on cellular entry factors for MuAstV infection that are unique to mucus-secreting, IDO1-expressing goblet cells (Cortez, Livingston, et al., 2023).

Only certain in vitro cell types are susceptible to astrovirus infection, of which Caco-2 cells are the gold standard for propagation of the virus. Caco-2 cells are immortalized human colorectal adenocarcinoma cells, which can be differentiated to recapitulate an intestinal epithelial cell layer. Interestingly, while all classic serotypes (HAstV-1-8) can infect and replicate in Caco-2 cells in vitro, only HAstV-2 can infect baby hamster kidney

(BHK) cells, and only HAstV-1 can infect human colorectal carcinoma epithelial (HTC) cells in vitro. This suggests that while these classic serotypes are similar to one another, they may require unique cellular entry factors (Brinker, Blacklow, and Herrmann, 2000). It is likely that astroviruses require numerous cellular attachment factors based on observed differences between human serotypes. One such potential entry factor is extracellular signal-regulated protein kinase 1/2 (ERK1/2). The ERK1/2 cellular signaling pathway is necessary to human astrovirus replication, and ERK becomes activated early in infection (Moser and Schultz-Cherry, 2008b). Similarly, human immunodeficiency virus type 1 (HIV-1) requires ERK for cellular entry (Liu et al., 2002).

It is hypothesized that the virus enters the host cell via clathrin-mediated pathways, as clathrin inhibitors can block HAstV-8 replication, although this has not been tested for other serotypes (Méndez, Muñoz-Yañez, et al., 2014). Also, electron microscopy (EM) evidence has shown clathrin-coated pits containing astrovirus virions during early infection (Donelli et al., 1992). In addition, silencing Rab7 (Ras-associated binding protein 7) expression impacts human astrovirus replication, which indicates a role for late endosome maturation in the viral life cycle. Bafilomycin A, which inhibits acidification of endosomes and lysosomes, also blocks astrovirus replication, further supporting a role for the endosome (Méndez, Muñoz-Yañez, et al., 2014).

Once astrovirus virions have entered the cell and uncoated, proteolytic processing of the capsid and translation occurs (Méndez, Murillo, et al., 2013). This results in production of a viral replicase complex which can begin the production of negative-sense RNA from the genomic RNA (gRNA). Formation of negative strand RNA is followed by formation of double-stranded RNA (dsRNA), the replicative form of the genome (Fuentes et al., 2011; Guix, S. Caballero, Bosch, et al., 2005; S. Y. Jang et al., 2010).

1.4.2 Viral replication, assembly, and release

Details of the replication mechanism for astroviruses are unknown, although it is suggested that replication is cytoplasmic (Méndez, Muñoz-Yañez, et al., 2014). Some positive sense ssRNA viruses such as severe acute respiratory syndrome coronavirus 2 (SARS-CoV-2) and hepatitis c virus (HCV) utilize double-membrane vesicles (DMVs) as replication organelles, and double-membrane organelles have been observed during astrovirus replication (Cortese et al., 2020; Romero-Brey et al., 2012; Snijder et al., 2020; Twu et al., 2021). However, their role in replication has not yet been determined. It should also be noted that astrovirus nsp1a has been shown to colocalize with the endoplasmic reticulum (ER), suggesting a potential site of origin for replication (Guix, S. Caballero, Bosch, et al., 2004). Some strains of astrovirus localize close to the nucleus and ER. It is likely that similarly to other viruses, the astrovirus UTRs recruit host cellular machinery to aid in viral replication (Y. Liu, Wimmer, and A. V. Paul, 2009; Méndez, Murillo, et al., 2013; Pogue, Huntley, and T. Hall, 1994).

Although the replication mechanism of AstV is unknown, researchers have been able to observe the appearance of dsRNA intermediates and capsid for different strains

of astrovirus at specific time points. It has also been shown that astrovirus virions are initially processed within the cell by caspases from VP90 to VP70 (Del Rocío Banos-Lara and Méndez, 2010; Méndez, Fernández-Luna, et al., 2002; Méndez, Salas-Ocampo, and Arias, 2004; Payne, 2017).

Finally, astrovirus exits the cell through an unknown non-lytic mechanism. After viral egress from the cell, the capsid is further processed by trypsin-like proteases extracellularly to produce infectious virions (Méndez, Fernández-Luna, et al., 2002). It is unknown whether virions exit the cell in exosomes or via other processes. One study showed that Yuc8-infected Caco-2 cells produce more CD63 and Alix-containing extracellular vesicles than mock-inoculated Caco-2 cells at 18 hpi. CD63 and Alix are common exosome markers. At this same time point, the majority of extracellular virus associated with vesicle membranes, supporting a role for exosomes in cellular exit during infection (Baez-Navarro et al., 2022). If this is the case, it is likely the virion needs to exit the organelle to be processed by trypsin-like proteases prior to infecting another cell. The same study showed that treatment with Triton X-100 prior to treatment with trypsin significantly increased the amount of infectious virions in cell supernatants. It will be necessary to explore these results with different astrovirus strains, as well as determine whether there are other organelle-associated markers on the exit vesicles to find their source. Generally, there is little cell death associated with astrovirus replication and cellular exit (Cortez, Sharp, et al., 2019; Hargest, Davis, et al., 2021; Hargest, Bub, et al., 2022; Koci, L. A. Moser, et al., 2003; V. A. Meliopoulos et al., 2016; L. A. Moser, Carter, and S. Schultz-Cherry, 2007).

1.5 Host Immune Response to Astrovirus Infection

1.5.1 Innate immune response

Upon infection with a positive sense ssRNA (+ssRNA) virus, there are many common pathways upregulated by mammalian cells. Specifically, pathways associated with the innate immune system are crucial to initially battling viral infection. +ssRNA viruses share evolutionarily conserved pathogen-associated molecular patterns (PAMPs) that trigger pattern recognition receptors (PRRs) within the infected cell. PRRs trigger interferon (IFN) pathways, and IFN I and III pathways commonly upregulate interferon-stimulated genes (ISGs) for innate immune response. Downstream of ISG activation are common cellular responses such as proinflammatory response, interference with viral replication, and induction of cell death. However, it is widely known that astrovirus infection does not induce cell death (Nelemans and Kikkert, 2019). While our work has shown a transcriptional upregulation of antiviral and IFN pathways, there is a lack of inflammatory response to astrovirus infection.

Our laboratory has shown that neutralization of IFN-β leads to higher viral titers, and this may relate to barrier permeability response in vitro (S. A. Marvin et al., 2016). However, induction of IFN-β tends to occur only after viral replication in vitro, indicating

that the type I IFN response is delayed and ineffective despite the sensitivity of astrovirus to exogenous IFN (Guix, Pérez-Bosque, et al., 2015). While IFN response is delayed in vitro, it appears to be important to viral clearance. We showed that interferon-α/β receptor (IFNaR) knockout (IFNaR-/-) mice shed murine astrovirus for significantly longer periods of time than wildtype (WT) mice. In addition, human intestinal enteroids (HIEs) infected with the VA-1 strain of astrovirus demonstrate type I and III IFN response much more strongly than infected Caco-2 cells. VA-1 also appears to be sensitive to exogenous IFN expression (Kolawole et al., 2019). Another study of human intestinal organoids supported the induction of IFN pathways in different cell types in response to HAstV-1 infection using single cell RNA sequencing (scRNA-seq) (Triana et al., 2021).

Among processes downstream of type I IFN signaling is the induction of STAT1, which controls numerous antiviral responses. In STAT1-/- mice, astrovirus increased in replication and shedding compared to WT mice. This again supports a role for the innate immune response in suppressing astrovirus replication, although astrovirus can successfully replicate even during activation of type I IFN and STAT1 pathways (Yokoyama et al., 2012).

In addition to type I IFN and STAT1 response, astrovirus induces cytokine TGF-β activity in vitro and in vivo (L. Xu et al., 2023). This response is a potential candidate for the lack of inflammatory response during astrovirus infection, as TGF-β can be immunosuppressive.

Another early immune response utilized to suppress viral infection and activate inflammatory pathways is the complement system. Studies have demonstrated that expression of astrovirus coat protein (CP), which composes the capsid, suppresses complement activation in two ways. First, CP binds directly to C1q (Complement Component 1q), downregulating further complement activation. This was true for HAstV-1-4 strains. C1q is the activation molecule for the classical complement pathway, which leads to tagging of infected cells for elimination by phagocytosis (Bonaparte et al., 2008). The same group then asked whether astrovirus CP can affect the mannose-binding lectin (MBL) complement pathway. MBL is capable of inducing opsonization or lysis of pathogens. The MBL pathway also appears to be targeted by astrovirus. The CP protein is capable of binding MBL directly, resulting in reduced lectin response (Hair et al., 2010). In these ways, astrovirus further suppresses the initial host antiviral response.

1.5.2 Adaptive immune response

The adaptive immune response to astrovirus is understudied. It has been suggested that T and B cells may play a role in viral clearance, due to the fact that Rag1-/- mice take longer to clear murine astrovirus infection compared to WT mice (Yokoyama et al., 2012). Although murine astrovirus infection differs greatly from human astrovirus infection, previous research has shown that astrovirus-specific T cells can be found in the small intestine of humans, as well (Molberg et al., 1998). It is clear that humans develop an antibody response to astrovirus infection, with upwards of 70% of adults having antibodies

to astrovirus (Kurtz and Lee, 1978; Kurtz, Lee, et al., 1979). In two T-cell immunodeficient children, astrovirus infection was shown to persist with no detectable antibodies, suggesting that the adaptive immune system is important for clearance of astrovirus in humans (Wood et al., 1988). However, in a turkey model of astrovirus infection, the adaptive immune response to TAstV infection was lacking (Koci, Kelley, et al., 2004). Immunity across strains of human astrovirus also needs to be explored, as a child was observed with HAstV-3-associated diarrhea and was infected with HAstV-1 9 months later (Guix, S. Caballero, Villena, et al., 2002).

There is a lack of adaptive immune response in patients infected with astrovirus neurological disease (AstV-ND). Within the brain, the importance of the innate immune response is then heightened. AstV-ND can be fatal in many cases, and the brain response includes microglial and macrophage activity (Maximova et al., 2022).

1.6 Cellular Responses to Astrovirus Infection

When our laboratory demonstrated that neutralization of IFN-β enhanced viral replication of astrovirus in vitro, we also observed that type I IFN response protects cells from increased barrier permeability during astrovirus infection. We now know that astrovirus induces epithelial-mesenchymal transition (EMT), a process usually induced during cancer cell growth to facilitate metastasis. During these studies, it was found that this EMT pathway is TGF-β-dependent, suggesting another important role for TGF-β during astrovirus infection. Epithelial cell-specific proteins were decreased by 24 hours post-infection, and mesenchymal cell-specific proteins increased concurrently. During this time, infected epithelial cells also lost polarity. The sodium/potassium adenosine triphosphatase (Na/K-ATPase) transporter, generally localized to the basolateral membrane, showed disrupted localization, migrating to the apical side of the cell during infection with HAstV-1. However, this phenotype did not translate to the non-classical VA-1 strain, which showed no evidence of upregulating EMT during infection (Hargest, Bub, et al., 2022).

While it is not yet clear which other cellular processes are manipulated by astrovirus during infection, one study attempted to discern which host cell factors may be involved in Yuc8 (HAstV-8) strain astrovirus replication using density gradient centrifugation and free-flow zonal electrophoresis (FFZE). This experiment followed by tandem mass spectrometry revealed a variety of host factors. When RNA interference was utilized to determine the importance of these factors, it became clear that different branches of metabolism were important to astrovirus replication, including fatty acid, cholesterol, and phospholipid metabolism. It remains unclear what role these specific pathways play in astrovirus replication and whether this applies to other human astrovirus strains. In addition, this study showed that proteins from the Golgi, ER, mitochondria, and nucleus were isolated from Yuc8-containing fractions (Murillo et al., 2015). This suggests that specific membrane fractionation and imaging experiments are required to elucidate binding partners and membranes involved in astrovirus replication.

1.7 Epidemiology and Disease

Gastroenteritis is an illness associated with diarrhea, nausea, vomiting, and dehydration. It is a global disease burden, resulting in millions of deaths per year in children. Gastroenteritis can be caused by a variety of pathogens, including bacteria and viruses, with many cases being linked to viral infection. Astroviruses are some of many viruses that can induce acute diarrheal gastroenteritis.

1.7.1 Clinical features and diagnosis in humans

Astroviruses typically cause diarrhea within 2 days of infection in symptomatic patients. Other sequelae associated with gastroenteritis such as vomiting, dehydration, and headache have also been recorded in astrovirus-infected patients. However, some people infected with astrovirus have no symptoms (Stuempfig and Seroy, 2018). Astrovirus is transmitted through the fecal-oral route, as well as through food and water.

Although astrovirus infection can become severe, it is usually not fatal. Those most at risk for severe astrovirus infection include immunocompromised and elderly populations. However, AstV infection can be dangerous. There have been multiple recorded instances of astrovirus viremia allowing entry to the brain, although the mechanism of entry into the central nervous system (CNS) is unknown. These cases are primarily in immunocompromised patients. When astrovirus enters the brain, infection is often accompanied by encephalitis, meningitis, and death. It is currently unknown whether astrovirus replicates in brain cells or only infects them, leading to inflammation in the brain. Although cases of astrovirus in the brain are not commonly recorded, this is likely due to a lack of screening for astrovirus in cases of encephalitis and meningitis. The rate of astrovirus infection in these disease states is likely higher than previously appreciated, and screening for astrovirus should become common practice for these patients.

1.7.2 Animal disease

A wide variety of species can become infected with astrovirus. Commonly across species, young animals including lambs, calves, pigs, turkeys, and pups experience diarrhea (Guy and Barnes, 1991; Koci, Seal, and Schultz-Cherry, 2000; Martella et al., 2011; M. Shimizu et al., 1990; Snodgrass and Gray, 1977; Woode et al., 1985). Although diarrhea has been observed in mice infected with astrovirus, MuAstV infection occurs often in laboratory mouse colonies with little to no pathogenicity and unsustained immune response (Kjeldsberg and Hem, 1985). Even in severely immunodeficient mice, astrovirus fails to induce symptoms commonly seen in symptomatic human infection (Morita et al., 2021). In one study, dams and litters were infected with MuAstV. The mice showed no symptoms despite shedding virus in feces for weeks post-infection, as well as demonstrating MuAstV levels in intestines and other organs (Compton, Booth, and Macy, 2017). Our laboratory has also observed murine astrovirus in the small and large intestine, as well as the lung, spleen, blood, and

stomach, causing no histopathology. Therefore mice could function as an effective model of asymptomatic, but not symptomatic, astrovirus infection in the laboratory setting (Cortez, Sharp, et al., 2019).

Some animals experience more severe astrovirus-associated symptoms, including birds. Both turkeys and chickens experience decreased hatch size and weight gain, better known as runting-stunting syndrome (RSS), as well as nephritis (Koci and Schultz-Cherry, 2002; Pantin-Jackwood et al., 2011). In 1987, one survey found that flocks of turkeys presenting enteric disease symptoms were infected with astrovirus at a rate of 78%, demonstrating that astrovirus infection of turkeys is more common than infection with other enteric viruses in diseased flocks (Reynolds, Saif, and Theil, 1987). This has direct implications for economic impact in the food industry, as astrovirus-infected avian species experience high rates of mortality. Baby turkeys infected with turkey astrovirus (TAstV) have become an excellent disease model to imitate symptomatic human astrovirus infection, as their symptoms closely mimic those of humans infected with astrovirus.

Further, some species experience neurological symptoms mimicking human astrovirus infection. In a group of cows with encephalitis, roughly one in four were infected with bovine astrovirus (BoAstV) as shown by reverse transcription PCR (Bouzalas et al., 2014). Another study revealed that a domestic sheep infected with ovine astrovirus (OvAstV) had encephalitis and ganglionitis, inflammation of ganglia which are crucial for brain cell signaling. Further analysis showed that OvAstV was related to neurotropic BoAstV (Pfaff et al., 2017). The relationship of these distinct mammalian strains of astrovirus to one another suggests similar disease pathogenesis.

1.7.3 Epidemiology

Classical human astrovirus (HAstV) infections tend to be more common than MLB and VA infections. Epidemiological data is typically recorded in symptomatic patients, as asymptomatic patients have not been routinely screened for astrovirus infection. However, there is a likelihood that there are widespread asymptomatic astrovirus infections that go unrecorded. Asymptomatic cases may be the result of immune response built from prior infection, which could explain why cases can range from mild to severe.

It is estimated that almost 4 million cases of astrovirus diarrhea occur each year (Mead et al., 1999). In 1991, a gastroenteritis outbreak in over 4700 children and adults over a span of 5 days in Osaka, Japan was traced back to astrovirus infection through RT-PCR and EM (Oishi et al., 1994). Another outbreak of HAstV-3 in military recruits with gastroenteritis was recorded in 1997 in France (Belliot, Laveran, and Monroe, 1997). Since then, a majority of epidemiological data reported on astrovirus infections has occurred in children screened during gastrointestinal illness. Primarily, testing includes RT-PCR, enzyme-linked immunosorbent assay (ELISA), and EM.

Globally, children under 5 years of age with acute gastroenteritis are infected with astrovirus at rates between 4 to 9% (Cortez, V. A. Meliopoulos, et al., 2017; De Grazia et al., 2011; Gabbay et al., 2007; Gaggero et al., 1998; Guerrero et al., 1998; Guix, S. Caballero, Villena, et al., 2002; Holtz et al., 2014; L. Lu et al., 2021; Pager and Steele, 2002; Palombo and Bishop, 1996; Pang and Vesikari, 1999; Qiao et al., 1999; Reither et al., 2007; Resque et al., 2007; Unicomb et al., 1998). For persistent cases, rates may approach closer to 15% (Khamrin et al., 2016; Unicomb et al., 1998). Although astrovirus is less common than rotavirus within these gastroenteritis populations, astrovirus infection is generally more common than adenovirus and bacterial gastroenteritis cases.

Within the population of children infected with astrovirus causing gastrointestinal illness, HAstV-1 is the most common strain, causing between 50 to 95% of AstV cases (Cortez, Freiden, et al., 2017; De Grazia et al., 2011; Gabbay et al., 2007; Gaggero et al., 1998; L. Lu et al., 2021; Pang and Vesikari, 1999). In a 3-year study of patients with gastroenteritis in Barcelona, a pediatric group recorded that over 34% of astrovirus-infected patients were hospitalized, with over 13% of these infections being nosocomial among oncologic patients (Guix, S. Caballero, Villena, et al., 2002). Immunocompromised children are especially at risk. In one study of immunocompromised children in Memphis, Tennessee, HAstV-1 made up 50% of astrovirus infections, followed by VA-2, MLB-1, HAstV-1, HAstV-5, and HAstV-8 (21%, 13%, 11%, n=1, and n=1 respectively) (Cortez, Freiden, et al., 2017). In another report, a patient with standard-risk B-cell acute lymphoblastic leukemia and CNS leukemia had neurological symptoms and was screened for infection. Cerebrospinal fluid (CSF) metagenomic next-generation sequencing (mNGS) revealed that the patient was positive for VA-1 infection. Another patient with KMT2A-rearranged relapsed refractory acute myeloid leukemia and respiratory syncytial virus (RSV) infection showed similar symptoms to the previous patient. Use of mNGS again revealed infection with VA-1. The first patient was treated for astrovirus infection for eight months, along with modified scheduled chemotherapy. She survived and has since shown improvement in neurological symptoms. The second patient received palliative care, as his leukemia was incurable, and he experienced further neurological deterioration before dying with renal and respiratory failure seven weeks post-diagnosis (Bami et al., 2022). These case studies emphasize the importance of screening for astrovirus infection among immunocompromised patients showing neurological symptoms.

As children get older, they are less likely to experience symptomatic astrovirus infection, and this is supported by a lower number of recorded cases in adult populations. However, elderly populations are an exception and can experience astrovirus infection at higher rates than their younger adult counterparts. One elderly population in Scotland experienced an outbreak of gastroenteritis associated with HAstV-5 (Jarchow-Macdonald et al., 2015). An elder care facility had 80% of patients and 44% of staff infected with astrovirus during a gastroenteritis outbreak. The first 9 days of this outbreak were associated with calicivirus infection, and HAstV-1 infections followed during days 16-22 (J. Gray et al., 1987). Based on this report and other cases of viral coinfection with astrovirus, it is possible

that previous insult from a gastrointestinal infection can prime the intestine for astrovirus infection (Cortez, Freiden, et al., 2017; Guerrero et al., 1998; Guix, S. Caballero, Villena, et al., 2002; L. Lu et al., 2021; Resque et al., 2007). Finally, astrovirus was also detected in a gastroenteritis outbreak in an elderly population in Australia (Marshall et al., 2007).

There is evidence that astrovirus cases could be seasonal, occurring primarily in the winter months. This was recorded in groups of children under age 5 with gastroenteritis in Australia (Mustafa, Palombo, and Bishop, 2000; Palombo and Bishop, 1996), children with gastroenteritis in Barcelona (Guix, S. Caballero, Villena, et al., 2002), and children with gastroenteritis in South Africa (Pager and Steele, 2002). It has been suggested that astrovirus could be more stable in cold weather because of this observation. However, viruses transmitted via fecal-oral route such as coxsackieviruses and other enteroviruses show peak infection in the spring and fall. It is possible that with improved screening of astrovirus, different seasonal patterns may be recorded (Pons-Salort et al., 2018; Xing et al., 2014).

Typically, MLB and VA strains have been recorded in fewer cases of gastrointestinal illness than classical strains. This was observed in the aforementioned study of children with gastrointestinal illness in Memphis, TN (Cortez, Freiden, et al., 2017). However, this could be due to a lack of previous testing for MLB and VA strains. One study found the opposite. In Japan, children with gastroenteritis were evaluated, and 16% were positive for astrovirus, with MLB-1 and MLB-2 being the predominant strains. Within the infected MLB and HAstV groups, boys had higher rates of infection than girls. Notably, peak infection months were March through May in this study, contrary to previous evidence suggesting that astrovirus infection peaks in the winter. In addition, over half of the patients had other viral coinfections (Khamrin et al., 2016). Since then, the same authors have found a higher prevalence for MLB and VA strains than classic HAstVs in a population of children in Japan with acute gastroenteritis from 2014 to 2021 (Okitsu et al., 2023). MLB-1 was also the predominant strain over HAstV-1 in a group of people in Germany from 2018 to 2019 (Niendorf et al., 2022). This demonstrates the need for continuous screening of astrovirus infections among patients with gastroenteritis globally. It is likely that infections are not being recorded, and other epidemiological factors could affect distribution of infections, symptoms, and strains associated with outbreaks.

1.8 Treatment and Prevention

Typical treatments for AstV infection include hydration to avoid further loss of fluids and medication for improvement of symptoms, such as antidiarrheals. In addition, one elderly patient diagnosed with astrovirus infection was successfully treated with intravenous immunoglobulin (IVIG), and his symptoms improved dramatically within 24 hours (Björkholm et al., 1995).

A promising treatment for astrovirus is nitazoxanide. Nitazoxanide is an FDA approved anti-infective drug. Our laboratory has found that it blocks astrovirus replication in Caco-2 cells if administered within up to 8 hours post-infection. This was the case for multiple lab-adapted serotypes, as well as clinical astrovirus isolates. It also reduced symptoms and viral titers in turkeys infected with TAstV, suggesting that it could improve symptoms for patients with gastroenteritis (Hargest, Sharp, et al., 2020). In the aforementioned case reports of immunocompromised pediatric cancer patients, nitazoxanide was administered as part of the astrovirus infection treatment regimen, alongside IVIG (Bami et al., 2022).

There is no vaccine for astrovirus infections, but development of a vaccine is certainly possible. Due to evidence showing that infection can lead to development of protective antibodies, this may become an effective option in the future for prevention of disease. Work has already begun to determine which targets may be suitable for astrovirus vaccination. One group explored HAstV-2, as different strains of HAstV-2 have relatively high heterogeneity. HAstV-2-neutralizing monoclonal antibody PL-2 (MAb PL-2) was unable to bind recombinant HAstV-2-Oxford capsid spike domain (Spike-2-Oxford). Crystal structure analysis revealed that Spike-2-Oxford is locked in a downward conformation, preventing its binding to MAb PL-2. When proline 463 was mutated to a serine, the downward conformation lock was resolved, allowing MAb PL-2 to bind the spike protein. Recombinant HAstV-2-Spain capsid spike domain (Spike-2-CDC-Spain) on the other hand was able to bind MAb PL-2. Spike-2-CDC-Spain notably has a serine at residue 463, rather than a proline. They next immunized rabbits with recombinant Spike-2-CDC-Spain and found that polyclonal antibodies produced were able to neutralize all HAstV-2 strains (Bogdanoff et al., 2018). This study shows promise for finding an effective antigen for astrovirus vaccination, but further work is needed to determine whether a multivalent vaccine could be effective for all human astrovirus serotypes.

Prevention is currently focused on interrupting human-to-human transmission through good hygiene practices, as well as decontamination of water supplies through addition of chlorine and decontamination of surfaces and objects that may have viral particles with Virkon S solution. Virkon S solution is a disinfectant that is more stable than bleach and is effective against many viruses, including highly pathogenic avian influenza. These practices are essential to interrupting nosocomial infections. During the worldwide SARS-CoV-2 pandemic in 2020, one study found that acute gastroenteritis cases dropped significantly, likely due to implementation of good hygiene and decontamination practices (Okitsu et al., 2023).

Antiviral approaches against positive sense RNA viruses Although positive sense RNA viruses vary widely in pathogenesis and symptoms, it is possible that common elements of viral replication may be targeted for broad antiviral treatment. As previously mentioned, little is known about the replication process of astrovirus within host cells. It is likely that astrovirus manipulates host membranes, similarly to other positive sense RNA

viruses, in order to replicate and escape the cell without inducing cell death. Understanding the replication mechanism of astrovirus is essential for finding potential antiviral treatments.

One study found that both SARS-CoV-2 and HCV utilize double membrane vesicles to replicate and that these DMVs can be targeted using a specific inhibitor, PIK-III, in order to reduce DMV formation and viral replication (Twu et al., 2021). Although these viruses cause different types of disease, both are positive sense RNA viruses and replicate using similar mechanisms. It is possible that astrovirus utilizes a similar mechanism, and its replication organelle could prove to be an effective target to halt replication.

1.9 Summary

Human astrovirus infection is becoming more broadly studied and screened for, but there is a significant lack of information related to entry, replication, and cellular exit mechanisms for HAstVs. In addition to its ability to cause gastrointestinal disease, HAstV can cause neurological disease such as encephalitis, with a greater likelihood for these occurrences in immunocompromised patients. Despite this, the replication organelle and mechanism of its formation during astrovirus infection has yet to be determined. Understanding the process of astrovirus replication would greatly improve our ability to find targeted treatments for the disease. The high mortality rate accompanying astrovirus-associated neurological disease demonstrates that early detection and more specific antivirals are necessary to subdue astrovirus infection.

We hypothesize that astrovirus induces formation of double-membrane vesicles for replication, similarly to other positive sense, single-stranded RNA viruses. This work will elucidate the mechanism of induction of replication organelles and the host cellular machinery required for this process during human astrovirus infection.

Chapter 2

Viral Manipulation of Host Cellular Machinery

The gastrointestinal (GI) tract has multiple lines of defense against pathogen invasion. It is covered by a layer of mucus, containing commensal bacteria and antimicrobial proteins secreted by cells. This protective layer can keep some pathogens at bay. However, infection of intestinal epithelial cells is inevitable. As a result, intestinal epithelial cells have additional mechanisms to fight pathogen invasion, with some responses being specific for viral infection (Duan, 2016; Kayisoglu, Schlegel, and Bartfeld, 2021; Vancamelbeke and Vermeire, 2017).

Upon infection, epithelial cells are capable of recognizing pathogen-associated molecular patterns (PAMPs) corresponding to viruses via pattern recognition receptors (PRRs), which trigger the antiviral immune response. Aside from generating cytokines and chemokines for immune cell activation and recruitment, there are cellular pathways that can be repurposed to fight viral infection of the epithelium, including autophagy, the unfolded protein response (UPR) and cell cycle. Autophagy, the recycling pathway of the cell, can selectively target and remove intracellular pathogens upon infection (Oh and H. K. Lee, 2014). The UPR is responsible for inducing endoplasmic reticulum (ER) stress within the cell to mitigate the clearance of misfolded and accumulated host and viral proteins in the overwhelmed ER during infection. This protective mechanism typically encourages cell survival. Along the same lines, virus-infected cells can transition into cell cycle arrest to avoid supporting viral replication. These processes are interconnected, in that ER stress can increase autophagy and induce cell cycle arrest, autophagy can regulate the cell cycle and ER stress, and the cell cycle can induce autophagy and regulate ER stress. These three pathways also maintain the biological switch from a state of cell survival to cell death when necessary.

However, antiviral mechanisms can be manipulated or overwhelmed during viral infections due to viral interference with host cellular machinery. Viruses have evolved to avoid triggering cellular responses that might threaten their replication cycles or to suppress them once they are underway. Additionally, viruses have developed tactics to repurpose existing cellular pathways for their own benefit. Among these cellular pathways are the same mentioned previously, autophagy, ER stress, and the cell cycle.

2.1 Autophagy

Autophagy is a catabolic process by which cells recycle cargo to the lysosome using double-membrane vesicles. While lysosomes were discovered in 1955, autophagy was defined later in 1963 as a process by which cargo is delivered to lysosomes for degradation (De Duve et al., 1955; De Duve, 1963). Autophagy can function at basal levels within the cell, picking up cytoplasmic cargo and delivering it to the lysosome for degradation within 5-10 minutes (Fujita et al., 2008). However, certain triggers can upregulate the autophagy pathway for specific reasons. For instance, starvation is a well-characterized autophagy inducer, which leads to uptake of proteins in the cytosol for recycling of their amino acids for further use by the cell. While autophagy was discovered in 1963, it was not until 30 years later that researchers had an understanding of starvation as a trigger for the pathway, first demonstrated in yeast and confirmed in mammals (Mizushima, Yamamoto, et al., 2004; Takeshige et al., 1992). Other triggers such as hypoxia and genotoxic stress can also induce autophagy with differing downstream effects (Bellot et al., 2009; Nishida et al., 2009).

Autophagy is responsible for degradation of not only proteins, but also organelles such as depolarized mitochondria, ER fragments, endosomes, and multiple forms of ribonucleic acid (RNA) (Aizawa et al., 2016; Fraser et al., 2019; Fujiwara, Furuta, et al., 2013; Fujiwara, Hase, et al., 2015; Hase et al., 2015; Lemasters, 2005; Schuck, Gallagher, and Walter, 2014). Although this cargo can be selectively delivered to an autophagosome, autophagy has been historically viewed as a random uptake of cytosolic contents. More recently, researchers have shown that specific cargo can be broken down via autophagy selectively, and the autophagy machinery involved can vary depending on type of cargo (Anding and Baehrecke, 2017).

2.1.1 Autophagy machinery

The canonical, starvation-related autophagy pathway includes four main phases; initiation, phagophore nucleation, autophagosome elongation and maturation, and fusion with the lysosome. Initiation of autophagy during cellular starvation is reliant upon upstream factors such as adenosine monophosphate-activated protein kinase (AMPK) and mammalian target of rapamycin (mTOR) (Egan et al., 2011; Joungmok Kim et al., 2011; J. W. Lee et al., 2010; Shang et al., 2011). Prior to starvation, mTOR can phosphorylate unc51-like autophagy activating kinase 1 (ULK1) at Serine 757 (S757) to inhibit autophagy initiation. However, upon starvation, AMPK phosphorylates ULK1 at S317 and S777 for activation of the ULK1 preinitiation complex (Joungmok Kim et al., 2011). ULK1 is a kinase responsible for phosphorylation and activation of other autophagy factors. The preinitiation complex consists of ULK1, PTK2/FAK family-interacting protein of 200kDa (FIP200), and ATG13 (C. H. Jung et al., 2009). Once ULK1 is active, it phosphorylates Beclin1, a member of the phosphatidylinositol-3 kinase (PtdIns3K) complex.

There are three classes of phosphoinositide-3 kinase (PI3K) complexes. The class I PI3K complex (PI3KC1) is part of the well-established PI3K-AKT-mTOR pathway, which suppresses autophagy. The class III PtdIns3K, or PI3KC3 is responsible for production of phosphatidylinositol-3 phosphate (PtdIns3P), a key component of autophagosome membranes (Obara et al., 2008). Class II PI3Ks (PI3KC2) are also considered pro-autophagy, contributing to the formation of PtdIns3P. G-protein-coupled receptors (GPCRs) and tyrosine kinases are responsible for the activation of PI3KC1 and PI3KC2 for production of phosphoinositide and phosphatidylinositol phosphates (Petiot et al., 2000; Xinlei Yu, Long, and Shen, 2015).

PI3KC3 consists of a central kinase, VPS34, bound to Beclin1 and other proteins that can promote or inhibit autophagy-related function (Xinlei Yu, Long, and Shen, 2015). The complex can transiently bind ATG14 and AMBRA1 (activating molecule in Beclin 1-regulated autophagy) for autophagosome formation (Di Bartolomeo et al., 2010; Itakura, Kishi, et al., 2008; Maria Fimia et al., 2007; Matsunaga et al., 2009; Yun Zhong et al., 2009; Yu Zhong et al., 2014). It can also bind UVRAG (UV radiation resistance-associated gene protein) to play a role in autophagosome maturation (Funderburk, Q. J. Wang, and Yue, 2010; Itakura, Kishi, et al., 2008; C. Liang et al., 2008). Once PI3KC3 is active and producing PtdIns3P, other proteins can be recruited to the site of the forming phagophore to assist in autophagosome maturation.

A key component of the starvation-induced autophagy pathway is the microtubule-associated protein light chain 3 (LC3) conjugation machinery. Autophagy-associated proteins act in a cascade of reactions to conjugate LC3 to phosphatidylethanolamine (PE). In an Adenosine Triphosphate (ATP)-dependent process, ATG7, an E1-like enzyme, and ATG10, an E2-like enzyme conjugate ATG5 to ATG12. ATG5-ATG12 then complexes with ATG16L1 and is delivered to phagophore membranes. ATG7 reacts similarly with LC3, followed by an E2-like enzymatic reaction between LC3 and ATG3. Finally, LC3 is conjugated to PE via an E3-like enzymatic reaction mediated by the ATG5-ATG12-ATG16L1 complex (Kuma, Mizushima, et al., 2002; Mizushima, Noda, and Ohsumi, 1999). This canonical pathway is often referred to as ATG5- and ATG7-dependent for this reason (Mizushima, Noda, Yoshimori, et al., 1998). LC3-PE is also known as LC3-II, while its unbound form is known as LC3-I. LC3-II is membrane- bound and is widely regarded as a marker of autophagy (Y.-K. Lee and J.-A. Lee, 2016). Quantifying the ratio of LC3-II to LC3-I while blocking lysosomal fusion is common practice for measuring autophagic flux. LC3 turnover is required for autophagosome maturation under starvation conditions (Klionsky et al., 2021; Tsukada and Ohsumi, 1993).

The final step of autophagosome fusion with the lysosome depends on a wide array of machinery, including microtubules and actin filaments which guide the organelles together (Kimura, Noda, and Yoshimori, 2008; Monastyrska et al., 2009; Pu et al., 2016; Ravikumar et al., 2005), as well as SNAP receptor (SNARE) (Bas et al., 2018; J. Gao, Reggiori, and Ungermann, 2018; Itakura, Kishi-Itakura, and Mizushima, 2012; Saleeb et al.,

2019; Takáts et al., 2013) and Ras-associated binding (Rab) proteins which facilitate fusion (Hegedűs et al., 2016; Johansson et al., 2007; Jordens et al., 2001; McEwan et al., 2015; H. Wang et al., 2015). Upon formation of the autolysosome, the inner membrane of the autophagosome and the cargo within are degraded in the acidic pH by lysosomal enzymes such as cathepsins (Mizushima, Levine, et al., 2008; Schroder et al., n.d.; Tsuboyama et al., 2016; Xiong and M. X. Zhu, 2016).

2.1.2 Alternative autophagy

Not all autophagy pathways involve the total components of the starvation-induced autophagy machinery. For instance, during erythropoiesis, mitochondria are degraded through the autophagy pathway to give way to mature red blood cells. This process is independent of the ATG5 and ATG7 LC3 conjugation machinery (Nishida et al., 2009; Ji Zhang et al., 2009). Erythrocytes are not the only cells to utilize an LC3-independent mechanism for autophagosome formation. Multiple cell types produce autophagosomes even in the absence of ATG5 and ATG7 activity to degrade a variety of cargo beyond mitochondria. Isolation membranes for these autophagosomes originate from the trans-Golgi network with TGN38 localization rather than ER calnexin-containing sites. Phosphatidylinositol 3-phosphate (PI3P)-recruited protein WD-repeat protein interacting with phosphoinositides (WIPI2), but not always its family member WIPI3, is generally required for canonical autophagy. In this alternative ATG5-independent pathway, WIPI3 is necessary for formation of autophagosomes from trans-Golgi sites (Yamaguchi et al., 2020). In place of LC3 conjugation machinery, Rab9 has been postulated to be involved in this alternative autophagy pathway. In its absence, the pathway cannot proceed, and Rab9 overexpression reduces LC3-associated autophagosomes while increasing Rab9-associated autophagosomes (Mareninova et al., 2022). Tripartite motif containing 31 (TRIM31) is another protein that is indispensable for ATG5/7-independent autophagic clearance of bacteria within intestinal epithelial cells specifically (Ra et al., 2016).

Alternative autophagy pathways can be specific and selective for cargo being degraded, involving differing types of machinery to aid in cargo delivery to autophagosomes. For example, mitochondrial degradation, referred to as mitophagy, requires additional autophagy components unique to mitochondrial sequestration and shuttling to the autophagosome. This is referred to as the PTEN-induced kinase1, phosphatase and tensin homologue-induced kinase 1 (PINK1) and PARKIN machinery and has been recognized for its role in Parkinson's Disease (Matsuda et al., 2010; D. Narendra et al., 2008; D. P. Narendra et al., 2010; Vives-Bauza et al., 2010). Pexophagy, autophagic degradation of peroxisomes, requires selective autophagy chaperone p62, also known as sequestosome-1 (SQSTM1), for shuttling to the autophagosome (Zientara-Rytter and Subramani, 2016). SQSTM1 recognizes ubiquitinated cargo and directs such cargo to the autophagosome. Similarly, leaky lysosomes that can damage cells are ubiquitinated and colocalize with SQSTM1 before their ultimate degradation via autophagy, termed lysophagy (Anding and Baehrecke, 2017). Not only are organelles selectively degraded, but also specific proteins and enzymes can be

targeted for unique purposes during selective autophagy. Hexokinase 2 (HK2) is one such enzyme which can be ubiquitinated by tumor necrosis factor receptor-associated factor 6 (TRAF6) before its recognition by SQSTM1 for autophagy. This enzyme has an essential role in glycolysis, and its specific degradation has consequences in cancer pathogenesis (Jiao et al., 2018). These types of selective autophagy are not necessarily ATG5/7-independent, again showing the flexibility of the host cell in supporting autophagy using a variety of machinery.

Some autophagy pathways can also be activated through differing upstream triggers. For instance, autophagy activated under genotoxic stress involves tumor protein 53 (P53) activation of protein phosphatase magnesium-dependent 1 delta (PPM1D) and receptor-interacting protein kinase 3 (RIPK3) through differential phosphorylation of ULK1. PPM1D is responsible for dephosphorylating ULK1 at S637, and RIPK3 phosphorylates and activates ULK1 at S746, unique phosphorylation sites which lead to autophagy induction independently of AMPK and mTOR activity (Torii et al., 2020).

Importantly, autophagy machinery is dysregulated within the context of a wide variety of diseases, including cancer, beta thalassemia, bacterial infection, and viral infection (Lechauve et al., 2019; Levine and Kroemer, 2008). Unsurprisingly, autophagy can be manipulated by cancer cells through control of metabolism and other pathways, and modulation of autophagy can increase the efficacy of cancer treatment (Cufí et al., 2011; S. K. Yeo et al., 2016; Y. Zhou, Rucker III, and B. P. Zhou, 2016). Similarly, viruses have become capable of manipulating autophagy machinery for replication purposes (**Figure** 2.1).

2.1.3 Autophagy during viral infection

Negative regulation of the viral life cycle by autophagy

Being that autophagy is a degradation pathway, it is unsurprising that there is evidence of autophagic degradation of pathogens, referred to as xenophagy. Bacteria in particular are targetable by ubiquitination and phosphorylation, patterns that are recognizable by selective autophagy chaperones (Tumbarello et al., 2015; Wild et al., 2011; Y. T. Zheng et al., 2009). The autophagy pathway can function as an immune effector to target and destroy intracellular pathogens before these pathogens can cause excessive damage or be allowed to further replicate within the host cell. This is the case for picornaviruses, which can be targeted by the autophagy pathway for degradation of viral RNA using galectin 8 as a sensor (Staring et al., 2017). Human immunodeficiency virus-1 (HIV-1) factor Vif is also degraded by autophagy, preventing further HIV-1 replication (Valera et al., 2015). Similarly to certain types of bacteria, Chikungunya virus (CHIKV) can also become ubiquitinated and degraded by autophagy, while Sindbis virus (SV) can be targeted to autophagosomes independently of ubiquitin pathways (Judith et al., 2013; Orvedahl, MacPherson, et al., 2010; Orvedahl, Sumpter Jr, et al., 2011). During vesicular stomatitis virus (VSV) infection, the

Figure 2.1: Autophagy During Viral Infection. A. Antiviral activity of autophagy. Viruses and their proteins including Sindbis virus (SV), vesicular stomatitis virus (VSV), picornaviruses, human immunodeficiency virus (HIV) protein Vif, and Chikungunya virus (CHIKV) can be directly degraded by autophagy. VSV actively inhibits autophagy to prevent its own degradation. Additionally, Epstein-Barr virus (EBV) and herpes simplex virus type 1 (HSV-1) antigens are processed via autophagy for antigen presentation. B. Evasion and manipulation of autophagy by viruses. HSV, Kaposi's sarcoma-associated herpesvirus (KSHV), and human cytomegalovirus (HCMV) inhibit initiation of autophagy via Beclin. KSHV also targets LC3 machinery. Human parainfluenza virus 3 (HPIV3) and severe acute respiratory syndrome coronavirus 2 (SARS-CoV-2) inhibit autophagosome-lysosome fusion. Dengue virus (DENV) promotes lipophagy for energy production during replication. Hepatitis C virus (HCV), SARS-CoV-2, tomato bushy stunt virus (TBSV), and carnation Italian ringspot virus (CIRV) manipulate the PI3K complex for double membrane vesicle (DMV) replication organelle formation.

PI3K-Akt pathway is downregulated, leading to an increase in autophagy and a decrease in viral replication (Shelly et al., 2009).

Autophagy can also indirectly target viral infection. For instance, Epstein-Barr virus (EBV) antigen presentation of EBV nuclear antigen 1 (EBNA1) is facilitated via autophagy, and blocking lysosomal degradation causes accumulation of EBNA1-containing autophagosomes in cells (Paludan et al., 2005). Similarly, cells infected by herpes simplex virus type 1 (HSV-1) have increased MHC class I presentation of viral antigens due to autophagy (English et al., 2009). Autophagy is also upregulated during HSV-1 infection for the purpose of degradation of viral deoxyribonucleic acid (DNA). Aside from regulating replication of the virus, this process also helps to avoid sustained immune activation and injury to host tissue (Q. Liang et al., 2014). In all, autophagy is a helpful antiviral tool during infection.

Evasion and manipulation of autophagy by viruses

Due to the role of autophagy in actively preventing viral replication, some viruses have evolved to not only evade, but also manipulate autophagy machinery for their benefit. HSV, Kaposi's sarcoma-associated herpesvirus (KSHV), and human cytomegalovirus (HCMV) fight against autophagy's antiviral properties by interacting with Beclin to inhibit initiation of the pathway (Mouna et al., 2016; Pattingre et al., 2005; Tallóczy et al., 2002). KSHV is also able to target LC3 conjugation machinery directly (J.-S. Lee et al., 2009). The human parainfluenza virus 3 (HPIV3) phosphoprotein (P) promotes viral replication by preventing the autophagosome from fusing with the lysosome (Ding et al., 2014). Severe acute respiratory syndrome coronavirus 2 (SARS-CoV-2) ORF3a protein similarly blocks lysosomal fusion

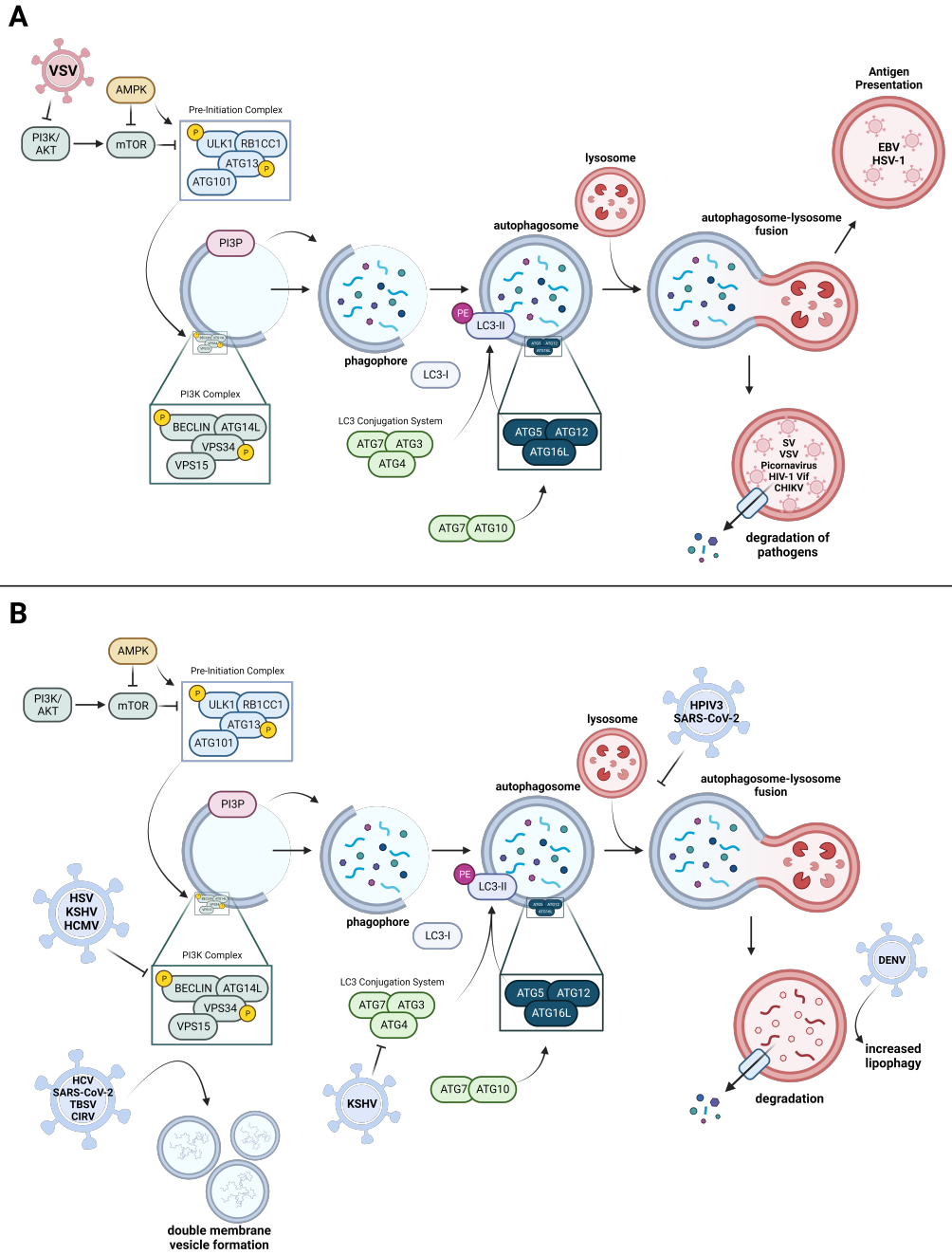

Figure 2.1: Autophagy During Viral Infection.

and enhances viral replication (Hayn et al., 2021; Miao et al., 2021; Qu et al., 2021; Y. Zhang et al., 2021). In another indirect manner, dengue virus (DENV) promotes lipophagy, the autophagic degradation of fatty acids, to increase ATP production to aid in viral replication, supporting a unique role for other metabolic pathways in the viral life cycle (Heaton and Randall, 2010).

Viruses can actively prevent canonical autophagy functions to avoid degradation and detection. However, viruses can also manipulate specific parts of autophagy machinery to promote their replication. Positive sense single stranded RNA (+ssRNA) viruses are experts at exploiting autophagy machinery. Many +ssRNA viruses utilize double-membrane vesicles (DMVs), which strongly resemble autophagosomes, as replication organelles (ROs). It has also been hypothesized that DMVs have a second purpose, protecting viral RNA from innate immune sensors within the host cell (Y. Choi, Bowman, and J. U. Jung, 2018). Due to the fact that these replication organelles share characteristics with autophagosomes, many studies have attempted to discern the role of autophagy machinery in formation of DMVs during viral replication.

A variety of viruses utilize PI3KC3 for formation of DMVs, including SARS-CoV-2 and hepatitis C virus (HCV). Chemical inhibition of PI3KC3 using inhibitor PIK-III or knockdown of PI3KC3 components VPS34 and Beclin1 significantly reduces DMV formation and viral replication for both SARS-CoV-2 and HCV (Twu et al., 2021). It has also been shown that phosphatidylinositol 4-kinase (PI4K) is involved in DMV formation during HCV and SARS-CoV-2 infection, suggesting that both PI3P and PI4P are membrane components of ROs. Coxsackievirus B3 (CVB3) utilizes PI4KIIIβ, but not PI3K machinery in formation of its ROs during infection (Mohamud et al., 2020). Poliovirus (PV) also uses PI4KIIIβ to form PI4P-rich DMVs (Mosser, Caliguiri, and Tamm, 1972). Tomato bushy stunt virus (TBSV) and carnation Italian ringspot virus (CIRV) are positive sense RNA viruses that utilize VPS34 and PI3P for formation of their peroxisomal and mitochondrial ROs in yeast cells, respectively (Z. Feng et al., 2019). Not all ROs require PI3KC3 specifically, but the role of lipid kinases in viral replication is clearly significant.

Previous work has suggested a role for PI3K in astrovirus replication using wortmannin and Ly294002, which are pan-PI3K inhibitors. Using these inhibitors resulted in reduction in astrovirus infection at the time of infection and for a few hours after. However, it is unclear whether this difference carries through the process of viral replication and which PI3K complex is responsible for these differences due to the use of the broad inhibitors and lack of mechanistic experiments (Tange et al., 2013). An alternative to determine whether astrovirus is affected by inhibition of the autophagy-specific PI3KC3 would be the specific PIK-III inhibitor, which binds a hydrophobic pocket only present in PI3KC3 and not PI3KC1 or PI3KC2.

While upstream PI3K machinery is involved in DMV formation for multiple viruses, the literature is varied regarding involvement of LC3 conjugation machinery in DMV formation. Showing an increase in LC3-II formation during viral infection is insufficient

to support a role for LC3 in formation of DMVs and viral replication. Because increased LC3 turnover may coincide with canonical autophagy pathways and antiviral mechanisms discussed previously, it is necessary to show that an absence of LC3 conjugation activity affects viral replication and DMV formation directly. For instance, PV clearly utilizes LC3 machinery for DMV formation, as LC3 is localized on replication organelle membranes, and targeting LC3 machinery via RNA interference greatly reduces PV yield (Jackson et al., 2005). A similar approach was taken to demonstrate the importance of LC3 conjugation machinery to foot and mouth disease virus (FMDV) and CVB3 replication (O'Donnell et al., 2011; J. Wong et al., 2008).

On the other hand, involvement of LC3 conjugation in HCV replication has been recently clarified. Although interference with ATG5 impacts initiation of HCV replication through transient interactions with HCV RNA polymerase NS5B, LC3 conjugation specifically is not required for DMV formation (Dreux et al., 2009; Guévin et al., 2010). The ATG5-12 conjugate is necessary for HCV replication, but not due to its role in LC3 turnover (Fahmy and Labonté, 2017). While showing the involvement of PI3KC3 in HCV replication and DMV formation, Twu and colleagues also showed that the ATG5-12/16L1 complex is not necessary for HCV replication. The same was true for SARS-CoV-2. Thus, DMV formation is PI3K-dependent and LC3-independent for SARS-CoV-2 and HCV, two unique +ssRNA viruses. This suggests that although +ssRNA viruses may exhibit a wide variety of pathology and symptoms, a common and targetable PI3K-dependent mechanism may be employed for replication.

Biogenesis of viral-induced DMVs

Since autophagy is a highly targetable pathway, researchers have also ventured to answer the question of DMV biogenesis. Autophagosomes can originate from multiple intracellular organelles, including the ER, ER-Golgi Intermediate Compartments (ERGIC), and mitochondrial membranes (L. Ge et al., 2013; Hailey et al., 2010). The ER was the first demonstrated site of observed phagophore formation (Axe et al., 2008; Hayashi-Nishino et al., 2009). It follows that DMVs formed during viral replication can originate from the ER (Roingeard et al., 2022). Coronaviruses generate their replication organelles from ER membranes (Cortese et al., 2020; Cottam et al., 2011; Knoops, Kikkert, et al., 2008; Mihelc, Baker, and Lanman, 2021; Prentice et al., 2004). This is also the case for HCV, arteriviruses, and noroviruses (Doerflinger et al., 2017; Knoops, Bárcena, et al., 2012; Romero-Brey et al., 2012). Interestingly, while DMVs can contain calnexin, an ER marker, HCV-induced DMVs have much higher cholesterol content than ER membranes, and SARS-CoV-2 replication is also reliant upon cholesterol (Hoffmann et al., 2021; D. Paul et al., 2013). This suggests that even if the ER is the source membrane material for DMVs, it becomes modified during their formation.

Although there is evidence for the ER as the site of biogenesis for DMVs, it is possible that in the absence of ER membrane sources, other organelles could compensate for the lack

of membrane material to form the site of biogenesis. Enteroviruses have been observed by electron microscopy (EM) to originate from both ER and Golgi membrane structures (Melia et al., 2019). The ER is the initial source of replication organelles for enterovirus, followed by the trans-Golgi membrane which disassembles and contributes lipids to budding ROs.

2.2 Endoplasmic Reticulum Stress During Viral Replication

Beyond its potential role as the site of DMV biogenesis, the ER regulates other facets of viral replication. The well-characterized unfolded protein response (UPR) pathway is responsible for maintaining correct protein folding and homeostasis within the host cell. When misfolded proteins accumulate, the cell faces ER stress, a state in which a multi-channel signaling pathway is triggered to restore the UPR and cellular homeostasis. Misfolded proteins can collect in the ER due to inability to fold the proteins or inability to recognize the misfolded proteins (J. H. Lin, Walter, and Yen, 2008).

Viral infection often leads to ER stress, and the UPR is induced, resulting in reduced cell death. This can be beneficial for viral replication, allowing the cell to survive and viral replication factories to continue producing progeny. On the other hand, ER stress can induce apoptosis if the stress upon the cell is prolonged during viral infection (J.-A. Choi and Song, 2020; S. Li, Kong, and Xilan Yu, 2015; V. Prasad and Greber, 2021). Therefore, the role of ER stress during viral replication is double-edged.

2.2.1 UPR pathways

Three pathways comprise the UPR in mammalian cells, including inositol-requiring enzyme 1 (IRE1), activating transcription factor 6 (ATF6), and PKR-like endoplasmic reticulum kinase (PERK) pathways. Each of these pathways can affect protein folding and homeostasis. IRE1 specifically is conserved among eukaryotic cells and leads to activation of mRNA X-box-binding protein 1 (XBP1) splicing. When XBP1 becomes spliced, it acts as a transcription factor, translocating to the nucleus and binding ER stress-response elements (ERSE) (Calfon et al., 2002; Misiewicz et al., 2013; Yoshida et al., 2001). ERSEs activate protein folding and degradation responses to maintain homeostasis within the cell. Interestingly, IRE1α is present in all cell types, and IRE1β is only present in intestinal epithelial cells (Bertolotti et al., 2001). IRE1β deficiency is known to cause faster inflammatory bowel disease (IBD) in mice, with higher ER chaperone immunoglobulin heavy-chain binding protein (BiP) levels. BiP is a marker often used to indicate ER stress. This suggests that IRE1β could play an important role in disease pathogenesis within the intestine, independent of IRE1α activity. IRE1 also has a role in upregulation of macroautophagy pathways (K. Castillo et al., 2011).

The ATF6 and PERK pathways can be similarly upregulated within the UPR. When ER stress occurs, ATF6 translocates to the Golgi and is cleaved into its transcription factor form, ATF6α. ATF6α activates pathways associated with ER stress response and tends to favor apoptosis within stressed cells (Gotoh et al., 2002; Nakanishi, Sudo, and Morishima,

2005; Ye et al., 2000). The PERK arm of the UPR is focused on stalling the protein misfolding process by stalling protein translation as a whole in response to ER stress. PERK is a kinase that phosphorylates eIF2α (eukaryotic translation initiation factor 2A) to inhibit translation (Harding et al., 2000; Hao-Yuan Jiang, L. Jiang, and Ronald C Wek, 2007; R. Wek, Jiang, and Anthony, 2006).

2.2.2 ER stress manipulation during viral infection

As previously mentioned, ER stress can be beneficial or detrimental to viral replication. Therefore, some viruses directly activate parts of the UPR, while actively suppressing others for specific purposes (**Figure** 2.2). Studies related to astrovirus modulation of ER stress are limited. While it has been established that astrovirus proteins can localize to the ER, there has only been one study investigating the role of ER stress in astrovirus infection. This work showed that protein kinase R (PKR), which normally phosphorylates eIF2α to cause a decrease in protein translation, is upregulated at 6 hpi during astrovirus infection. Phosphorylation of eIF2α was increased by 12 hpi. This is a common response of host cells to viral infection, meant to decrease translation of viral proteins. However, the delay in eIF2α phosphorylation suggests an interference of astrovirus with this pathway. Further, the authors found that this process occurred independently of the PERK pathway, suggesting an ER stress-independent mechanism (Tomoyasu Isobe et al., 2019). Therefore, the role of ER stress during astrovirus infection needs to be further investigated to clarify any changes in the UPR during infection and whether these changes affect viral replication.

For some positive sense RNA viruses, ER stress activation leads to apoptosis. This is the case for Bovine Diarrhea Virus (BDV), which modulates apoptosis via the PERK arm of the UPR (R. Jordan et al., 2002). During Japanese Encephalitis Virus (JEV) infection, viral proteins build up in the ER, leading to activation of C/EBP Homologous Protein (CHOP) and JEV-induced apoptosis (Su, C.-L. Liao, and Y.-L. Lin, 2002). Interestingly, DENV upregulates UPR pathways and XBP1, leading to autophagy and enhanced viral replication. However, ER stress during DENV infection actually protects the cell from cell death processes (Datan et al., 2016; Umareddy et al., 2007; C.-Y. Yu et al., 2006). This could certainly be the case for astrovirus, as it is a non-lytic virus.

Other positive sense RNA viruses modulate ER stress, but the effect of that activation on cell death has not been described. This includes HCV, which upregulates ATF6 for viral protein folding. HCV also increases IRE1, but XBP1 splicing is repressed during infection. Lastly, HCV actively inhibits PERK to prevent translational attenuation (Tardif, Waris, and Siddiqui, 2005). Both SARS-CoV and gamma coronavirus infectious bronchitis virus (IBV) modulate ER stress response pathways. SARS-CoV activates ATF6, but not IRE1 or PERK pathways. However, there is evidence that the 8ab SARS protein interacts with IRE1α, and the spike protein increases BiP levels during infection (Chan et al., 2006; Karagöz et al., 2017; Sung et al., 2009). IBV activates the IRE1 pathway, but not XBP1 splicing, for induction of an ATG5-independent, Beclin-dependent autophagy pathway during infection, supporting

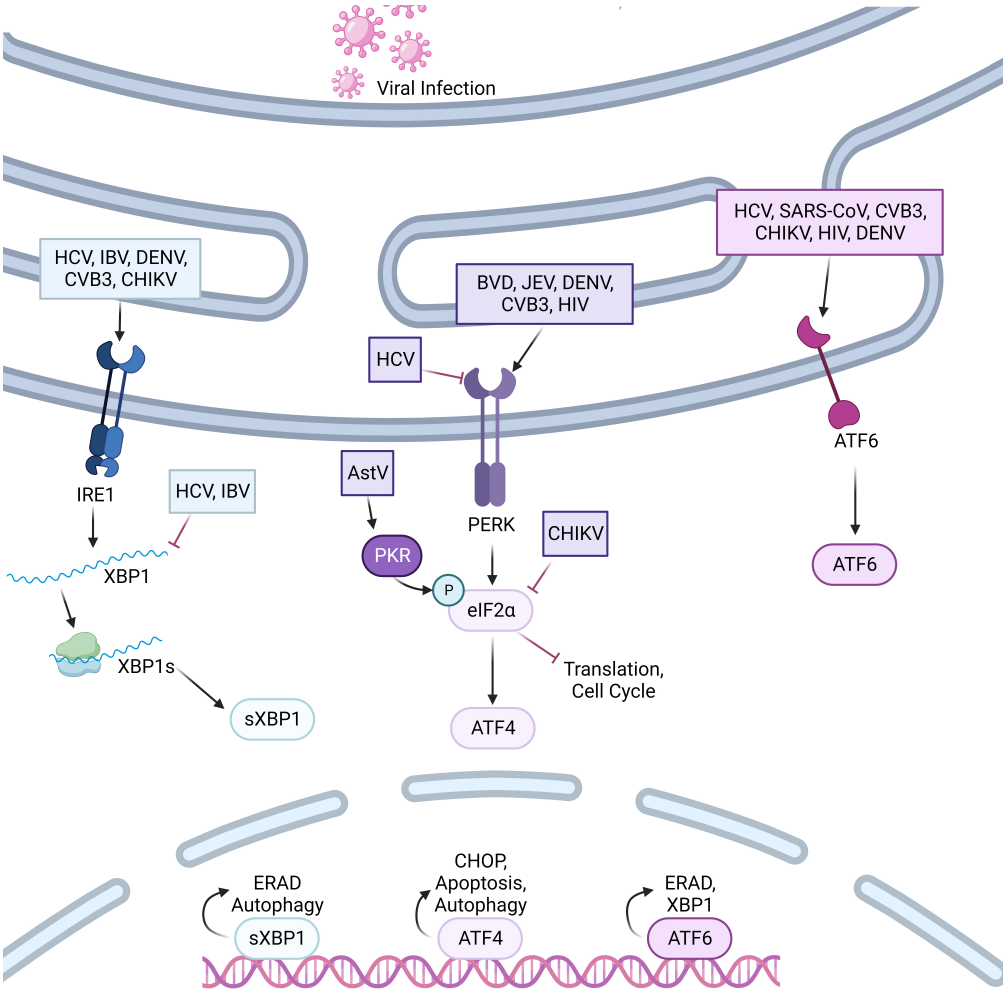

Figure 2.2: Viral Manipulation of the Unfolded Protein Response Pathways. Viruses activate or inhibit arms of the Unfolded Protein Response (UPR) pathways to benefit their replication. Hepatitis C virus (HCV), dengue virus (DENV), infectious bronchitis virus (IBV), Coxsackievirus B3 (CVB3), and Chikungunya virus (CHIKV) activate the IRE1 arm of the UPR. HCV and IBV also negatively regulate XBP1 splicing. bovine diarrhea virus (BDV), Japanese encephalitis virus (JEV), human immunodeficiency virus (HIV), DENV, and CVB3 also activate the PERK arm of the UPR. HCV negatively regulates PERK. Astrovirus (AstV) activates PKR in a PERK-independent manner. CHIKV negatively regulates eIF2α. Severe acute respiratory syndrome coronavirus (SARS-CoV), HCV, CVB3, CHIKV, HIV, and DENV all activate the ATF6 arm of the UPR.

another link between ER stress and autophagy induction during viral infection (Fung and D. X. Liu, 2019). Another study showed that thapsigargin, an ER stress activator, was antiviral during infection with three types of CoVs. Thapsigargin treatment also reduced autophagy in CoV infection (Shaban et al., 2021). CVB3, CHIKV, and HIV are more examples of pathogens that increase UPR activation during infection, but more should be studied to make conclusions on the importance of ER stress to viral replication (Colli et al., 2019; Lindl et al., 2007; Rathore, M.-L. Ng, and Vasudevan, 2013).

Knowing that positive sense RNA viruses modulate ER stress for their own benefit justifies studying the role of the UPR in astrovirus infection. Not only is ER stress capable of modulating viral protein folding, but it also directly affects autophagy, cell death, and even the cell cycle. Each of these areas are understudied in astrovirus infection, and a better understanding of the role of these pathways could lead to more efficiently targeted treatments.

2.3 Cell Cycle Arrest During Viral Replication

Yet another cellular process manipulated by viruses during infection is the cell cycle. The cell cycle is necessary to govern overall cellular health and whether a cell is fit to grow and divide. Billions of cells in the human body go through this process daily. Regulation of the cell cycle is famously evaded by cancer cells, which maneuver around checkpoints to continue their own growth and division processes. However, the cell cycle is meant to prevent exactly that occurrence. When a cell is healthy and properly functioning, it will only grow and divide after passing cell cycle checkpoints. Even with these checkpoints in place, a cell can be vulnerable to a variety of stressors. Viruses are one such stressor able to exploit the cell cycle to promote their replication processes.

2.3.1 Stages of the cell cycle

The four stages of the cell cycle are Gap 1 (G1), Synthesis (S), Gap 2 (G2), and Mitosis (M). During G1 phase, the cell grows and produces more protein, nucleic acids, and organelles to be distributed to daughter cells. In S phase, the cell duplicates its DNA. Next, the cell prepares for division, organizing its new contents during G2 phase. Finally, the cell divides into two identical daughter cells during M phase. This process is necessary to keep the body functioning daily, but not in all cell types. For instance, some cells are fully differentiated and will not divide further. At this point, the cell enters an alternate Gap 0 (G0) phase, in which it becomes quiescent (Barnum and O'Connell, 2014; Schafer, 1998).

For different phases of the cell cycle, the cell must pass checkpoints that determine whether it is ready to move on to the following stage. For instance, if not enough nutrients have accumulated during G1 phase, the cell will not begin S phase (Killander and Zetterberg, 1965b; Killander and Zetterberg, 1965a). Similarly, if there is DNA damage during G1, the cell will not move into S phase to avoid replication of mutation-containing cells (Giono and

Manfredi, 2006). Once the cell passes the G1/S checkpoint, it enters S phase. If the cell has not replicated its DNA correctly by the end of S phase, it will not enter into G2 (Nishitani and Lygerou, 2004). Finally, there are many events that can go wrong during cell division in M phase. If the cell fails to divide properly, it will not pass the M phase (McLean et al., 2011).

At each checkpoint of the cell cycle, proteins called cyclins and cyclin-dependent kinases (CDKs) govern whether the cell moves forward to the next stage. Only when the proper cyclin binds its associated CDK will the cell cycle gain permission to move forward (Jeffrey et al., 1995). This is because CDKs activate cyclins so that they can phosphorylate downstream targets, enabling downstream replication activities within the cell (De Bondt et al., 1993). Cyclins D and E are necessary for progression through G1 phase, followed by Cyclin A in S phase, and finally Cyclin B in M phase. Cyclin D binds CDK4/6, Cyclin E binds CDK2, Cyclin A binds CDK2 and CDK1, and Cyclin B binds CDK1. Therefore, although a cyclin may be present in the cell, it is not until it is bound by its partner CDK that it becomes active in cell cycle progression (Łukasik, Załuski, and Gutowska, 2021; Pavletich, 1999).

Other proteins are also essential for cell cycle regulation, including tumor suppressors like P53 and retinoblastoma protein 1 (RB1). These proteins interact directly with cell cycle components so that a cell will only continue growth and division if it is ready. This is why mutations in p53 and Rb1 are often associated with cancer. Without management of these cell cycle checkpoints by tumor suppressors, the cell may grow uncontrolled (Engeland, 2022).

2.3.2 Viral manipulation of the cell cycle

Unsurprisingly, the cell cycle can be manipulated by viruses during infection. Different viruses cause cell cycle arrest in unique phases of the cell cycle for specific reasons (**Figure** 2.3). For instance, viruses that can induce G1 phase arrest include SARS-CoV, EBV, HCMV, HSV1, and influenza A virus (IAV) (J. P. Castillo and Kowalik, 2004; Cayrol and Flemington, 1996; C.-J. Chen, Sugiyama, et al., 2004; C.-J. Chen and Makino, 2004; Sinclair et al., 2000; Yuan, Shan, et al., 2005; Yuan, J. Wu, et al., 2006). During IAV infection, pRb and cyclins D and E are decreased, and p21 is increased. This is a recipe for G1 arrest (Yuan He et al., 2010). Interestingly, during HSV1 infection, pRb is hypophosphorylated, which supports G1 arrest. However, CDKs normally involved in modulation of pRb activity are not decreased (Diwan, Lacasse, and Schang, 2004; Schang, Phillips, and Schaffer, 1998). In fact, it has been shown that these CDKs may benefit HSV1 infection through modulation of RNAPII function (Durand and Roizman, 2008).

Therefore, cell cycle arrest during viral infection is not straight-forward. In fact, some viruses manipulate multiple stages of the cell cycle. For example, while EBV protein Zta induces G1 arrest, EBV protein LMP-1 induces G2/M arrest (K.-S. Yeo, Mohidin, and

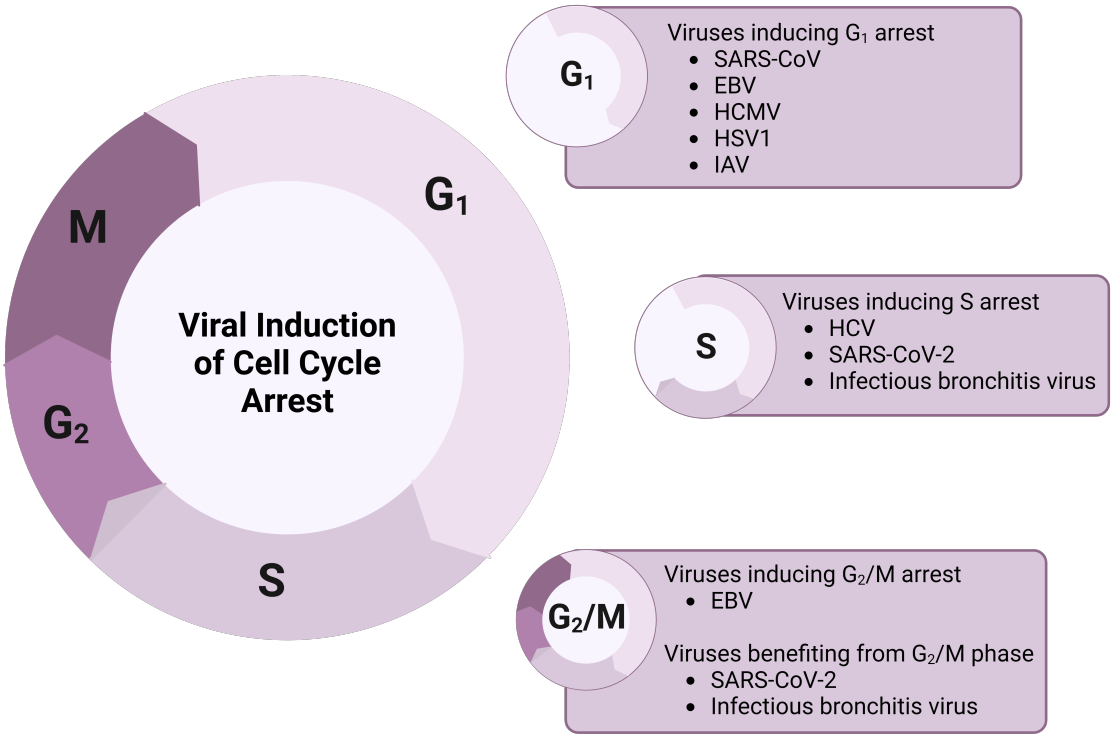

Figure 2.3: Viral Induction of Cell Cycle Arrest. Viruses induce cell cycle arrest during different phases of the cell cycle to support replication and exit from the host cell.

C.-C. Ng, 2012). This suggests that different cell cycle phases are beneficial for specific viral life cycle stages, not just G1 phase.

Viruses that modulate S and G2/M phases include HCV, KSHV, human papillomavirus type 1 (HPV1), reovirus serotype 3, SARS-CoV-2, IBV, and HCV (Järviluoma and Ojala, 2006; Poggioli, Dermody, and Tyler, 2001; Stark and W. R. Taylor, 2006). HCV interestingly shows biphasic regulation of S phase, with an increase in cells in S phase, followed by arrest (Munakata et al., 2007; Otsuka et al., 2000; Ruggieri et al., 2003; X.-J. Yang et al., 2006). SARS-CoV-2 and IBV both show an accumulation of cells in S and G2/M phases following infection. When cells are synchronized to G2/M phase, there is an increase in SARS-CoV-2 and IBV replication (Dove et al., 2006; Sui et al., 2023). This indicates that there is a benefit to DNA replication and cellular division stages of the cell cycle for viral infection. In observing this phenomenon across viral families, researchers have suggested that the benefit comes from the host cellular machinery available during this "pseudo-S phase" (Bagga and Bouchard, 2014). While DNA replication is occurring in the cell, DNA viruses thrive. The reason for arrest during RNA virus infection may also be related to availability of host cellular organelles. During preparation stages for division, there is an abundance of ER and Golgi membranes available to aid in viral replication and assembly. Therefore, modulation of the cell cycle by viruses is beneficial for replication and assembly purposes.

2.4 Research Aims

In these studies, I aimed to determine the site of replication for human astrovirus serotype 1 (HAstV-1) and involvement of host cellular machinery in the process. Although other studies have begun to find cellular pathways that affect astrovirus replication, no research thus far has elucidated which cellular machinery is necessary to replication organelle formation. I hypothesize that astrovirus induces double-membrane vesicle formation for replication using some host autophagy machinery.

2.4.1 Aim 1: Identify the replication organelle for HAstV-1

Using electron microscopy (EM) and UV-inactivated virus, we showed that astrovirus induces double-membrane vesicle (DMV) formation during infection of human Caco-2 cells. There are no DMVs formed in mock-inoculated cells, and astrovirus virions associate closely with the DMVs within HAstV-1-infected cells. In addition, UV-inactivated virus does not induce DMV formation upon cellular inoculation, suggesting that formation of DMVs is replication-dependent.

2.4.2 Aim 2: Determine what host cellular machinery is necessary for astrovirus-induced replication organelle formation

Through reverse transcription polymerase chain reaction (RT-PCR), a variety of host cellular machinery involved in vesicular trafficking, autophagy, and cell death were analyzed for transcriptional changes. Upstream autophagy machinery from the PI3K complex stood out as significantly upregulated. Single-cell RNA sequencing (scRNA-seq), western blotting, siRNA knockdowns, and use of inhibitors confirmed this upregulation and importance of the autophagy-specific PI3K complex for astrovirus replication.

This project has revealed the site of replication and a therapeutic target for astrovirus replication. In addition, we have supported the role of autophagy-specific PI3KC3 as a common positive strand ssRNA virus replication factor. We have also shown that PI3KC3 inhibition is effective for reduction of VA1 replication, as well, suggesting that the mechanism spans clades of astrovirus. This research will lead to new insights for astrovirus replication and novel opportunities for inhibition of replication.

2.4.3 Aim 3: Determine major differences in host cellular processes during astrovirus infection

Using single cell RNA sequencing on HAstV-1-infected Caco-2 cells, differences in major cellular pathways and gene expression were elucidated. Among dysregulated pathways of interest were lysosomal activity, endoplasmic reticulum (ER) stress, and cell cycle arrest. Lysosomal activity was further studied using flow cytometry and western blotting and showed no significant dysregulation of the pathway despite significant transcriptional differences.

ER stress was further explored using various inhibitors, confocal microscopy, electron microscopy, and western blotting. During astrovirus infection, ER fragments appear to rearrange and consolidate near the nucleus. Electron microscopy showed close association of ER fragments with double membrane vesicles, suggesting an origin for DMVs at the ER. In addition, nucleation promoting factor (NPF) WHAMM (WASP Homolog associated with Actin, Golgi Membranes and Microtubules) was significantly upregulated at the transcriptional and translational level. WHAMM has been previously associated with budding of autophagosomes from ER membranes, which could be a mechanism for DMV formation during viral replication. Use of ER stress inducer thapsigargin significantly reduced astrovirus staining, suggesting that the endoplasmic reticulum plays a role in viral replication. ER stress inhibitor ceapin had no effect on astrovirus replication, meaning that the ATF6 arm of the ER stress pathway is likely not responsible for this phenotype.

Lastly, single cell RNA sequencing data suggested a major disruption in the cell cycle at 24 hours post-infection (hpi) in astrovirus-infected Caco-2 cells compared to earlier time points of infection and mock controls. Further exploration of the dataset showed that the G2M checkpoint pathway was significantly downregulated at 24 hpi in infected cells, and

astrovirus-infected cells were transcriptionally accumulating in G1 phase. Bystander cells were not affected. To further explore this, immunoblotting was employed. Immunoblots showed a significant decrease in S and G2/M-associated proteins geminin and Cyclin A2 at 24 hpi in HAstV-1 samples compared to mock-inoculated samples. There was also a significant increase in CDK6, a kinase essential for G1 phase of the cell cycle, at 24 hpi in HastV-1 samples compared to mock-inoculated samples. Finally, a significant decrease in G1-associated Cyclin D1 indicates cell cycle arrest in G1 phase.

Astrovirus infection disrupts multiple elements of cellular homeostasis. The astrovirus infected cell is arrested in G1 phase, likely to prevent cell death. This surviving cell experiences ER membrane rearrangement and manipulation of the UPR, supporting activation of autophagy machinery required for replication. The autophagy machinery does not include changes in lysosomal activity which could disrupt astrovirus survival and exit from the cell (**Figure** 2.4).

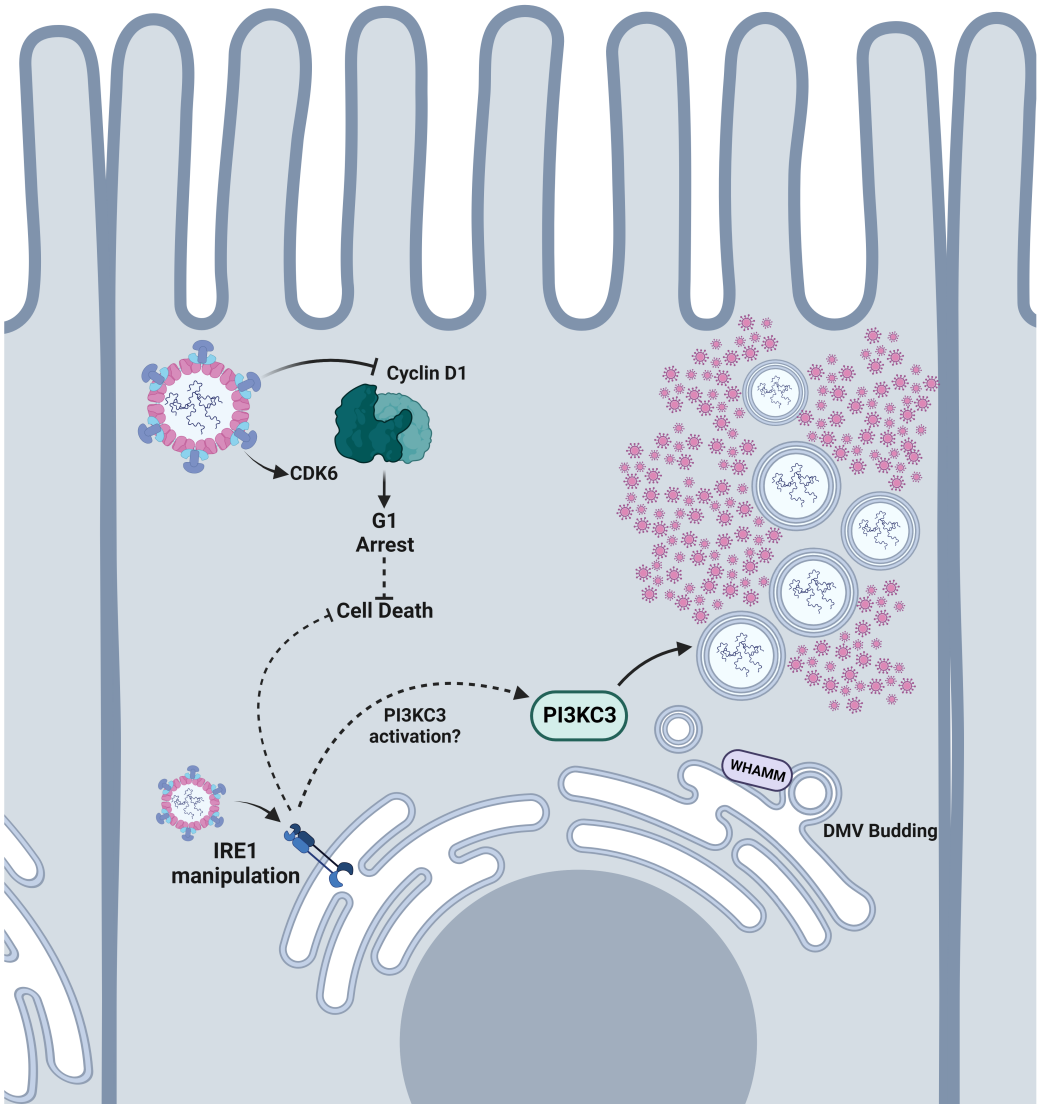

Figure 2.4: Astrovirus Modulation of Host Cellular Machinery. Representative schematic of astrovirus manipulation of host cellular machinery. We have determined that astrovirus infection induces PI3KC3-dependent formation of double membrane vesicle (DMV) replication organelles (ROs). These DMVs may bud from the endoplasmic reticulum (ER), and interference with the ER stress pathway affects astrovirus replication. Lastly, the cell cycle is arrested in G1 phase during astrovirus replication, which may also contribute to cellular survival.

Chapter 3

Discovery of the Replication Organelle for Human Astrovirus[1]

NOTE: This chapter refers frequently to content in **Appendix A**. When using Adobe Acrobat, after going there, return to the last viewed page using quick keys Alt/Ctrl+Left Arrow on PC or Command+Left Arrow on Mac. For the next page, use Alt/Ctrl or Command + Right Arrow. See **Preface** for further details.

3.1 Introduction

For information regarding cell and virus propagation, transmission electron microscopy (EM), RT2 Profiler, 10X single cell RNA sequencing, immunofluorescent staining, immunoblotting, RT- PCR, and Huh-7.5 RavZ doxycycline induction, please refer to the Materials and Methods section found in Appendix A.

3.2 Additional Methods

Transmission electron microscopy Caco-2 cells were plated in a six-well plate (3.5 × 10^5). After 48 h, appropriate samples were inoculated with supernatants taken from VA-1-infected (Multiplicity of infection (MOI) 10) Caco-2 cells in serum-free media for 1 h. Following virus adsorption, inoculum was replaced with fresh media. At 48 and 72 hpi, cells were fixed in 2.5% glutaraldehyde/2% paraformaldehyde (PFA) in 0.1 M Cacodylate Buffer.

293T cells were plated in a six-well plate (4 x 10^5). After 48 h, appropriate samples were inoculated with supernatants taken from human astrovirus serotype 1 (HAstV-1)-infected (MOI 10) or mock-inoculated Caco-2 cells in serum free media for 1 h. Following

[1]Reproduced with permission from the American Society of Microbiology. Theresa Bub et al. (2023). "Astrovirus replication is dependent on induction of double membrane vesicles through a PI3K-dependent, LC3-independent pathway". In: *Journal of Virology*. DOI: 10.1128/jvi.01025-23. URL: https://journals.asm.org/doi/10.1128/jvi.01025-23. (**Appendix A**).

virus adsorption, inoculum was replaced with fresh media. At 24 hpi, cells were fixed in 2.5% glutaraldehyde/2% paraformaldehyde (PFA) in 0.1 M Cacodylate Buffer.

Alternatively, 293T cells were transfected with HAstV-1-associated plasmids gifted to our laboratory by the Lennemann lab at University of Alabama at Birmingham. These plasmids are named ORF1ab, ORF1a, ORF1ab - protease, and ORF1a - protease. 293T cells were transfected using the Lipofectamine 2000 Reagent kit, per manufacturer's instructions, with 5 µg of each plasmid, Opti-MEM, and Lipofectamine 2000 Reagent in serum free media. At 24 hours post-transfection, cells were observed using the EVOS FL cell imaging system to confirm transfection through GFP expression. Once confirmed, cells were fixed in 2.5% glutaraldehyde/2% paraformaldehyde (PFA) in 0.1 M Cacodylate Buffer.

Following fixation, samples were post-fixed in osmium tetroxide and contrasted with aqueous uranyl acetate. Samples were dehydrated by an ascending series of ethanol to 100% followed by 100% propylene oxide. Samples were infiltrated with EmBed-812 and polymerized at 60°C. Embedded samples were sectioned at 70 nm on a Leica (Wetzlar, Germany) ultramicrotome and examined in a ThermoFisher Scientific (Hillsboro, OR) TF20 transmission electron microscope at 80 kV. Digital micrographs were captured with an Advanced Microscopy Techniques (Woburn, MA, USA) imaging system. Unless otherwise indicated, all reagents are from Electron Microscopy Sciences (Hatfield, PA, USA).

3.3 Double Membrane Vesicle Replication Organelles Form During HAstV-1 Infection in a PI3KC3-Dependent Manner

Electron microscopy (EM) showed that HAstV-1 infection induces formation of double-membrane vesicles (DMVs) at 24 hours post-infection (hpi), while mock-inoculated cells did not form DMVs in Caco-2 cells. DMVs continued to form at 36 hpi in HAstV-1-infected cells (**Figure** A.1a). Inoculation of Caco-2 cells with UV-inactivated HAstV-1 did not induce DMV formation, demonstrating that formation of DMVs is replication-dependent (**Figure** A.1b).

Previous research showed that phosphatidylinositol-3 kinase (PI3KC3) is necessary for severe acute respiratory syndrome coronavirus 2 (SARS-CoV-2) and hepatitis C virus (HCV) replication. One study also suggested that PI3K may be involved in astrovirus replication, although nonspecific inhibitors were utilized to demonstrate this. Therefore, we employed a specific PI3KC3 inhibitor, PIK-III, to determine whether the autophagy-specific complex was involved in astrovirus replication. Upon inhibition with PIK-III during infection, electron microscopy revealed a significant decrease in DMV formation (**Figure** A.2a), accompanied by a significant decrease in astrovirus capsid staining and double stranded RNA (dsRNA) replication intermediates in a dose-dependent manner at 24 hpi (**Figure** A.2b, SA.1a). We also observed a dose-dependent decrease in genome copies of astrovirus in cell supernatants and lysates from PIK-III-treated compared to DMSO control cells at 24 hpi (**Figure** A.2c). Finally, there was significantly less infectious virus

in cell supernatants of Caco-2 cells treated with PIK-III prior to infection, compared to DMSO-treated controls (**Figure** A.2d). To determine whether PIK-III affects VA-1 infection similarly, we infected Caco-2 cells with VA-1 and treated them with either PIK-III or DMSO. We again found a significant decrease in VA-1 infection in a dose-dependent manner in PIK-III-treated cells compared to DMSO controls (**Figure** SA.1b).

Next, to confirm the importance of the autophagy-specific PIK3C3 to astrovirus replication, we employed siRNA knockdown of Beclin, a PIK3C3 component. When Beclin was knocked down during infection, genome copies in cell lysates, capsid staining, and dsRNA staining were all significantly decreased compared to siRNA control (siControl) (**Figure** A.3a-d).

3.4 Additional Autophagy Machinery is Not Required for HAstV-1 Replication

Knowing that PI3KC3 is important for astrovirus replication and DMV formation, we sought to determine whether other autophagy machinery was necessary for astrovirus replication. Transcriptionally, only upstream components of the autophagy machinery were upregulated at 24 hpi in HAstV-1-infected compared to mock-inoculated Caco-2 cells. LC3 (microtubule-associated protein light chain 3) machinery was either unchanged or downregulated at 24 hpi in HAstV-1-infected cells, and immunoblotting confirmed no change in ATG5 or ATG7 protein expression (**Figure** A.4a-b). To confirm, we used an siRNA knockdown of ATG5 and found no change in lysate genome copies, capsid staining, or dsRNA staining during infection (**Figure** A.4c-d, SA.2a, , SA.2c-d). Finally, an Huh-7.5 cell line with doxycycline-inducible expression of RavZ was utilized to confirm this in a different cell line. RavZ is a protease that can specifically cleave LC3, disabling it from becoming conjugated to phosphatidylethanolamine (PE) and participating in autophagosome formation. We confirmed the cleavage activity of RavZ and found it made no difference in genome copies of astrovirus found in cells or supernatants during infection (**Figure** A.4e, SA.2b).

3.5 Single Cell RNA Sequencing in HAstV-1 and MuAstV Infection

Single cell RNA sequencing (scRNA-seq) was utilized to determine whether changes in autophagy machinery occurred in infected or bystander cells during HAstV-1 infection of Caco-2 cells (**Figure** A.5a, SA.3, Table 1). We found that only infected cells showed an upregulation of PIK3C3-associated genes, while bystander cells downregulated these genes (**Figure A.5c**). To address whether these changes in autophagy machinery span different species, we utilized a scRNA-seq dataset previously obtained in our laboratory for mice

infected with murine astrovirus (MuAstV). Again, PI3KC3 was only upregulated in infected, not bystander cells in mice (**Figure** A.5d).

3.6 VA-1 Replication Organelles

As shown in our publication, PIK-III successfully inhibits both HAstV-1 and VA-1 replication. To determine whether VA-1 also forms DMVs during replication, we infected Caco-2 cells with VA-1 for 48, 72, or 96 hours and performed electron microscopy. To our surprise, well-defined DMVs were not observed during VA-1 infection. However, double-membrane structures resided close by to virions. Qualitatively, there were far fewer membranous structures around VA-1 virions compared to HAstV-1. This indicates that although PIK-III reduces formation of DMV replication organelles during HAstV-1 infection, PIK-III may also target phosphatidylinositol 3-phosphate (PI3P)-containing membranes other than DMVs during viral replication (**Figure** 3.1).

3.7 Determination of Viral Components Involved in DMV Formation During Infection

To begin to understand which parts of the astrovirus genome are essential for DMV formation, we first infected or inoculated 293T cells with HAstV-1 or mock control respectively for 24 hours to determine whether DMVs form in 293T cells during astrovirus infection. We also transfected 293T cells with ORF1ab, ORF1a, or ORF1 plasmids containing a mutation in the protease domain, disabling protease activity. These samples were submitted for electron microscopy. Representative images showed that HAstV-1-infected 293T cells produce DMVs associated with HAstV-1 virions similarly to Caco-2 cells. Mock-inoculated cells do not produce DMVs. Each of the plasmids did not induce DMV formation (**Figure** 3.2).

3.8 Discussion

Our work demonstrates that the replication organelle for HAstV-1 is a double-membrane vesicle. DMVs form during HAstV-1 infection in Caco-2 cells in a replication-dependent manner and require PI3KC3 machinery for formation. DMVs do not require LC3 conjugation machinery for formation despite this being a key component of autophagosome formation. Formation of DMVs and upregulation of PI3KC3 machinery only occurs in HAstV-1-infected and not bystander cells. These data closely mimic findings for SARS-CoV-2 and HCV, positive sense single stranded RNA viruses that also utilize PI3KC3 but not LC3 to form DMV replication organelles. Despite the major differences between these viruses, HAstV-1, SARS-CoV-2, and HCV use similar strategies to support their replication by manipulating host cellular machinery and repurposing it for replication organelle formation. This suggests that targeting PI3KC3 machinery could be a broad therapeutic option utilized to interrupt infection with positive sense RNA viruses, regardless of their pathogenic differences.

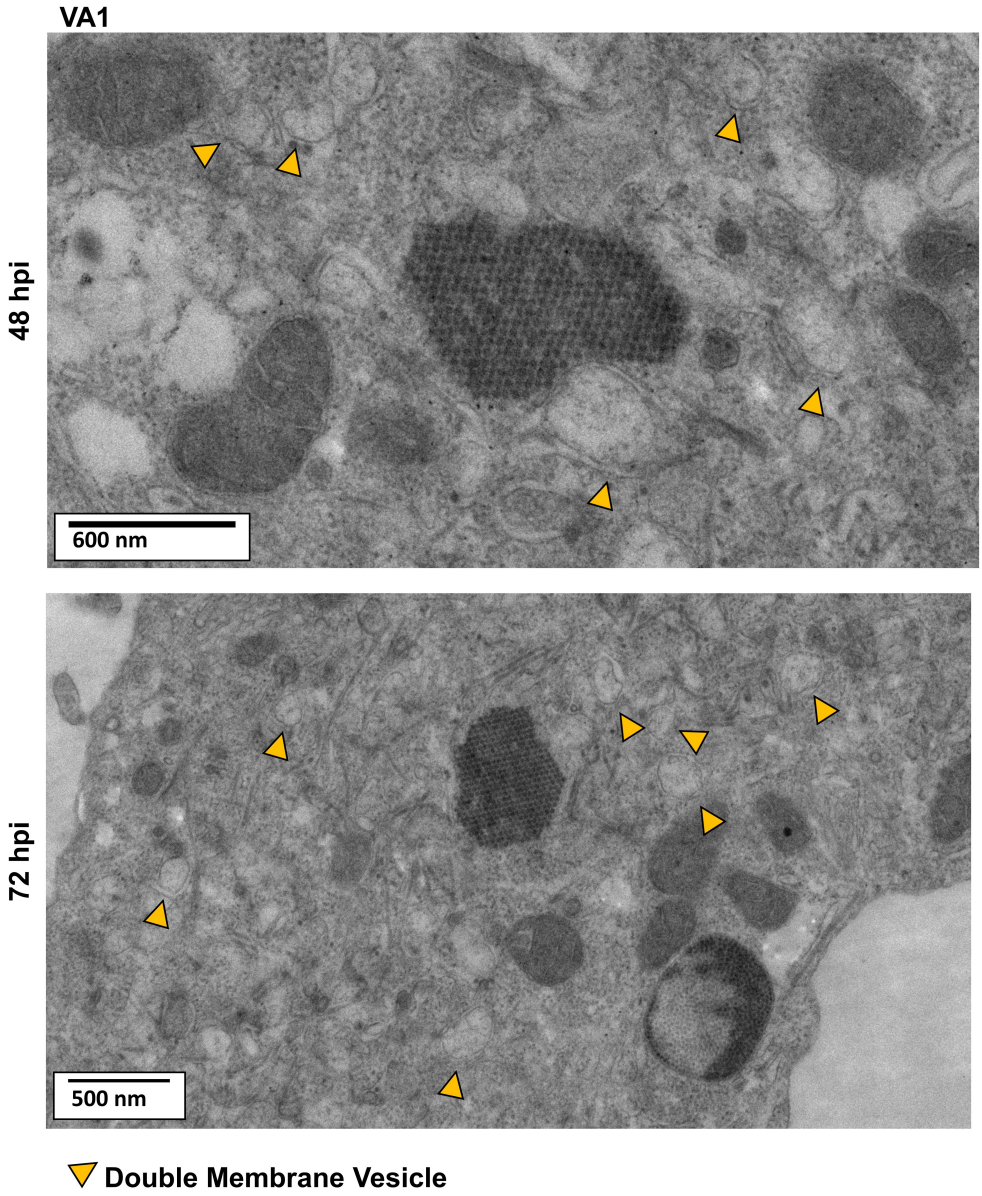

Figure 3.1: Astrovirus VA-1 Replication Organelles. Electron microscopy (EM) shows clusters of VA-1 virions in Caco-2 cells infected with VA-1 for 48 or 72 hours. Double membrane vesicles (DMVs) are noted with arrows.

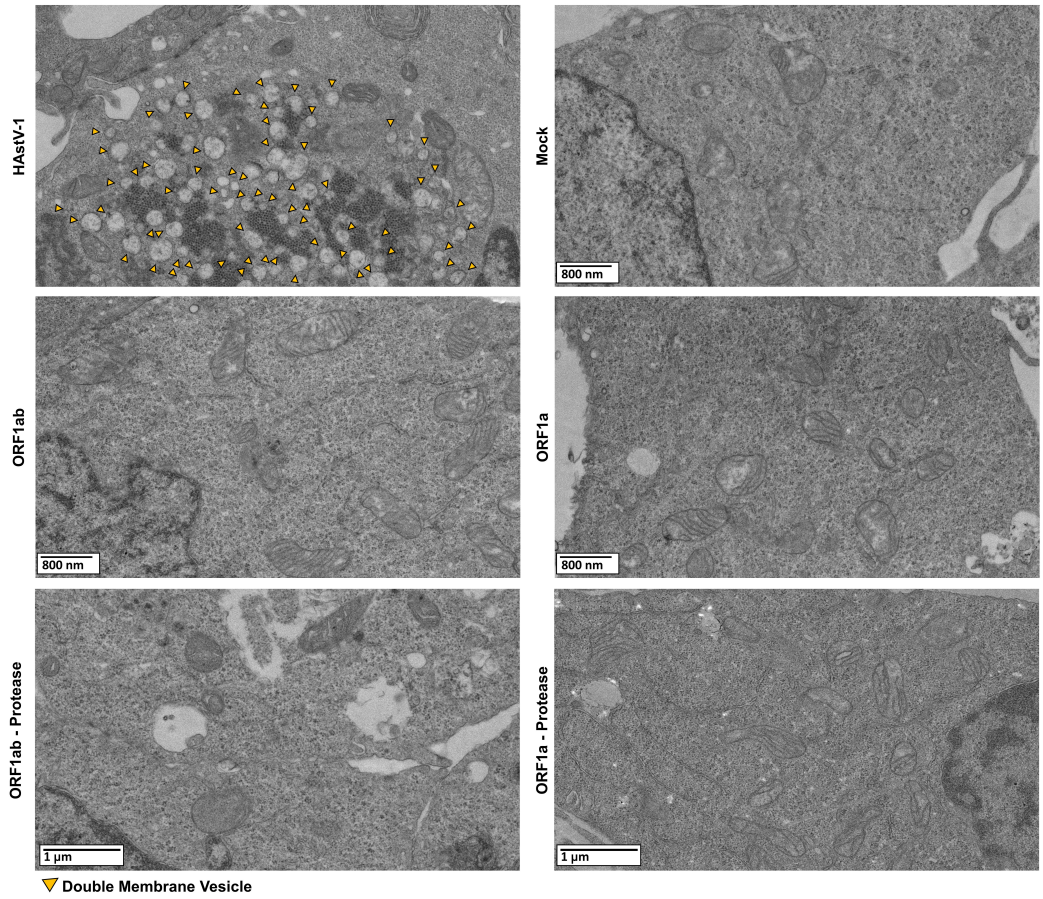

Figure 3.2: Astrovirus-Induced DMVs in 293T Cells. Electron microscopy (EM) shows that HAstV-1 infection induces double membrane vesicle (DMV) formation in 293T cells, but not mock-inoculated cells. 293T cells transfected with ORF1ab, ORF1a, or ORF1ab and ORF1a with a mutation in the protease domain also did not show DMV formation.

VA-1 infection is also significantly reduced by inhibition of the PI3KC3 complex, although replication organelles for VA-1 did not closely resemble DMVs observed in HAstV-1-infected Caco-2 cells by electron microscopy. Given the role of PI3KC3 in general formation of PtdIns3P, it is possible that this membrane component could be required for different types of replication organelle formation. It will be beneficial to determine whether PI3KC3 is activated through canonical upstream autophagy machinery such as activation of the ULK1 complex during astrovirus infection. If PI3KC3 is activated through a canonical mechanism, more therapeutic targets may be utilized in interruption of DMV or RO formation during HAstV-1 or VA-1 infection. Given that an upregulation of AMPK (Adenosine Monophosphate-Activated Protein Kinase)-associated gene PRKAA1 was observed during HAstV-1 infection of Caco-2 cells, it is possible that AMPK activates ULK1, leading to activation of PI3KC3 through canonical autophagy-associated mechanisms. However, if activation of PI3KC3 is independent of AMPK and ULK1 machinery, novel targets may be identified for interference with PI3KC3 complex activation. This could have implications for other diseases during which PI3KC3-dependent canonical and alternative autophagy pathways are upregulated.

Regardless of RO membrane arrangement, the fact that inhibition of PI3KC3 is a strain-spanning tactic for reduction of astrovirus infection suggests that despite differences among astrovirus strains, a common therapeutic target may be possible for astrovirus infection. Not only is PI3KC3 important for human astrovirus strains, but our data also suggest that murine astrovirus (MuAstV) infection may follow a similar pattern. PI3KC3 is upregulated in infected, but not bystander cells during MuAstV infection. This suggests that although human astrovirus infection is phenotypically unique from MuAstV infection, a common replication mechanism may also span species of astrovirus.

Finally, we showed that 293T cells infected with HAstV-1 also produce DMVs. When we transfected 293T cells with plasmids to produce ORF1ab, ORF1a, or ORF1ab and ORF1a mutants lacking protease, we found that none of these induced DMV formation. This does not necessarily mean that ORF1a and ORF1ab do not induce DMV formation. Because we have found that DMVs form in a replication-dependent manner in Caco-2 cells, it may be necessary to produce infectious astrovirus mutants to address the involvement of each part of the astrovirus genome in DMV formation.

Chapter 4

Disruption of Host Cellular Processes by Astrovirus

4.1 Introduction

Upon infection with a virus, it is inevitable that a host cell's machinery will be disrupted in a variety of ways. Host cellular machinery has evolved to fight viral infection through unique mechanisms, including upregulating degradation pathways like autophagy and modulating endoplasmic reticulum (ER) stress-associated pathways that might benefit viral replication. Not only this, but cells may attempt to disrupt viral replication by modulating cell cycle response during infection. However, just as host cells have responded successfully to lessen viral replication, viruses have evolved to evade such responses for their own survival.

Although autophagy machinery can be upregulated to promote viral degradation, we have shown that astrovirus upregulates only portions of the canonical autophagy pathway to promote its own replication in double membrane vesicles (DMVs). Some viruses can be degraded by autophagosomal delivery to the lysosome, thwarting their viral life cycle. Yet some others can disrupt lysosomal activity to avoid this fate. Here, we investigate whether lysosomal activity is affected by astrovirus infection.

Further, we have attempted to discern the origins of astrovirus-induced DMVs to determine whether other organelles and cellular pathways are involved in or necessary for viral replication. In the process, we have found that similarly to other positive sense RNA viruses, astrovirus DMVs may originate from the ER. It is also possible that astrovirus infection disrupts unfolded protein response (UPR) homeostasis and affects ER stress, similarly to other viruses.

Lastly, many viruses disrupt cell cycle progression to benefit replication. Our data show that astrovirus arrests cells in G1 phase. This could be a mechanism employed to support replication or to disrupt cell death pathways.

4.2 Methods

4.2.1 Immunoblotting

Caco-2 cells were plated in a six-well plate (3.5×10^5). At 48 h post-plating, cells were inoculated with supernatants taken from human astrovirus serotype 1 (HAstV-1) (Multiplicity of Infection (MOI) 10) or mock-inoculated Caco-2 cells in serum-free media for 1 h. Following virus adsorption, inoculum was replaced with fresh media. At the proper time point, 0, 4, 8, or 24 hpi, cells were collected in 250 µL radioimmunoprecipitation assay (RIPA) lysis buffer (Abcam) containing 1× protease inhibitor cocktail (Pierce) on ice. Samples were vortexed briefly and kept on ice for 30 min. Samples were frozen at –80°C until used. Sample protein concentration was determined using BCA Protein Assay Kit (Pierce). Equal concentrations of protein were prepared under reducing conditions and separated by sodium dodecyl sulfate-polyacrylamide gel electrophoresis (4%–20% tris-glycine 1.0 mm Mini Protein Gels from Invitrogen (XP04200BOX). Gels were transferred to polyvinylidene fluoride (PVDF) membranes using the iBlot 2 transfer stacks (ThermoFisher IB24002). Membranes were probed for protein with respective primary antibodies and IRDye 680RD goat anti-rabbit IgG secondary antibody using the ThermoFisher iBind device according to manufacturer's instructions. Primary antibodies included β-Actin (Cell Signaling 4970S) at 1:1,000, Cathepsin D (CTSD) (Abcam ab72915) at 1:1,000, WHAMM (Abcam ab122572) at 1:1000, Geminin (Abcam ab195047) at 1:1,000, Cyclin-Dependent Kinase 6 (CDK6) (Abcam ab124821) at 1:1,000, Cyclin D1 (Abcam ab134175) at 1:1,000, Cyclin A2 (Abcam ab211735) at 1:1,000, Rb (Abcam ab181616) at 1:1,000, p-Rb (Abcam ab47474) at 1:1,000.

4.2.2 Flow cytometry

Caco-2 cells were plated in a six-well plate (3.5×10^5). At 24 h post-plating, cell media was replaced with serum free media. At 48 h post-plating, 24-hour infection or inoculation cells were inoculated with supernatants taken from HAstV-1-infected (MOI 10) or mock-inoculated Caco-2 cells in serum-free media for 1 h. Following virus adsorption, inoculum was replaced with fresh media. At this point, control cells in starvation groups were treated with serum-free media, or rapamycin control cells were treated with 500nM rapamycin. At 72 h post-plating, 1 hour infection or inoculation cells were inoculated with supernatants from HAstV-1-infected (MOI 10) or mock-inoculated Caco-2 cells in serum free media for 1h. Following virus adsorption, inoculum was removed and cells from all groups were collected by scraping in 2% FBS/PBS (FACS Buffer). Cells were centrifuged at 250xg for 5 minutes at 4°C. Samples were resuspended in FACS Buffer.

LAMP1 staining

Cells stained for lysosomal associated membrane protein 1 (LAMP1) were then blocked in human FC block on ice for 10 minutes at 4°C (Biolegend 422301, 1:300 in FACS Buffer). Cells were washed in 300 µL FACS buffer. Cells were then stained with Zombie Aque

Fixable Viability Kit (Biolegend 423102, 1:100 in PBS) for 15 minutes at 4°C in the dark. Cells were washed in 300 µL FACS buffer. Cells were then fixed and permeabilized using the BD Biosciences Cytofix/Cytoperm Kit solution (554714, 250 µL per sample) for 40 minutes at 4°C. Cells were washed in 300 µL cytoperm buffer. Finally, LAMP1-APC antibody was diluted in cytoperm wash, and cells were incubated in LAMP1 buffer for 1 hour in the dark at 4°C (BioLegend 328620, 1:100 in cytoperm wash). Cells were washed in 300 µL cytoperm buffer. Finally, cells were resuspended in 300 µL FACS buffer for flow cytometry analysis and kept in the dark at 4°C until use.

CTSB enzymatic activity kit

Cells stained for cathepsin B (CTSB) activity (BioRad ICT9151) were transferred into 490 µL of cellular assay buffer. R110-$(RR)_2$ solution was prepared per manufacturer's instructions. 10 µL of the staining solution was added to each cell sample. Cells were incubated for 60 minutes at 37°C, avoiding light. Cells were resuspended every 20 minutes. Cells were washed in FACS buffer and stained with Zombie Aque Fixable Viability Kit (Biolegend 423102, 1:100 in PBS) for 15 minutes at 4°C in the dark.

Flow cytometry analysis

Samples were analyzed using a 17-color LSR Fortessa (4 lasers) and DiVa software. Single color stains were used to set parameters for each channel, and isotype controls were tested. 10,000 events were collected per sample. Samples were analyzed using FlowJo v10 software. Cells were gated by singlets, followed by viable cells, followed by either LAMP1 positive or CTSB positive cells, depending on the experiment. Cell frequency and mean fluorescence intensity were calculated. Plots were made using GraphPad Prism v9.

4.2.3 10x single cell RNA sequencing and analysis

For information of single cell RNA sequencing and analysis, visit **Appendix A**.

4.2.4 Confocal microscopy

Confocal microscopy images were acquired with the help of Dr. George Campbell at the Cell and Tissue Imaging Center which is supported by SJCRH and NCI P30 CA021765. Caco-2 cells were plated on ibidi µ-Slide 8 Well high Polymer chamber slides at a density of 4×10^4 cells per well. At 48 hours post-plating, cells were inoculated with supernatants taken from HAstV-1-infected (MOI 10) or mock-inoculated Caco-2 cells in serum free media for 1 hour. Following virus adsportion, inoculum was replaced with fresh media. At 24 hpi, cells were fixed in 4% paraformaldehyde (PFA) in PBS at room temperature for 20 minutes. Cells were washed in PBS. Next, 0.1% Triton X in PBS was utilized to permeabilize the cells for 15 minutes at room temperature. Cells were washed in PBS and blocked in 5% normal goat serum (NGS) in PBS for 1 hour at room temperature. Cells were washed in

PBS, and antibodies were diluted in 1% NGS/PBS. Primary antibodies included Calnexin (Invitrogen PA5-34754) at 1:1000 and J2 (SciCons 10010500) at 1:100. Cells were incubated in antibody solution overnight at 4°C. The next day, samples were washed in PBS. Cells were incubated in secondary antibody solution for 45 minutes in the dark. Secondary antibodies included Alexa Fluor 488 goat anti-Rabbit (Invitrogen A11008) at 1:1000, Alexa Fluor 555 goat anti-Mouse (Invitrogen A21422) at 1:1000, and Hoechst (ThermoFisher H3569), 1:2000 in 1% NGS/PBS. Cells were again washed in PBS, and samples were finally fixed in Prolong Gold Antifade Mountant (Invitrogen). Prepared samples were imaged on a Zeiss LSM 780 Observer.Z1 using a Plan Apochromat 63X/1.4 objective lens. A 1024 x 1024 pixel array, final pixel size of 88nm, and pixel dwell time of 1.27 µs was used. Based on the green channel, a 1 AU pinhole size was selected. For each channel, the gain was set to 500. A 405nm diode laser was utilized for Hoechst fluorescence, and 410-495 nm light was detected using an alkali PMT. A 488 nm multi-line Argon laser was utilized for Alexa Fluor 488 fluorescence, and 499-579 nm light was detected using a GaAsP PMT. Finally, a 561 nm DPSS laser was utilized for Alexa Fluor 555 fluorescence, and 588-712 nm light was detected using an alkali PMT. Acquisition was completed using Zen Black 2012 SP 5 (14.0.28.201).

4.2.5 ER stress inhibition experiments

Caco-2 cells were plated in a 96-well plate (2.5 x 10^4). At 48 hours post-plating, cells were inoculated with supernatants taken from HAstV-1-infected (MOI 10) or mock-inoculated Caco-2 cells in serum free media for 1 hour. Following virus adsportion, the inoculum was replaced with fresh media or media containing 1 µg thapsigargin (thermofisher, T7458), ceapin-A7 (Millipore Sigma, SML2330-5MG), or DMSO control. At 24 hpi, cells were fixed in 100% methanol. Cells were washed in PBS and incubated in primary antibody solution containing astrovirus capsid monoclonal antibody 8e7 (Invitrogen MA5-16293) at 1:100 or J2 (SciCons 10010500) at 1:100 in 1% NGS/PBS for 1 hour at room temperature. Cells were washed in PBS. Cells were incubated in secondary antibody solution containing Alexa Fluor 488 goat anti-Mouse (Invitrogen A10680) at 1:1000 and and Hoechst (ThermoFisher H3569) at 1:2000 in 1% NGS/PBS for 45 minutes in the dark. Cells were again washed in PBS. Samples were imaged using the EVOS FL cell imaging system and analyzed using ImageJ 2.9.0/1.53t software. Focus-forming units (FFU) were calculated as previously described (S. Marvin, V. Meliopoulos, and S. Schultz-Cherry, 2014).

4.2.6 Statistical analysis

Data were analyzed by two-way ANOVA followed by Tukey's multiple comparisons test (western blots, flow cytometry, ER Stress FFU calculations, cell count and viability calculations) to determine statistical significance using GraphPad Prism version 9. Asterisks show statistical significance as follows: *, $P \leq 0.05$; **, $P \leq 0.01$; ***, $P \leq 0.001$; ****, $P \leq 0.0001$.

4.3 Astrovirus Disrupts Lysosomal Enzyme Processing, but Not Lysosomal Function During Replication

As previously reported, we used an RT2 Profiler array to assess differences in vesicular trafficking, autophagy, lysosome, and cell death-related genes during astrovirus infection. During this initial screen, we found that lysosomal enzymes CTSD and CTSB were significantly downregulated at 24 hours post infection (hpi) in HAstV-1 compared to Mock samples (**Figure** A.4a). This was supported by our single cell RNA sequencing (scRNA-seq) dataset in HAstV-1-infected Caco-2 cells, but not bystander or mock-inoculated cells (**Figure** A.5c).

To determine whether lysosomal enzymes were disrupted at the translational level, we used immunoblotting for CTSD during infection. At 24 hpi, prepro-CTSD and pro-CTSD were significantly downregulated in HAstV-1 compared to mock cell lysates. The mature form of CTSD was trending toward a reduction in HAstV-1 lysates compared to mock at 24 hpi, but did not reach significance (**Figure** 4.1a,c). To assess whether these differences were replication dependent, Caco-2 cells were inoculated with UV-inactive HAstV-1. In UV-inactive lysates, there was no change in any form of CTSD compared to replicating HAstV-1 lysates, suggesting that the disruption in CTSD processing is unique to cells infected with replicating astrovirus (**Figure** 4.1b,d).

Electron microscopy (EM) data was inconclusive regarding the amount of lysosomes in infected cells (**Figure** A.1a). To determine whether there are fewer lysosomes in astrovirus-infected cells compared to mock-inoculated lysates, we infected Caco-2 cells with HAstV-1 at an MOI of 10 or mock-inoculated cells. At 1 hpi and 24 hpi, cells were fixed and stained with lysosomal marker LAMP1 for flow cytometry. Caco-2 cells treated with rapamycin or starved for 24 hours were used as positive controls. Flow cytometry data showed an increase in LAMP1-expressing cells at 24 hpi in astrovirus compared to mock controls. However, there was no difference in LAMP1 MFI (mean fluorescence intensity) per cell (**Figure** 4.2a).

To assess whether there is a difference in lysosomal activity during infection, we employed a CTSB enzymatic activity kit for flow cytometry. Results demonstrated that HAstV-1-infected cells showed no difference in lysosomal activity compared to mock-inoculated cells at 1 hpi or 24 hpi (**Figure** 4.2b).

Altogether, these data suggest that although there is a disruption in enzymatic processing of CTSD during infection, astrovirus does not affect the amount or activity of lysosomes in infected cells. Although lysosomes are not disrupted, there is thus far no evidence of degradation of astrovirus particles by lysosomes during infection, suggesting that it may not be necessary for astrovirus to evade degradation by disrupting lysosomal activity.

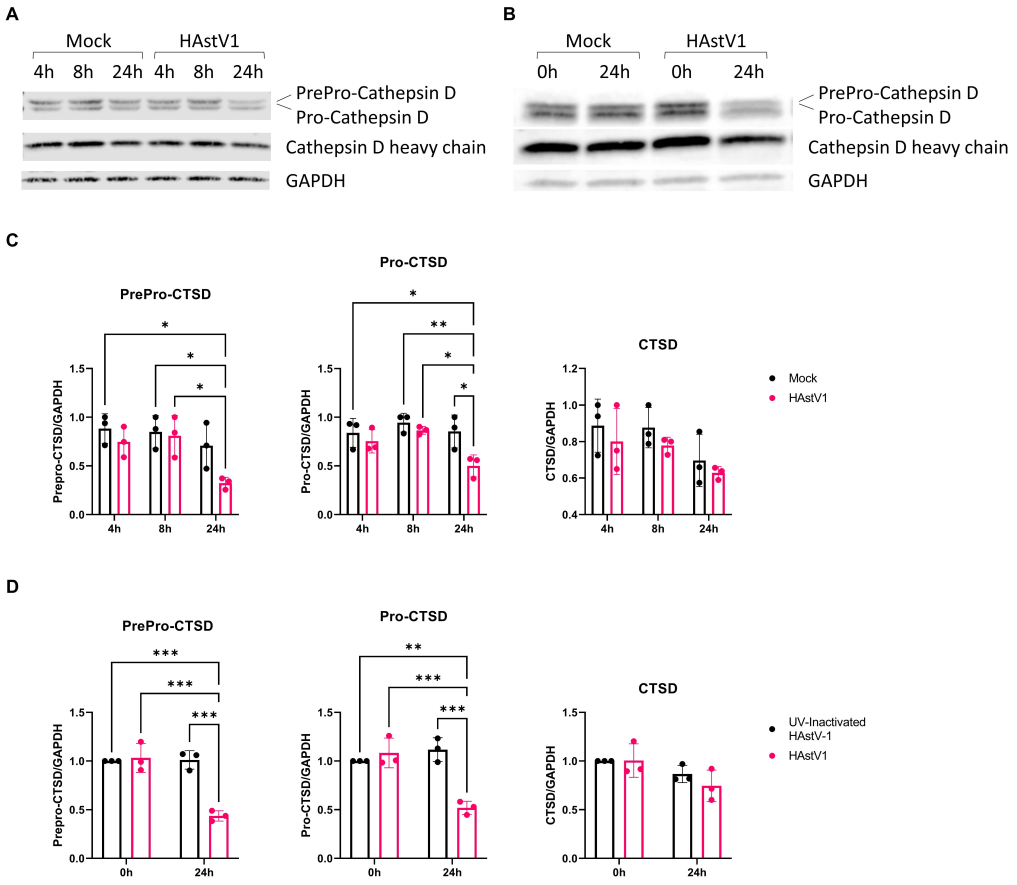

Figure 4.1: Lysosomal Enzyme Dysregulation During Astrovirus Infection. A,C. Immunoblots and quantification showing protein expression of lysosomal enzyme CTSD during astrovirus infection. B,D. Immunoblots and quantification showing protein expression of lysosomal enzyme CTSD during astrovirus infection or UV-inactivated astrovirus inoculation.

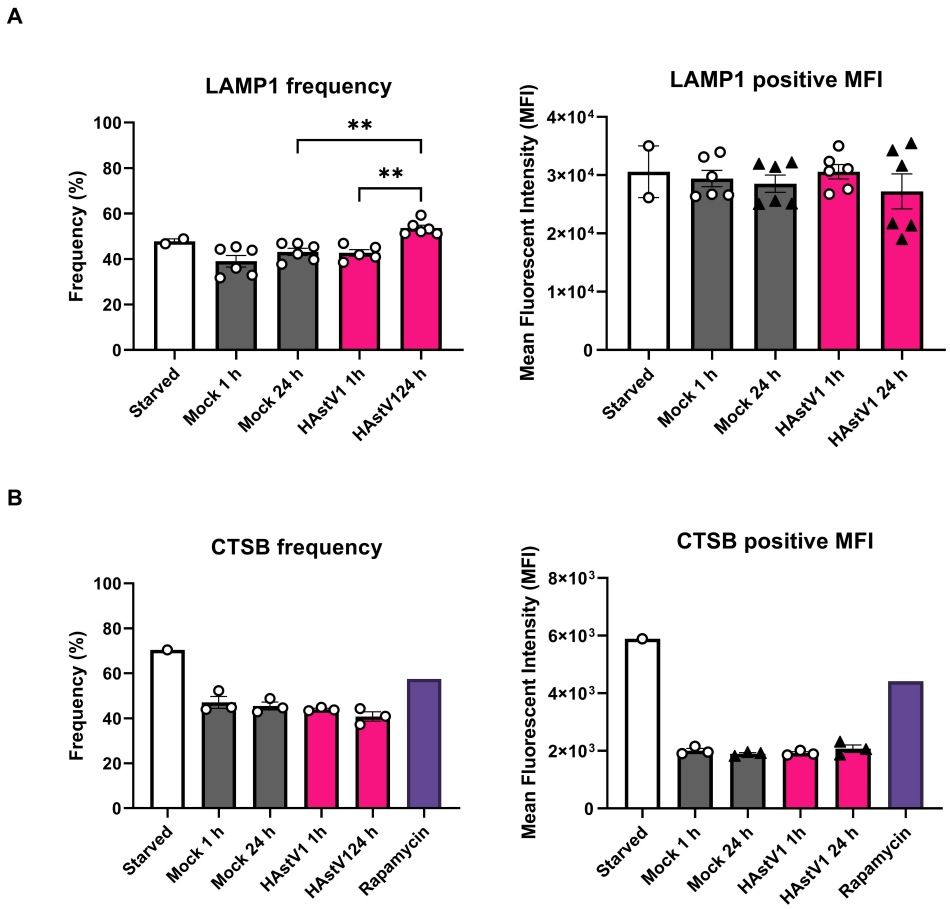

Figure 4.2: Lysosomal Quantity and Activity During Astrovirus Infection. A. Frequency and mean fluorescence intensity of LAMP1 lysosomal marker during astrovirus infection compared to mock inoculation or starvation positive control. B. Lysosomal enzyme CTSB activity frequency and mean fluorescence intensity during astrovirus infection compared to mock inoculation or starvation and rapamycin positive controls.

4.4 Dysregulation of Endoplasmic Reticulum Structure and Function During Astrovirus Infection

DMVs can originate from the ER during viral infection. To determine whether any ER-associated genes were dysregulated during astrovirus infection, we utilized our scRNA-seq dataset. We found that WHAMM (WASP homolog associated with actin, Golgi membranes and microtubules) was significantly upregulated in HAstV-1-infected Caco-2 cells at 24 hpi, compared to all other samples (**Figure** 4.3a-b). WHAMM is a nucleation promoting factor (NPF). A study demonstrated that WHAMM participates in phagophore budding from ER membranes during canonical autophagy (Kast and Dominguez, 2015). Therefore, we used immunoblotting to determine whether WHAMM protein is upregulated during infection. We infected Caco-2 cells with HAstV-1 or mock inoculated the cells for 8h and 24h. We collected lysates and blotted for WHAMM. We found that WHAMM significantly increased at 24 hpi in HAstV-1-infected, but not mock-inoculated Caco-2 cells (**Figure** 4.3c).

In observing previous electron microscopy data, we found that DMVs associated closely with ER fragments at 24 hpi in Caco-2 cells (**Figure** 4.3d). This prompted us to utilize confocal microscopy staining of calnexin to determine whether the ER associates with astrovirus double stranded RNA (dsRNA) intermediates during infection. We found that astrovirus-infected Caco-2 cells, but not bystanders, experienced a rearrangement of ER membranes. Calnexin staining became dense and closely associated with astrovirus dsRNA in infected cells, but remained diffuse in bystander cells (**Figure** 4.3e).

Calnexin is also a known marker of ER stress. Due to the role of ER stress in positive sense viral infections, we decided to explore whether the UPR is changed during astrovirus infection. Our scRNA-seq dataset provided evidence that the UPR was significantly downregulated in infected cells (**Figure** 4.4d). To gather more specific detail on which arms of the UPR may be affected, we investigated specific ER stress-associated genes. XBP1 was upregulated transcriptionally at 24 hpi and in HAstV-1-infected, but not bystander or mock-inoculated cells. This suggests involvement of the IRE1 (inositol-requiring enzyme 1) arm of the UPR during infection. ATF4 was slightly upregulated, indicating a potential activation of PERK (PKR-like endoplasmic reticulum kinase), and ATF6 (Activating Transcription Factor 6) was not changed (**Figure** 4.4a-b). When examining the 24 hour time point alone, ATF4 was downregulated in HAstV-1-infected cells (**Figure** 4.4c).

To further explore this, we treated Caco-2 cells with thapsigargin, an ER stress activator, or ceapin A7, an ATF6 inhibitor, to determine whether either would affect astrovirus replication. Ceapin had no effect on capsid or dsRNA expression during HAstV-1 infection. However, thapsigargin significantly reduced both capsid and dsRNA staining at 24 hpi in HAstV-1- infected cells. This suggests that broad activation of ER stress pathways negatively regulates astrovirus replication (**Figure** 4.5a-b). Importantly, there was no difference in cell viability with thapsigargin treatment compared to DMSO control. Interestingly, the viability of ceapin-treated HAstV-1-infected cells was lower than viability of ceapin-treated

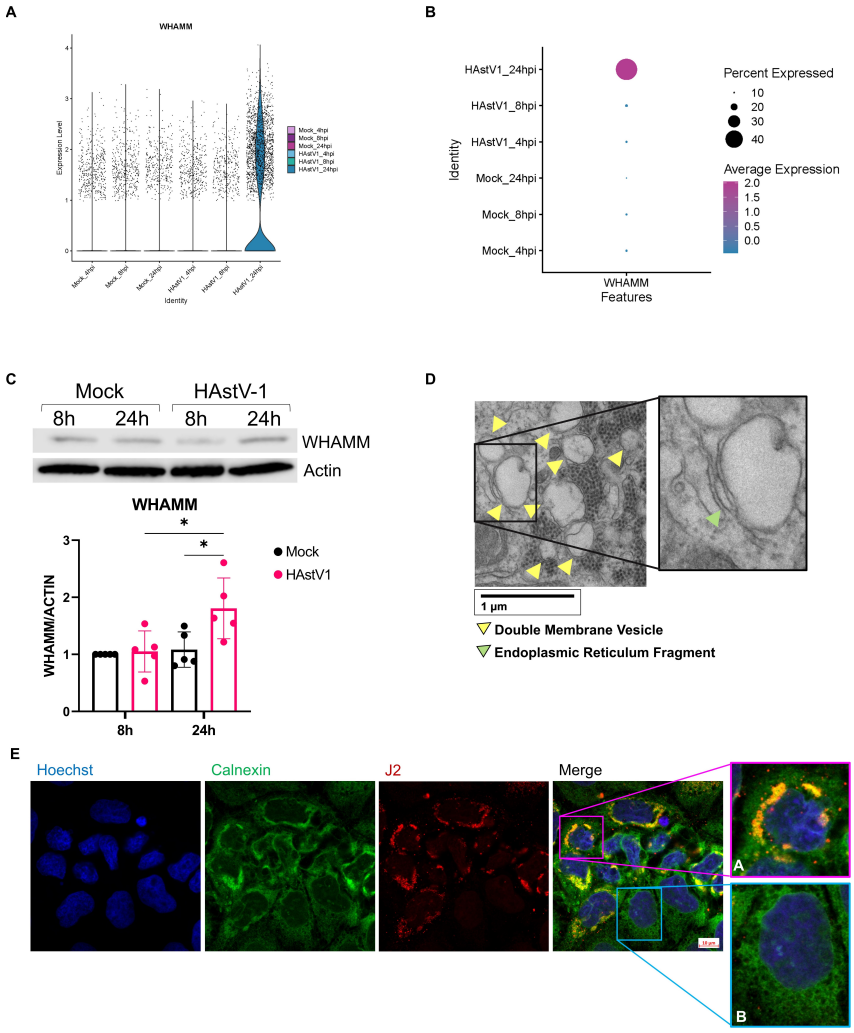

Figure 4.3: Endoplasmic Reticulum Dysregulation During Astrovirus Infection. A-B. Violin plot and dot plot showing expression of WHAMM over the course of astrovirus infection or mock inoculation in Caco-2 cells using single cell RNA sequencing. C. Immunoblot and quantification showing protein expression of WHAMM throughout astrovirus infection or mock inoculation in Caco-2 cells. D. Representative electron microscopy image showing endoplasmic reticulum (ER) fragment-associated double membrane vesicle. E. Representative confocal microscopy image showing calnexin ER marker and J2 astrovirus double stranded RNA intermediate marker at 24 hours post-infection in Caco-2 cells.

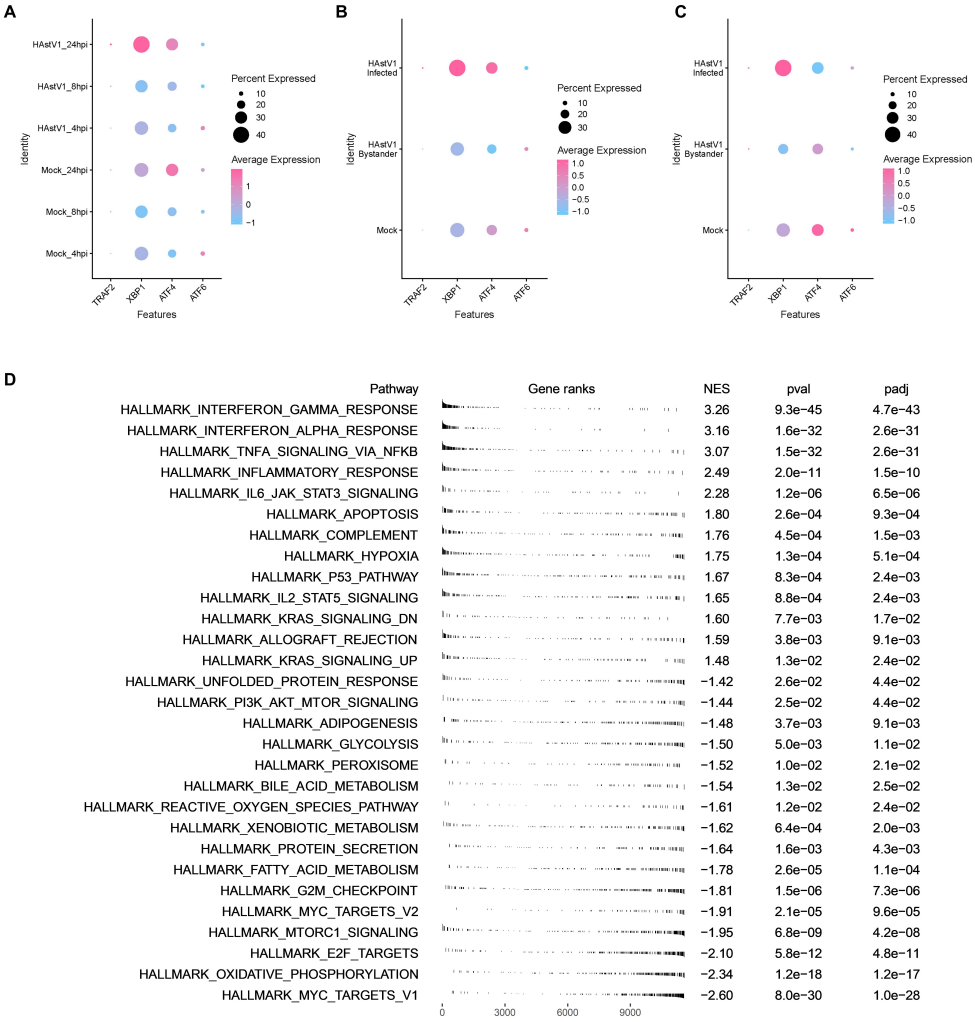

Figure 4.4: Endoplasmic Reticulum Stress Single Cell RNA Sequencing Data During Astrovirus Infection. A. Dot plot showing expression of endoplasmic reticulum (ER) stress markers throughout astrovirus infection or mock inoculation using single cell RNA sequencing (scRNA-seq). B. Dot plot showing expression of ER stress markers in astrovirus-infected, bystander, and mock-inoculated cells using scRNA-seq. C. Dot plot showing expression of ER stress markers at 24 hpi in astrovirus-infected, bystander, and mock-inoculated cells using scRNA-seq. D. Upregulated and downregulated pathways in an astrovirus-infected scRNA-seq cluster compared to uninfected clusters using Hallmark pathway analysis.

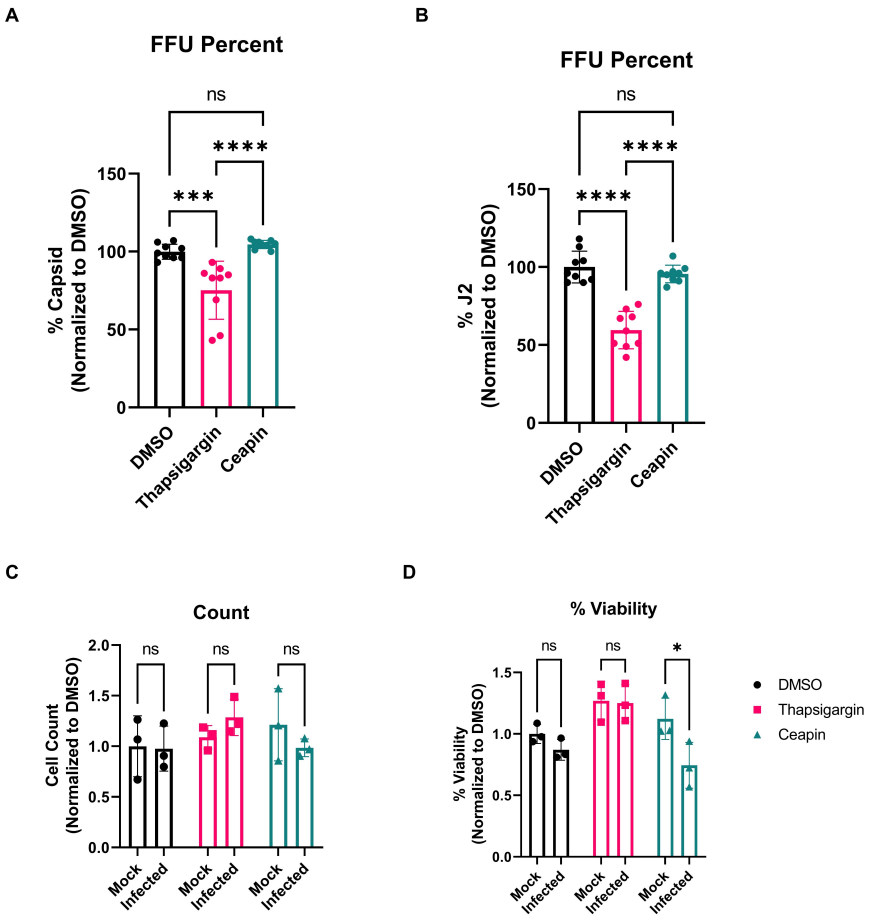

Figure 4.5: Endoplasmic Reticulum Stress Manipulation During Astrovirus Infection. A. Quantification of astrovirus capsid-expressing Caco-2 cells at 24 hours post-infection (hpi) after treatment with thapsigargin, ceapin, or DMSO control. B. Quantification of astrovirus double stranded RNA intermediate (J2) expressing Caco-2 cells at 24 hours post-infection (hpi) after treatment with thapsigargin, ceapin, or DMSO control. C. Cell count in DMSO, thapsigargin, or ceapin-treated Caco-2 cells at 24 hours post-treatment. D. Cell viability in DMSO, thapsigargin, or ceapin-treated Caco-2 cells at 24 hours post-treatment.

mock-inoculated cells. However, there was no difference in ceapin-treated cell viability compared to DMSO controls (**Figure** 4.5c-d).

4.5 Astrovirus Arrests Cells in G1 Phase of the Cell Cycle

Viral infection can lead to disruption of the cell cycle. To determine whether astrovirus is capable of regulating the cell cycle during infection, we utilized our scRNA-seq dataset. HAstV-1-infected cells, but not bystander or mock-inoculated cells, were primarily in Gap 1 (G1) phase, according to the transcriptional data (**Figure** 4.6a-b). Interestingly, using differential expression analysis, we found that the Gap 2/Mitosis (G2M) checkpoint is significantly downregulated in infected cells compared to bystander cells, indicating a dysregulation in the cell cycle (**Figure** 4.6c).

We further explored the scRNA-seq data for more specific analysis. Cyclins D1, D2, E1, E2, B1, B2, as well as CDK4, 2, and 1 genes were downregulated in HAstV-1-infected cells compared to mock-inoculated cells at 24 hpi (**Figure** 4.7a). Cyclins D1, D2, E1, B1, B2, as well as CDK4, 6, 2, and 1 genes were downregulated in HAstV-1-infected cells compared to bystander and mock-inoculated cells, as well (**Figure** 4.7b). This suggests reduced cell cycle progression from G1 and G2/M phases. Cell cycle-associated genes RB1, E2F1, E2F2, E2F3, BUB1, BUB1B, BUB3, ABL1, ANAPC1, ANAPC10, ANAPC11, ANAPC2, ANAPC4, ANAPC5, ANAPC7, ATM, and ATR were all downregulated in HAstV-1-infected compared to mock-inoculated cells at 24hpi, as well as in HAstV-1-infected compared to bystander and mock-inoculated cells (**Figure** 4.7c-d). RB1 hyperphosphorylation is required for progression from G1 to S (synthesis) phase. E2F genes are necessary for deoxyribonucleic acid (DNA) repair and progression through S phase. BUB and ANAPC genes are associated with mitosis progression. Finally, ATM and ATR are involved in arresting the cell cycle upon DNA damage. Therefore, the overall downregulation of these genes in multiple phases of the cell cycle suggests there may be additional influence of astrovirus infection on the cell cycle transcriptional program.

We also explored our murine astrovirus (MuAstV) scRNA-seq dataset. The most highly infected cell type was goblet cells (**Figure** 4.8b-c). We found that MuAstV-infected cells were again primarily in G1 phase compared to bystander and mock cells (**Figure** 4.8d). This phenotype is carried through in goblet cells (**Figure** 4.9).

We then investigated cyclin, CDK, and cell cycle-associated genes within our MuAstV scRNA-seq dataset. All cyclin and CDK genes were decreased in infected cells compared to bystander and mock-inoculated cells, except for CCND2 and CCND3, encoding cyclins D2 and D3. These were upregulated in infected cells (**Figure** 4.10a). Interestingly, Rb1, Abl1, and Anapc2, Anapc4, and Anapc7 were all upregulated in MuAstV-infected cells, while other cell cycle-associate genes were downregulated (**Figure** 4.10b). The combination of upregulation of Cyclin D2 and D3, as well as Rb1 would suggest an increase in cells progressing into the S phase in MuAstV infection. However, the decrease in CCND1 and

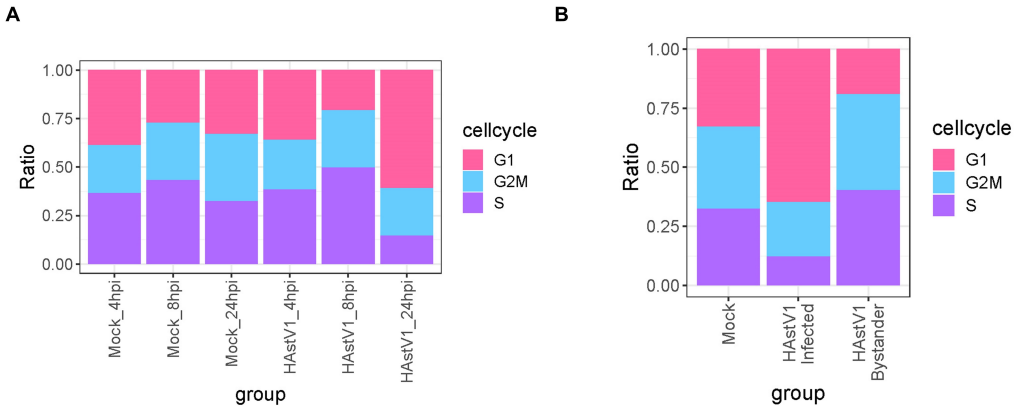

C

Pathway	Gene ranks	NES	pval	padj
HALLMARK_INTERFERON_ALPHA_RESPONSE		2.50	2.0e−07	9.8e−06
HALLMARK_MYC_TARGETS_V2		2.18	2.1e−04	2.6e−03
HALLMARK_KRAS_SIGNALING_DN		1.81	8.6e−03	5.4e−02
HALLMARK_WNT_BETA_CATENIN_SIGNALING		1.46	6.6e−02	2.4e−01
HALLMARK_INTERFERON_GAMMA_RESPONSE		1.89	2.1e−04	2.6e−03
HALLMARK_TNFA_SIGNALING_VIA_NFKB		1.78	5.7e−04	5.7e−03
HALLMARK_TGF_BETA_SIGNALING		1.43	1.1e−01	2.8e−01
HALLMARK_SPERMATOGENESIS		1.32	1.2e−01	2.8e−01
HALLMARK_INFLAMMATORY_RESPONSE		1.15	2.4e−01	4.1e−01
HALLMARK_ESTROGEN_RESPONSE_EARLY		1.18	1.5e−01	3.3e−01
HALLMARK_E2F_TARGETS		−1.32	5.9e−02	2.4e−01
HALLMARK_G2M_CHECKPOINT		−1.46	1.7e−02	9.3e−02
HALLMARK_EPITHELIAL_MESENCHYMAL_TRANSITION		−1.34	7.4e−02	2.4e−01
HALLMARK_OXIDATIVE_PHOSPHORYLATION		−1.52	4.5e−03	3.2e−02
HALLMARK_ANDROGEN_RESPONSE		−1.38	6.5e−02	2.4e−01
HALLMARK_MYC_TARGETS_V1		−1.64	8.5e−04	7.1e−03
HALLMARK_PROTEIN_SECRETION		−1.51	2.1e−02	1.0e−01
HALLMARK_MYOGENESIS		−1.56	2.6e−02	1.2e−01
HALLMARK_REACTIVE_OXYGEN_SPECIES_PATHWAY		−1.40	7.6e−02	2.4e−01
HALLMARK_MITOTIC_SPINDLE		−1.86	7.2e−06	1.8e−04

0 2000 4000 6000 8000

Figure 4.6: Human Single Cell RNA Sequencing Cell Cycle Data. A. Ratio of cells in G1, G2M, or S phase in each sample group from the human single cell RNA sequencing (scRNA-seq) dataset. B. Ratio of cells in G1, G2M, or S phase in mock, bystander, or HAstV-1-infected cells at 24 hpi in the human scRNA-seq dataset. C. Differential expression analysis of Hallmark pathways in HAstV-1-infected compared to bystander cells in the human scRNA-seq dataset.

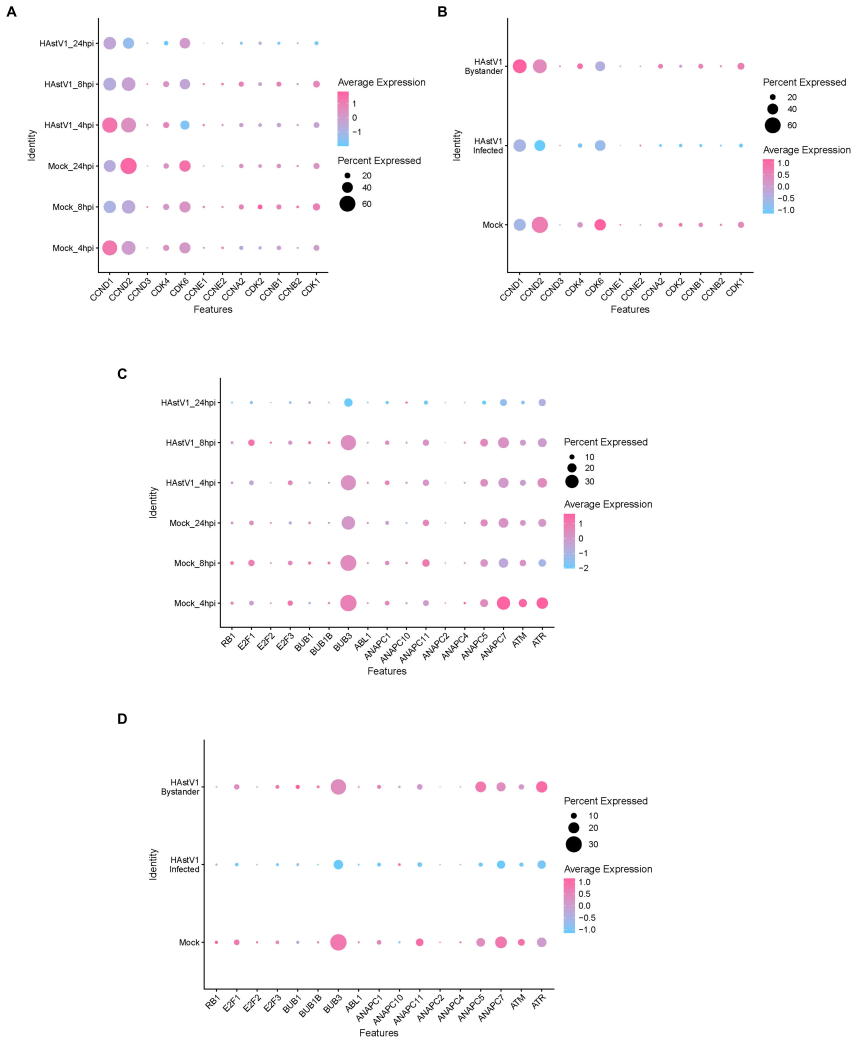

Figure 4.7: Human Single Cell RNA Sequencing Cell Cycle Gene Expression. A. Dot plot showing cyclin and CDK expression across samples in the human single cell RNA sequencing (scRNA-seq) dataset. B. Dot plot showing cyclin and CDK expression in mock, infected, and bystander groups at 24 hours post infection (hpi) in the human scRNA-seq dataset. C. Dot plot showing expression of cell cycle-associated genes across samples in the human scRNA-seq dataset. D. Dot plot showing expression of cell cycle-associated genes in mock, infected, and bystander groups at 24 hpi in the human scRNA-seq dataset.

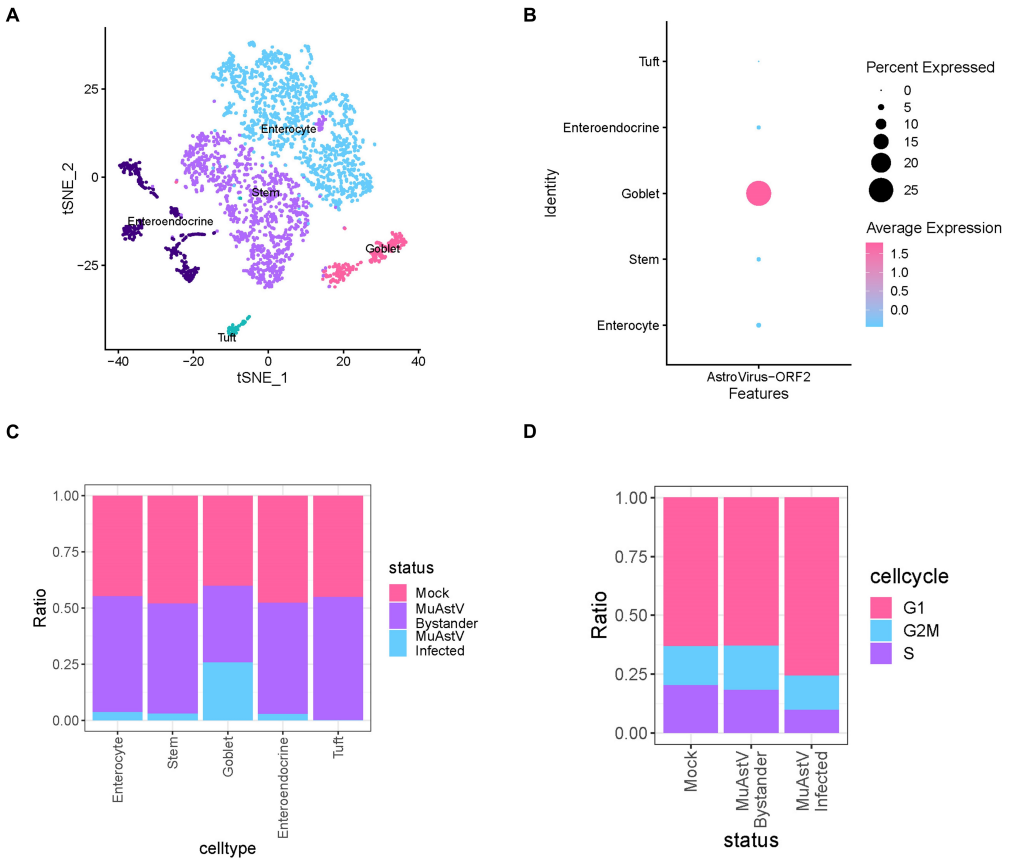

Figure 4.8: Mouse Single Cell RNA Sequencing Cell Cycle Data. A. tSNE plot showing cell types in the mouse scRNA-seq dataset. B. Astrovirus gene expression in different cell types from the mouse single cell RNA sequencing (scRNA-seq) dataset. C. Ratio of infected, bystander, and mock cells in each cell type. D. Ratio of G1, G2M, and S phase cells in mock, bystander, and infected groups.

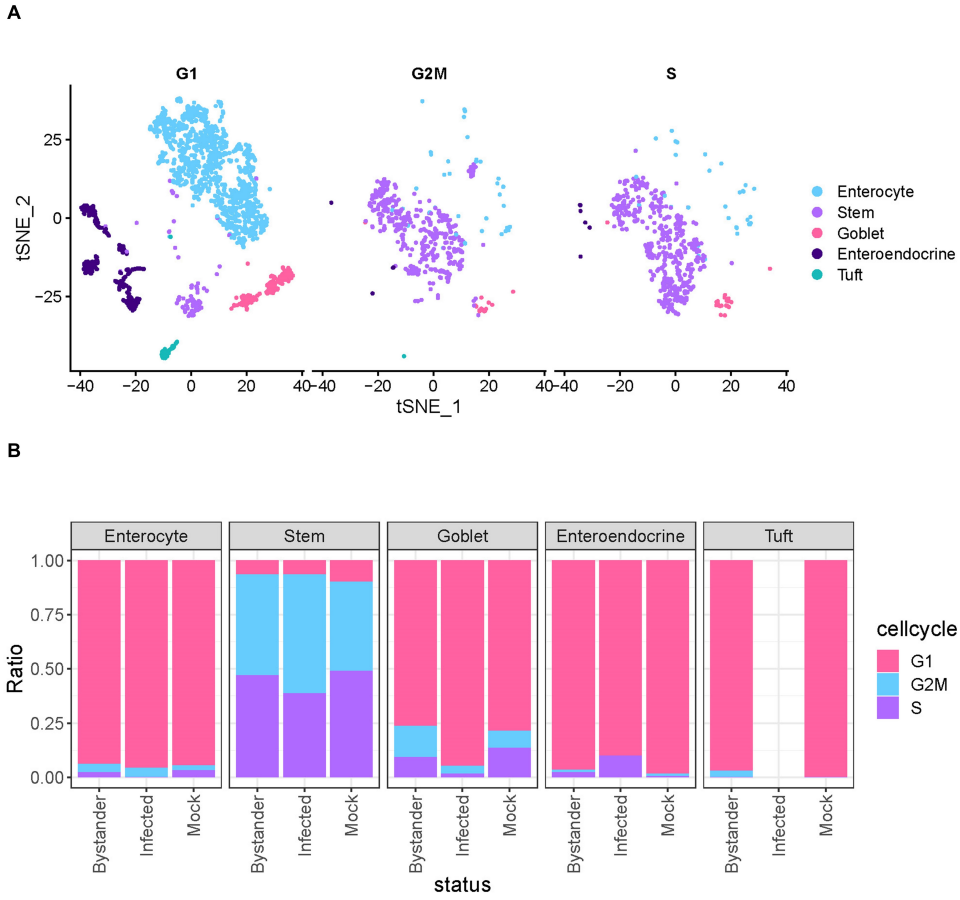

Figure 4.9: Mouse Single Cell RNA Sequencing Cell Cycle Data by Cell Type. A. tSNE plot showing cell types in the mouse scRNA-seq dataset and their respective cells in G1, G2M, or S phase. B. Ratio of G1, G2M, and S phase cells in mock, bystander, and infected groups by cell type. Note that viral transcripts were detected at low levels in tuft cells, resulting in no recorded cell cycle data for this group.

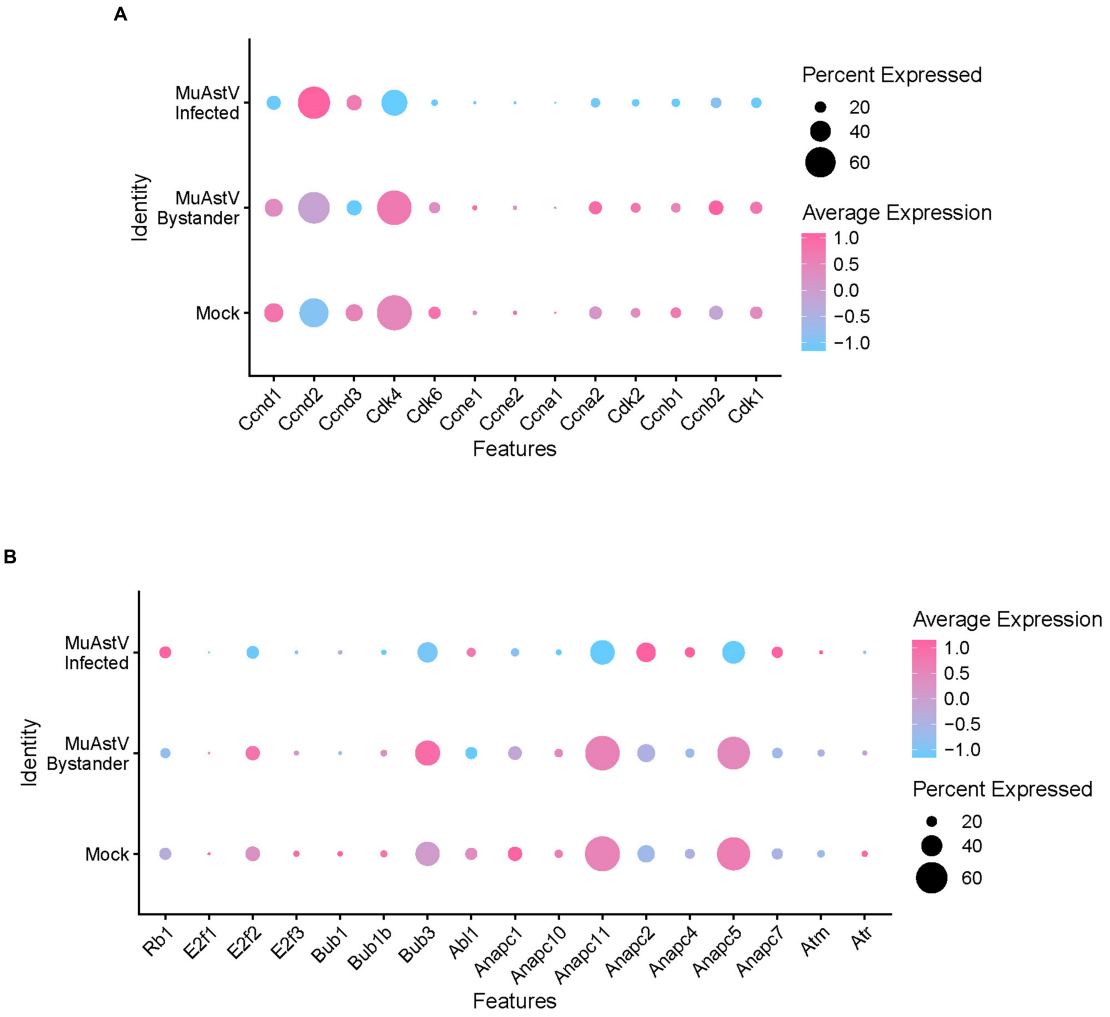

Figure 4.10: Mouse Single Cell RNA Sequencing Cell Cycle Gene Expression. A. Dot plot showing cyclin and CDK expression in mock, infected, and bystander groups in the mouse single cell RNA sequencing (scRNA-seq) dataset. B. Dot plot showing expression of cell cycle-associated genes in mock, infected, and bystander groups in the mouse scRNA-seq dataset.

CDK4/6 expression in infected cells suggests a lack of necessary G1 activity, supporting G1 arrest. These data suggest that astrovirus infection disrupts the cell cycle transcriptionally in both human and mouse infection.

To elucidate how these transcriptional changes translate to changes in protein, we employed immunoblotting for multiple cell cycle markers in HAstV-1-infected and mock-inoculated Caco-2 cell lysates at 0, 8, and 24 hpi. Geminin, a marker for S and G2/M phases, was significantly downregulated at 24 hpi in HAstV-1-infected lysates compared to mock-inoculated 24-hour lysates. Geminin levels were also significantly decreased in HAstV-1 24 hpi lysates compared to HAstV-1 0 hpi lysates, indicating a decrease in S, G2, and M phase cells throughout infection (**Figure** 4.11a). Geminin is typically degraded during metaphase and is not present in G1 phase. Similarly, cyclin A2 was significantly reduced in HAstV-1 24 hpi compared to mock-inoculated 24 hpi samples. As cyclin A2 is present during S phase, this again supports a decrease in S phase-associated cells in astrovirus-infected samples late in infection. Not only this, but degradation of cyclin A is necessary for G1 arrest (**Figure** 4.11d).

Finally, CDK6 and cyclin D1 were utilized as markers of G1 phase. CDK6 significantly increased at 24 hpi in astrovirus-infected samples compared to mock-inoculated 24-hour samples. Mock-inoculated samples showed a decrease in CDK6 over time, while HAstV-1-infected samples showed a significant increase in CDK6 over time (**Figure** 4.11b). This accumulation of CDK6 in HAstV-1 24 hpi samples indicates that cells are in G1 phase. However, without activation of CDK6 via binding to cyclin D, the cell cannot progress from G1 to S phase. Interestingly, cyclin D1 levels are significantly decreased in HAstV-1 24 hpi samples compared to HAstV-1 0 hpi samples and mock-inoculated 24-hour samples (**Figure** 4.11c). During genotoxic stress, cyclin D1 degradation is indicative of cell cycle arrest in G1 phase. Therefore, it is likely that this significant reduction in cyclin D1 is related to G1 arrest (**Figure** 4.12).

4.6 Discussion

Our work has shown that astrovirus manipulates parts of the autophagy machinery to form DMV replication organelles during infection. Here we show that although some autophagy machinery is involved in astrovirus replication, lysosomes are not dysregulated in the process. While there is a significant decrease in prepro-CTSD and pro-CTSD at 24 hpi, mature CTSD is not significantly decreased. In addition, the number of lysosomes and their enzymatic activity does not change during infection, as is evidenced by LAMP1 staining and CTSB activity measurement using flow cytometry. Therefore, astrovirus infection is not affected by lysosomal activity. This could be due to an active suppression of degradation pathways by astrovirus components during infection.

Upstream of DMV replication, we have determined that the ER is the site of origin for astrovirus-induced DMVs. With upregulation of NPF WHAMM transcriptionally

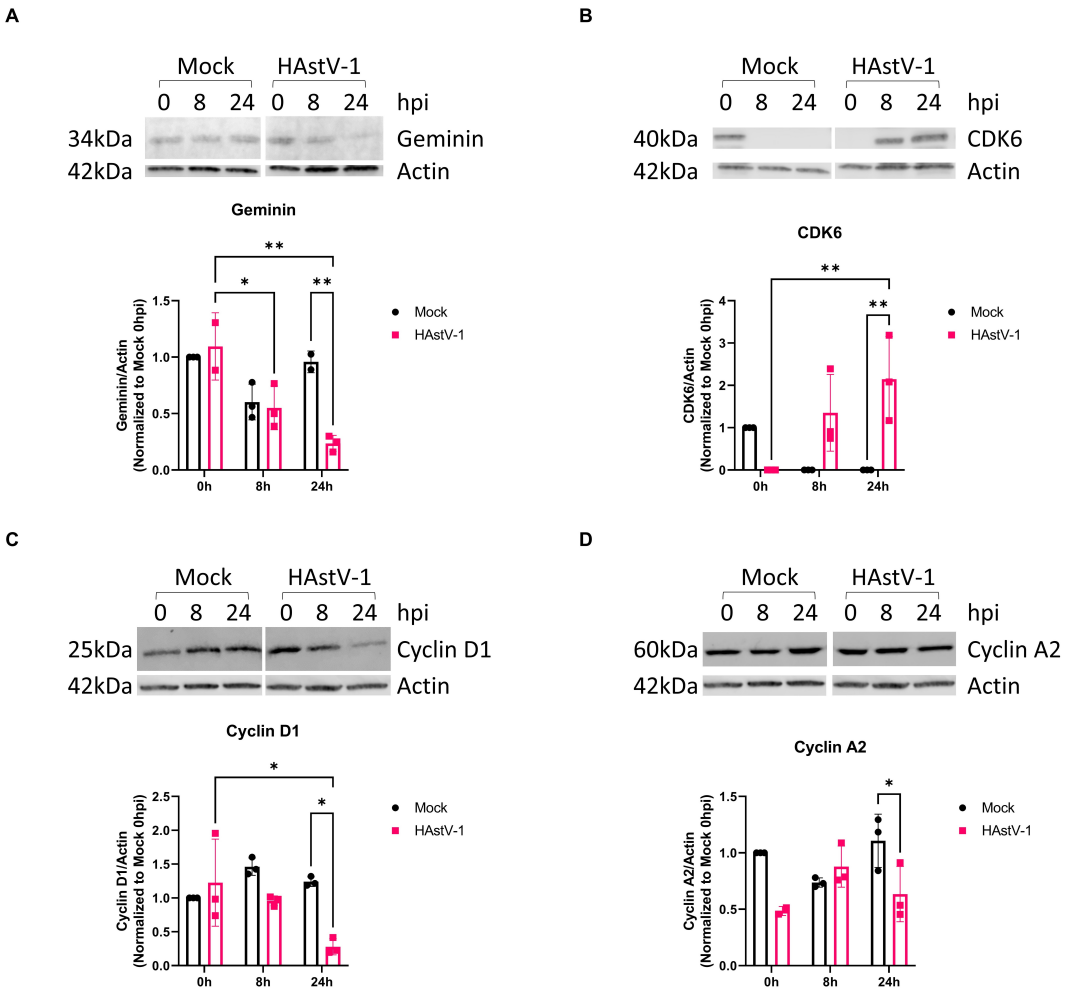

Figure 4.11: Cell Cycle Protein Expression During HAstV-1 Infection in Caco-2 Cells. A. Representative immunoblot and quantification of geminin expression during HAstV-1 infection or mock inoculation of Caco-2 cells. B. Representative immunoblot and quantification of CDK6 expression during HAstV-1 infection or mock inoculation of Caco-2 cells. C. Representative immunoblot and quantification of Cyclin D1 expression during HAstV-1 infection or mock inoculation of Caco-2 cells. D. Representative immunoblot and quantification of Cyclin A2 expression during HAstV-1 infection or mock inoculation of Caco-2 cells.

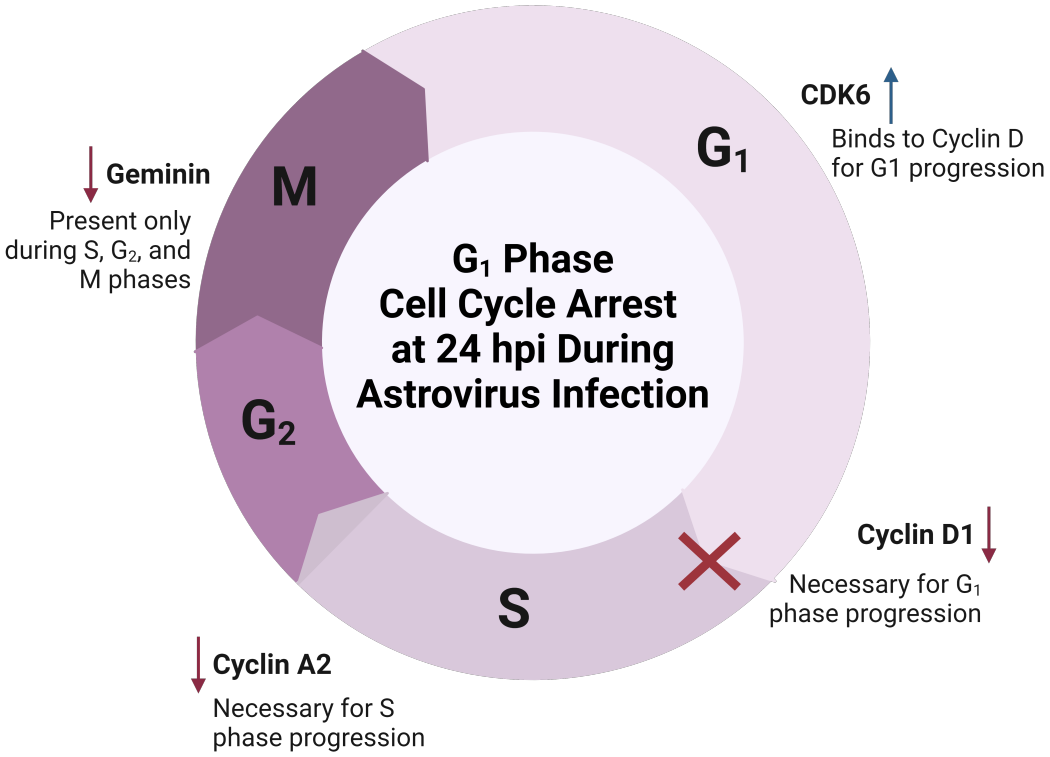

Figure 4.12: Model of Cell Cycle Arrest During Astrovirus Infection. Our data show a decrease in S and G2M phase-associated proteins geminin and Cyclin A2 at 24 hours post-infection (hpi) in HAstV-1 infected cells compared to mock-inoculated cells. There is also an increase in G1-associated CDK6, as well as a decrease in G1-associated Cyclin D1, indicating potential G1 phase arrest.

and translationally as well as EM evidence of ER fragments associated with DMVs, it is likely that DMVs bud from ER. This has been observed for coronaviruses, hepatitis c virus (HCV), and noroviruses. We also used confocal microscopy and stained for calnexin during infection. We found that ER membranes became condensed in infected cells, but not bystander cells.

Knowing that calnexin also serves as a marker of ER stress, we explored the dysregulation of ER stress-associated pathways in our scRNA-seq dataset. This data showed a significant downregulation in the UPR pathway in infected samples late in infection. When we explored expression of specific ER stress-associated genes, we found an upregulation of XBP1 and ATF4 in HAstV-1-infected cells at 24 hpi, as well as in infected compared to bystander cells. As XBP1 is downstream of the IRE1 pathway and ATF4 is downstream of the PERK pathway, we next employed ATF6 pathway inhibitor ceapin A7 and broad ER stress activator thapsigargin to determine whether ER stress changes astrovirus infection. Thapsigargin treatment reduced astrovirus infection significantly, while ceapin had no effect. This demonstrates that the ATF6 pathway is not important to astrovirus infection, but IRE1 and PERK pathways could modulate infection.

These findings align with evidence of IRE1 manipulation during coronavirus infection. The IRE1 pathway is activated, but XBP1 splicing is actively repressed, leading to activation of Beclin-dependent, ATG5-independent autophagy during Infectious bronchitis virus (IBV) replication. In addition, three separate coronaviruses showed reduced infection when cells were treated with thapsigargin during infection, leading to a downstream reduction in autophagy. It is possible that similarly to coronaviruses, astrovirus manipulates the IRE1 arm of the UPR to activate Beclin-dependent, LC3-independent autophagy for DMV formation during infection. Additionally, the IRE1β paralogue of IRE1α is present only in intestinal epithelial cells. In its absence, mice experience accelerated onset of inflammatory bowel disease. Therefore, the intestinal-specific IRE1β could be responsible for activation of autophagy machinery during astrovirus infection for formation of replication organelles.

Previous work explored the role of eukaryotic translation initiation factor 2A (eIF2α) signaling in astrovirus infection and found that it was upregulated in a PERK-independent manner. This could be the reason for increased ATF4 transcripts. However, eIF2α has further implications for the status of the cell during infection. Activation of eIF2α can lead to cell cycle arrest in G1 phase through decreased translation of cyclin D1.

To determine the cycling status of the cell during astrovirus infection, we explored which phase of the cell cycle infected cells most occupied. Our scRNA-seq data suggested that infected human and mouse cells were most often in G1 phase. We next employed immunoblotting to explore whether this transcriptional data translated to differences in cell cycle-associated proteins. A significant reduction in geminin and cyclin A2 in HAstV-1-infected lysates compared to mock-inoculated lysates suggested that cells were in G1 phase during infection. In support of this observation, CDK6 was significantly upregulated in HAstV-1-infected samples compared to mock. Finally, a significant reduction in cyclin D1

suggested that although the cells had readily available CDK6 for progression of the cell cycle, they were likely arrested in G1 phase with an absence of available cyclin D1 to bind the CDK6.

Severe acute respiratory syndrome coronavirus (SARS-CoV), Epstein-Barr virus (EBV), human cytomegalovirus (HCMV), herpes simplex virus type 1 (HSV1), and influenza A virus (IAV) each induce cell cycle arrest in G1 phase (J. P. Castillo and Kowalik, 2004; Cayrol and Flemington, 1996; C.-J. Chen, Sugiyama, et al., 2004; C.-J. Chen and Makino, 2004; Sinclair et al., 2000; Yuan, Shan, et al., 2005; Yuan, J. Wu, et al., 2006). This common tactic during viral infection may provide favorable conditions for replication since the host cell is producing more mRNA and protein during G1. Therefore, additional nucleotides and machinery involved in transcription and translation could be repurposed for viral replication. Arrest in G1 may also allow astrovirus time to assemble while preventing cell death responses. As we have shown using many different methods, astrovirus infection does not induce cell death. This observed cell cycle arrest in G1 phase may be responsible for the prevention of cell death to prolong viral replication in the host cell.

Therefore, our data show that astrovirus infection induces cell cycle arrest in G1 phase, reducing the risk of cell death. In this state of cellular survival, ER membranes are rearranged and the IRE1 arm of the UPR is manipulated to enhance replication, likely via activation of the PI3KC3-dependent, ATG5-independent autophagy machinery required to form replication DMVs. Finally, the formation of these DMVs is not accompanied by changes in lysosomal activity, suggesting that canonical autophagy-associated degradation pathways do not affect astrovirus replication.

Chapter 5

Conclusions and Future Directions

Astrovirus infection causes gastrointestinal disease but can become more serious in immunocompromised and elderly populations. For this reason, it is imperative that we gain a better understanding of how astrovirus infection manipulates host cellular responses to support its replication cycle. Here, I will discuss the discovery of the replication organelle (RO) for human astrovirus, the ways in which human astrovirus disrupts endoplasmic reticulum (ER) stress and cell cycle machinery during infection, the limitations of these studies, and future directions that may clarify the astrovirus life cycle further.

5.1 Discovery of the Replication Organelle for Human Astrovirus

In 1980, Gray and colleagues published an observation of double membrane organelles in astrovirus-infected lamb intestines (E. Gray, Angus, and Snodgrass, 1980). Since then, little has been done to discern the purpose of these structures. We hypothesized that double membrane vesicles (DMVs) form during astrovirus infection as replication organelles, similarly to the replication mechanism of other positive sense RNA viruses. Our work has added significant depth to the understanding of astrovirus replication. We have shown that human astrovirus serotype 1 (HAstV-1) infection leads to formation of DMVs in a replication-dependent manner. These DMVs are associated directly with HAstV-1 virions (Bub et al., 2023).

We hypothesize that the viral genome replicates inside the DMVS, and viral assembly occurs outside of the DMVs. RNA dependent RNA polymerases (RdRp) are often membrane-associated during viral infection (Moradpour et al., 2004; Venkataraman, B. V. Prasad, and Selvarajan, 2018). In the future, research should determine whether the astrovirus RdRp is localized inside the DMV and whether disruption of membrane association might reduce viral replication. Additionally, the viroporin encoded by the astrovirus genome, XP, may play a role in passage of viral genetic material through the DMV, enabling protection of the viral genetic material from immune sensors (Lulla and Firth, 2020; Wolff et al., 2020). Spatially, enclosing viral genetic material in a DMV would also be beneficial to viral replication so that genomes and replication machinery are not physically spread out in the cytoplasm. While double membrane vesicles were also observed in astrovirus

VA-1-infected Caco-2 cells by electron microscopy (EM), they did not always associate directly with clusters of VA-1 virions. This could suggest that VA-1-induced DMV formation is related to replication, but viral assembly can occur separately.

We next explored the role of PtdIns3K information of DMVs during HAstV-1 infection, as this complex has been previously implicated as a necessary feature of positive sense, single- stranded viral replication for severe acute respiratory syndrome coronavirus 2 (SARS-CoV-2) and hepatitis c virus (HCV) (Twu et al., 2021). We hypothesized that PtdIns3K is necessary to DMV formation during astrovirus replication. Inhibition of PtdIns3K with specific inhibitor PIK-III significantly reduced formation of DMVs and viral particles associated with them. Additionally, PIK-III treatment reduced capsid and double stranded RNA (dsRNA) staining during infection in a dose-dependent manner, whether cells were treated prior to or after infection with HAstV-1. The same was true for astrovirus VA-1, which is more closely related to astrovirus strains of other species than to HAstV-1. PIK-III treatment also resulted in significantly fewer genome copies of HAstV-1 in cell supernatants and lysates in a dose-dependent manner. Supernatants from PIK-III-treated, HAstV-1-infected cells also contained less infectious virus than DMSO-treated controls, suggesting that targeting phosphatidylinositol 3-kinase (PI3KC3) reduces not only initial replication, but also secondary infection (Bub et al., 2023).

The PI3KC3 complex is a key component of canonical autophagy machinery, aiding in the production of autophagosomes through formation of phosphatidylinositol 3-phosphate. Although autophagy can be an antiviral pathway, previous work has shown that autophagy machinery can be manipulated for viral replication. Due to the key role of PI3KC3 in canonical autophagy pathways within the host cell, we examined whether other autophagy machinery is involved in astrovirus replication. We showed that LC3 (microtubule-associated protein light chain 3) conjugation machinery is dispensable for astrovirus replication using doxycycline-inducible cleavage of LC3 in Huh-7.5 cells, as well as siRNA knockdown of ATG5, a necessary LC3 conjugation component (Bub et al., 2023). This suggests that astrovirus manipulates some, but not all the autophagy machinery to form its DMV replication organelles. This again demonstrates a similar thread between positive sense, single-stranded RNA viruses, as the same was true for SARS-CoV-2 and HCV.

It is possible that human astrovirus induces expression of additional phosphatidylinositol phosphate kinases for DMV formation during infection. Phosphatidylinositol 4-kinase (PI4Kα) can also affect viral replication and is localized to the endoplasmic reticulum (A. Balla and T. Balla, 2006; Mohamud et al., 2020; Mosser, Caliguiri, and Tamm, 1972; K. Wong, Meyers, and Cantley, 1997). Specifically, the PI4KA-G1 inhibitor has been implicated as a specific phosphatidylinositol 4-phosphate (PI4P) production inhibitor that disrupts replication of viruses (Bojjireddy et al., 2014; Twu et al., 2021). It is possible that in addition to targeting PI3KC3, targeting PI4K may also disrupt astrovirus replication.

However, it should be noted that targeting PI4K is not a safe therapeutic option. In generating a tamoxifen-inducible conditional knockout mouse model targeting the Pi4ka gene, researchers observed that ablation of Pi4ka causes lethality. Histopathology showed necrosis in stomach and intestinal cells. When dosed with a PI4K inhibitor, animals given the smallest dose survived but faced gastrointestinal abnormalities (Bojjireddy et al., 2014). Therefore, determining whether PI4Kα plays a role in DMV formation during astrovirus infection would help to further characterize the cellular machinery involved in the viral life cycle, but would not provide a new therapeutic target.

We have also shown that murine astrovirus-infected cells upregulate PI3K machinery and not LC3 machinery transcriptionally, suggesting potential for a species-spanning mechanism for astrovirus replication (Bub et al., 2023). Autophagy-deficient mouse models exist to help further clarify this work. To determine whether replication in mice is linked to a PI3KC3-dependent pathway, it would be beneficial to disrupt Beclin1 expression in mice. Beclin1 knockout mice have an embryonic lethal phenotype, while heterozygotes are viable with increased tumor formation. It is also necessary to consider that heterozygotes have heightened immune response to some viral infections (Kuma, Komatsu, and Mizushima, 2017). Therefore, an ideal model would be crossing Beclin1 floxed mice with Villin Cre mice to produce intestine-specific knockout of Beclin1. This would allow for specific analysis of the role of Beclin1 in gastrointestinal infection with astrovirus in vivo. Other autophagy-associated models for mice, including Atg5 floxed villin-cre mice, could also be utilized to determine whether there is any variation in host machinery manipulation by murine astrovirus (MuAstV). Notably, murine astrovirus is not an ideal model to relate to human astrovirus infections, as mice lack some phenotypic responses to astrovirus that are present in humans (Compton, Booth, and Macy, 2017; Cortez, Sharp, et al., 2019; Kjeldsberg and Hem, 1985; Morita et al., 2021). It would be more relevant to study the effects of PI3KC3 inhibition in a turkey model, as turkeys have similar symptoms during infection with TAstV compared to humans (Koci and Schultz-Cherry, 2002; Pantin-Jackwood et al., 2011; Reynolds, Saif, and Theil, 1987).

Although targeting the PI3KC3 complex shows promising preclinical results in astrovirus, SARS-CoV-2, and HCV in vitro infection models, it will be necessary to evaluate whether this specific inhibitor can be used as an antiviral therapeutic clinically. While PIK-III specifically binds a hydrophobic pocket unique to PI3KC3, other common inhibitors of the PI3KC3 complex broadly inhibit PI3KC1 and PI3KC2, as well. For instance, 3-MA, wortmannin, and LY294002 are reversible PI3KC3 inhibitors that also target PI3KC1. Thus far, all inhibitors of the PI3KC3 complex, whether specific or broadly reactive with PI3KC1 and PI3KC2, are preclinical and need sufficient testing in vivo to determine whether they could be effective in treating viral infections (G. Lu et al., 2022). Another beneficial therapeutic target to explore in the future is the astrovirus protease. With other viral infections such as HCV and HIV, inhibition of their viral protease activity is successful in attenuating viral replication and maturation (Hayes et al., 2022; Lv, Chu, and Yong Wang, 2015). These inhibitors come with concerns regarding toxicity, but an astrovirus protease

inhibitor may be a feasible alternate target to weaken viral infection.

Further studies should also explore the kinetics of astrovirus infection. We have shown that treatment of cells with PIK-III prior to infection or at 1 hpi is effective for reducing DMV formation and viral replication. However, it will be beneficial to determine whether PI3KC3 inhibition late in infection can prevent spread of the virus to neighboring cells. In our electron microscopy experiments, DMVs were observed no earlier than 24 hpi. It is certainly possible that DMVs form at earlier time points during infection and may be observed with a higher number of electron microscopy images taken. Regardless, viral replication should be measured throughout infection to determine when genome copies and infectious virus begin to be produced within the cell and released outside of the cell. With this information, a time course of PIK-III treatment could be utilized to determine whether there is a therapeutic window for treatment of cells infected with astrovirus.

While we have described the replication phase of the astrovirus life cycle, cellular exit of astrovirus remains understudied. Knowing that astrovirus utilizes DMVs to replicate may help to clarify the mechanism of cellular exit of this virus. Some viruses utilize their replication organelles to eventually exit the cell. In the future, studies should focus on determining whether astrovirus escapes the cell in an organelle and what the components of these organelles might be. Differential ultracentrifugation would help to determine what cellular structures astrovirus associates with. Tandem mass spectrometry would further clarify the components of these structures and potentially provide more therapeutic targets to prevent spread of astrovirus from one cell to another.

Additionally, it will be necessary to determine which parts of the astrovirus genome are important to DMV formation during infection to better understand the virus itself. While we did not observe DMV formation in 293T cells transfected with ORF1ab or ORF1a, this does not necessarily rule out their involvement in replication organelle biogenesis. Transfecting 293T cells with a plasmid to produce astrovirus nonstructural proteins (nsps) may not be the most efficient way to determine their involvement in the replication process. Future studies should employ infectious astrovirus mutants to clarify the role of each astrovirus protein in the viral life cycle. Selection of mutants should take into consideration viral titer to ensure that they are efficiently replicating. Newer Cryo-EM technology will also allow researchers to take more detailed images of astrovirus replication organelles. Studies of SARS-CoV-2 replication organelles have revealed a viral porin on the surface of DMV replication organelles, which serves as a passageway for viral RNA (Wolff et al., 2020). Using Cryo-EM, we will be able to elucidate whether astrovirus-induced DMVs also contain a surface porin. This may be the porin encoded by astrovirus alternative-frame ORFX (Lulla and Firth, 2020).

5.2 Astrovirus Manipulation of Host Cellular Processes During Infection

Since the autophagy pathway leads to degradation of cargo in the lysosome, we explored lysosomal dysregulation during astrovirus infection. During infection, picornaviruses, Chikungunya virus, Sindbis virus, human immunodeficiency virus (HIV)-associated protein Vif, and others can be degraded by the lysosome (Judith et al., 2013; Orvedahl, MacPherson, et al., 2010; Orvedahl, Sumpter Jr, et al., 2011; Staring et al., 2017; Valera et al., 2015). Other viruses such as SARS-CoV-2 and human parainfluenzavirus 3 (HPIV3) actively interfere with lysosomal function to prevent their own degradation (Ding et al., 2014; Hayn et al., 2021; Miao et al., 2021; Qu et al., 2021; Y. Zhang et al., 2021). We showed that while cathepsins are dysregulated transcriptionally and translationally during astrovirus infection, their activity, and the number of lysosomes per cell during astrovirus replication is not significantly different. These data suggest that the lysosome does not interfere with astrovirus replication as it does with other viruses. While this may be supported by our current data, it will be necessary to determine whether infectious astrovirus mutants are more susceptible to lysosomal degradation. This will clarify whether specific astrovirus proteins are actively preventing viral degradation during infection.

The site of biogenesis of replication organelles is another potential target to prevent viral infection. Therefore, we aimed to determine the site of origin of astrovirus-induced DMVs. Coronaviruses, HCV, arteriviruses, and noroviruses induce RO formation at the ER, which is also a common site for autophagosome biogenesis (Cortese et al., 2020; Cottam et al., 2011; Doerflinger et al., 2017; Knoops, Kikkert, et al., 2008; Knoops, Bárcena, et al., 2012; Mihelc, Baker, and Lanman, 2021; Prentice et al., 2004; Romero-Brey et al., 2012). Knowing that the astrovirus genome contains ER-localizing motifs, we turned our attention to the ER as a potential source of DMV membranes. Single cell RNA sequencing (scRNA-seq) data also suggested that astrovirus upregulates ER-associated WHAMM, a nucleation promoting factor that can aid in phagophore formation from the ER (Kast and Dominguez, 2015). We saw that this transcriptional difference translated to a significant increase in WHAMM at the protein level during astrovirus infection. We have attempted to produce WHAMM knockout (KO) Caco-2 cells, however they are not viable. A siRNA knockdown of WHAMM may clarify whether it is necessary for DMV formation and astrovirus replication. We further explored our electron microscopy data, which showed ER fragments associated with DMVs. Finally, confocal microscopy demonstrated that calnexin-associated ER fragments were condensed and reorganized in astrovirus-infected, but not bystander cells. Notably, calnexin also colocalized with astrovirus dsRNA, supporting a role for these membranous structures in astrovirus replication.

Altogether, our data suggest an ER origin for DMV replication organelles. If this is the case, disrupting the ER would help to clarify whether DMVs are able to originate from other sites such as the Golgi during infection. There are available ER protein transport inhibitors that may help to clarify this question (Kalies and Römisch, 2015). Additionally,

electron microscopy using immunogold labeling of ER or Golgi-associated markers such as calnexin or TGN38 respectively would help to determine whether DMVs associate with both ER and Golgi fragments.

After observing the restructuring of calnexin-associated ER fragments during infection, we hypothesized that ER stress could play a role in astrovirus infection. Our scRNA-seq data showed an upregulation in XBP1 and ATF4 transcripts later in astrovirus infection, in infected but not bystander cells. The scRNA-seq dataset also suggested that genes associated with the Hallmark unfolded protein response (UPR) pathway were significantly downregulated during astrovirus infection. We saw that treatment of astrovirus-infected cells with thapsigargin significantly decreased both capsid and dsRNA staining at 24 hpi, but ceapin treatment had no effect. Thapsigargin broadly activates ER stress, while ceapin inhibits the ATF6 (Activating Transcription Factor 6) arm of the pathway. In interpreting these data, we hypothesize that the IRE1 (inositol-requiring enzyme 1) arm of the UPR may be upregulated in response to astrovirus infection, leading to an increase in XBP1 transcripts. XBP1 activation can lead to upregulation of autophagy-associated genes. On the other hand, XBP1 transcripts are also upregulated during coronavirus infection. However, XBP1 splicing is decreased, which leaves it inactive. This process results in activation of PI3K-dependent, ATG5-independent autophagy during infectious bronchitis virus (IBV) replication (Fung and D. X. Liu, 2019). Therefore, it will be important to specifically target the IRE1 pathway to clarify whether XBP1 is spliced during astrovirus infection and to determine whether this affects PI3KC3 activity and DMV formation.

Previous work has also shown that astrovirus upregulates eIF2α (eukaryotic translation initiation factor 2A) phosphorylation in a PERK (PKR-like endoplasmic reticulum kinase)-independent manner (Tomoyasu Isobe et al., 2019). Our work supports an upregulation in eIF2α phosphorylation, as we observe an increase in ATF4 transcripts during infection. Additionally, eIF2α plays a role in Gap 1 (G1) phase cell cycle arrest. Specifically, eIF2α phosphorylation leads to decreased translation of cyclin D1, causing cell cycle arrest in G1 phase. Our scRNA-seq datasets for both human and mouse astrovirus infection show an increased proportion of cells in G1 phase. Using immunoblotting, we showed that geminin and cyclin A2 were downregulated during infection, suggesting that cells are in G1 phase. Further, G1-associated Cyclin-Dependent Kinase 6 (CDK6) was upregulated. Finally, cyclin D1 was translationally decreased, supporting arrest in G1 phase.

SARS-CoV, Epstein-Barr virus (EBV), human cytomegalovirus (HCMV), herpes simplex virus type 1 (HSV-1), and influenza A virus (IAV) are all capable of inducing G1 phase cell cycle arrest (J. P. Castillo and Kowalik, 2004; Cayrol and Flemington, 1996; C.-J. Chen, Sugiyama, et al., 2004; C.-J. Chen and Makino, 2004; Sinclair et al., 2000; Yuan, Shan, et al., 2005; Yuan, J. Wu, et al., 2006). Since G1 is a growth phase of the cell cycle, additional nucleotides and amino acids are present and could be repurposed for viral replication. Future studies should explore whether infected cells have enhanced nucleotide and amino acid metabolism compared to bystander cells or mock-inoculated cells.

EBV manipulates multiple stages of the cell cycle through expression of two proteins, Zta and LMP-1. Zta induces G1 arrest, while LMP-1 induces Gap 2/Mitosis phase (G2/M) arrest (K.-S. Yeo, Mohidin, and C.-C. Ng, 2012). Viruses can differentially regulate proteins and pathways for unique purposes throughout their life cycles. While our studies suggest cell cycle arrest in G1 phase for astrovirus, it will be necessary to explore whether this arrest lasts past the 24 hpi time point or whether G1 arrest is only necessary during active viral replication.

It would also be impactful to determine whether disruption of ER stress pathways affects cell cycle processes during astrovirus infection, as the UPR is linked to cell cycle regulation. Alternatively, synchronization of cells in specific stages of the cell cycle may affect the organization of ER membranes and their use in DMV formation during astrovirus infection. Additionally, the relationships between these host cellular processes and cell survival should be explored. It is widely known that astrovirus infection does not cause cell death (Cortez, Sharp, et al., 2019; Hargest, Davis, et al., 2021; Hargest, Bub, et al., 2022; Koci, L. A. Moser, et al., 2003; V. A. Meliopoulos et al., 2016; L. A. Moser, Carter, and S. Schultz-Cherry, 2007). It is certainly possible that manipulation of UPR pathways and cell cycle arrest are responsible for this cell survival during infection. Promoting cell survival would enable astrovirus to continue to replicate and exit the cell to continue its life cycle.

To confirm the findings of these studies related to autophagy, ER stress, and cell cycle regulation, additional tools and model systems should be developed. An enteroid model would be ideal to validate our results from Caco-2, Huh-7.5, and 293T cells. The cell lines utilized in these studies are helpful tools to learn basic information about astrovirus replication. However, using these methods and inhibitors in a model more closely reflective of the human intestine would allow us to characterize response to astrovirus infection in differing cell types. It would also allow us to begin to characterize the communication that occurs between infected and bystander cells. We have shown that the transcriptional response of bystander cells closely mimics that of mock-inoculated cells, rather than infected cells, for autophagy, ER stress, and cell cycle-associated genes. During the HCMV viral life cycle, infected cells have a unique proteomic profile when compared with immediate bystander cells. The bystander cells have suppressed cellular responses, which is attributed to HCMV creating a more susceptible immediate environment for replication (T. M. White and Goodrum, 2023). Astrovirus infection in both human Caco-2 cells and murine epithelial cells may behave similarly, given the scRNA-seq profiles we observe here. It will be necessary in the future to characterize the response of both bystander epithelial cells and circulating immune cells to determine whether their proteomic profiles indicate antiviral activity.

Additionally, the development of infectious astrovirus mutants would clarify the mechanism by which astrovirus regulates and exploits the host cellular machinery. Viral nonstructural proteins (nsps), proteases, and capsid proteins can induce unique cellular

responses. Determining the role of each of these proteins beyond viral replication would greatly develop our understanding of astrovirus and its life cycle.

Altogether, these studies demonstrate that astrovirus uses a replication mechanism similar to other positive sense, single stranded RNA viruses. It also manipulates cellular processes such as ER stress and cell cycle pathways to create a pro-replication environment. Unveiling the mechanisms by which astrovirus hijacks the infected host cell and suppresses bystander cell responses will undoubtedly reveal therapeutic targets, which could reduce the disease burden of astrovirus globally.

Appendix A

Chapter 3 Article: Astrovirus Replication Is Dependent on Induction of Double-Membrane Vesicles Through a PI3K-dependent, LC3-independent Pathway

NOTE: Navigation with Adobe Acrobat Reader or Adobe Acrobat Professional: To return to the last viewed page, use key commands Alt/Ctrl+Left Arrow on PC or Command+Left Arrow on Mac. For the next page, use Alt/Ctrl (or Command)+Right Arrow, respectively. For more commands please refer to the **Preface**.

Introduction

The published article was used with permission. Theresa Bub et al. (2023). "Astrovirus replication is dependent on induction of double membrane vesicles through a PI3K-dependent, LC3-independent pathway". In: *Journal of Virology*. DOI: 10.1128/jvi.01025-23. URL: https://journals.asm.org/doi/10.1128/jvi.01025-23.

Version of Record:

https://journals.asm.org/doi/10.1128/jvi.01025-23

Astrovirus Replication is Dependent on Induction of Double-Membrane Vesicles through a PI3K-dependent, LC3-independent Pathway

Theresa Bub[1,2], Virginia Hargest[1], Shaoyuan Tan[1], Maria Smith[1,3], Ana Vazquez-Pagan[1,3], Tim Flerlage[1], Pamela Brigleb[1], Victoria Meliopoulos[1], Brett Lindenbach[4,5] Harish N. Ramanathan[4,5], Valerie Cortez[6], Jeremy Chase Crawford[7], Stacey Schultz-Cherry[1]

[1]Department of Infectious Diseases, St. Jude Children's Research Hospital, Memphis, Tennessee, USA

[2]Integrated Program of Biomedical Sciences, Department of Microbiology, Immunology, and Biochemistry, University of Tennessee Health Science Center, Memphis, Tennessee, USA

[3]Graduate School of Biomedical Sciences, St. Jude Children's Research Hospital, Memphis, Tennessee, USA

[4]Department of Microbial Pathogenesis, Yale University, New Haven, Connecticut, USA

[5]Department of Comparative Medicine, Yale University, New Haven, Connecticut, USA

[6]Department of Molecular, Cellular, and Developmental Biology, University of California, Santa Cruz, California, USA

[7]Department of Immunology, St. Jude Children's Research Hospital, Memphis, Tennessee, USA

Abstract

Human astrovirus is a positive-sense, single-stranded RNA virus. Astrovirus infection causes gastrointestinal symptoms and can lead to encephalitis in immunocompromised patients. Positive-strand RNA viruses typically utilize host intracellular membranes to form replication organelles, which are potential antiviral targets. Many of these replication organelles are double-membrane vesicles (DMVs). Here, we show that astrovirus infection leads to an increase in DMV formation through a replication-dependent mechanism that requires some early components of the autophagy machinery. Results indicate that the upstream class III phosphatidylinositol 3-kinase (PI3K) complex, but not LC3 conjugation machinery, is utilized in DMV formation. Both chemical and genetic inhibition of the PI3K complex lead to significant reduction in DMVs, as well as viral replication. Elucidating the role of autophagy machinery in DMV formation during astrovirus infection reveals a potential target for therapeutic intervention for immunocompromised patients.

Importance

These studies provide critical new evidence that astrovirus replication requires formation of double-membrane vesicles, which utilize class III phosphatidylinositol 3-kinase (PI3K), but not LC3 conjugation autophagy machinery, for biogenesis. These results are consistent with replication mechanisms for other positive-sense RNA viruses suggesting that targeting PI3K could be a promising therapeutic option for not only astrovirus, but other positive-sense RNA virus infections.

Introduction

Astroviruses are positive-sense, single-stranded, non-enveloped RNA viruses that cause disease in a variety of mammals and birds (1–4). In humans, infection is often associated with gastrointestinal symptoms such as nausea, vomiting, loss of appetite, stomachaches, and diarrhea (4–7). However, astrovirus infections can also result in fatal encephalitis, particularly in immunocompromised individuals (2, 7–12). Astrovirus infections are typically under-reported despite high prevalence (13, 14), and there are significant gaps in knowledge about astrovirus pathogenesis including the mechanisms behind viral replication.

Many positive-sense, single-stranded RNA viruses including hepatitis C virus (HCV), coronaviruses, picornaviruses, and noroviruses utilize double-membrane vesicles (DMVs) as replication chambers during infection. These replication organelles shield viral RNA from recognition by intracellular pattern recognition receptors that could alert the immune system (15–22). It has been suggested that DMVs form with the aid of autophagy machinery. Generally, autophagy serves as the recycling system of the cell. During autophagy, double-membrane vesicles called autophagosomes deliver cytoplasmic material to the lysosome for degradation. Autophagy can also be selective, targeting specific cargo such as depolarized mitochondria, damaged endoplasmic reticulum (ER) fragments, and others. The lysosome then fuses with the autophagosome, and cargo is degraded due to lysosomal enzymatic activity and acidic pH, recycling it for further use by the cell (23–26). The formation of the autophagosome can vary depending on whether the pathway is canonical or non-canonical. The canonical autophagy pathway involves machinery first characterized in starvation-induced autophagy, including the ULK1 pre-initiation complex, the class III phosphatidylinositol 3-kinase (PI3K) complex required for production of phosphatidylinositol 3-phosphate (PI3P), and the LC3 conjugation system required for autophagosome maturation. Non-canonical pathways may utilize only some parts of the originally characterized autophagy machinery (27). Regardless of the pathway, these cellular components are often manipulated by viruses during infection to enhance viral replication.

Positive-strand RNA viruses can hijack components of the autophagy machinery to form DMVs, which share characteristics with autophagosomes. However, viral-induced DMVs can be distinct from autophagosomes. They are not always delivered to lysosomes for degradation, tend to be smaller in size compared to autophagosomes, and importantly, canonical autophagy machinery is not necessarily involved in the formation of these vesicles (15, 17–20, 22). Notably, viruses can induce the formation of DMVs from the ER, Golgi apparatus, mitochondria, and other sites in the cell, which may have virus-specific implications for antiviral therapies (19, 22, 28). Recent evidence has shown that DMV formation is independent of LC3 lipidation machinery in both severe acute respiratory syndrome coronavirus 2 (SARS-CoV-2) and HCV infection; instead, both viruses appear to rely on the PI3K complex for formation of PI3P in DMV membranes (21, 29). Coxsackievirus B3, on the other hand, induces DMV formation that is independent of PI3K and ULK1 machinery, relying instead upon PI4KIIIβ for formation of these vesicles (30–32). Although electron microscopy

images have shown association of lamb astrovirus with DMVs in lamb intestines (33), the role of autophagy in astrovirus infection has remained uncharacterized in both humans and animal models.

In the present study, we find that DMVs formed during astrovirus infection rely on a PI3K-dependent, LC3-independent autophagy pathway and may originate from the ER. This machinery is targetable and using an autophagy-specific PI3K inhibitor and specific small interfering RNA (siRNA) knockdown significantly reduces DMV formation and astrovirus replication. Targeting DMV formation through inhibition of the PI3K complex during astrovirus infection offers a potential therapy for astrovirus infection, and this therapy may further be applicable to other positive-sense RNA viruses.

Results

Astrovirus induces DMV formation during replication

A previous study showed that astrovirus infection in lambs resulted in the formation of DMVs (33). To determine if this was also true with human astroviruses, we performed transmission electron microscopy (TEM) on mock and human astrovirus-1 (HAstV-1)-infected Caco-2 cells at 8, 12, 24, and 36 h post-infection (hpi). Beginning at 24 hpi, HAstV-1-infected cells had widespread formation of DMVs of approximately 200–500 nm in size compared to mock-inoculated Caco-2 cells (Fig. 1A). The DMVs were associated with HAstV-1 virions. Induction of DMV formation was dependent on productive viral replication, as UV-inactivated virus failed to induce DMVs (Fig. 1B).

Inhibition of the PI3K complex significantly reduces astrovirus replication

Like autophagosomes, DMVs have a double membrane and can utilize components of the autophagy machinery during formation. A recent study of SARS-CoV-2 and HCV replication demonstrated that the PI3K complex involved in the formation of PI3P during autophagy is necessary to the formation of DMVs during viral replication (21). One study showed that pan-PI3K inhibitors wortmannin and LY294002 were effective in reducing HAstV-1 infection (34, 35). However, this study did not address which PI3K complex is necessary for astrovirus infection or which part of the replication pathway is affected by inhibition. To test whether the autophagy-specific class III PI3K complex is required for astrovirus replication, we infected Caco-2 cells with HAstV-1 and treated Caco-2 cells with PIK-III, a specific class III phosphatidylinositol 3-kinase (PI3KC3) complex inhibitor, or DMSO (dimethyl sulfoxide) at 1 hpi. At 24 hpi, the cells were fixed for TEM. PIK-III treatment significantly reduced the presence of DMVs and viral particles at 24 hpi, suggesting that the PI3K complex may support viral replication via formation of DMVs (Fig. 2A).

To determine whether inhibition of the PI3K complex affects astrovirus replication, we infected Caco-2 cells with HAstV-1 and treated cells with varying concentrations of PIK-III or DMSO at 2 h pre-infection or 1 hpi. At 24 hpi, we fixed and stained the cells for HAstV-1 capsid or dsRNA. We observed significantly less capsid and dsRNA staining in the PIK-III-treated Caco-2 cells compared to the DMSO control at 24 hpi, and this difference was dose-dependent. Pre-infection treatment with PIK-III was not significantly different from post-infection treatment (Fig. 2B; Fig. S1a). We then repeated the experiment, collecting cells and supernatants at 24 hpi, and extracted RNA to quantify HAstV-1 genome copies. Similarly, we found that PIK-III decreased HAstV-1 genome copies in both cell lysates and supernatant significantly in a dose-dependent manner (Fig. 2C). Then, using supernatants from these cells, we found that cells that had been treated with PIK-III after HAstV-1 infection produced significantly less infectious virus than cells treated with DMSO (Fig. 2D). Finally, to determine whether this PI3K-dependent replication mechanism expands to other human astrovirus genotypes, we infected Caco-2 cells with the human astrovirus VA-1 strain and treated them with varying concentrations of PIK-III or DMSO at 1 hpi. At 48 hpi, we fixed and stained the cells for VA-1 capsid and observed significantly less VA-1 infection in Caco-2 cells treated with PIK-III compared to DMSO controls in a dose-dependent manner (Fig. S1b). These experiments suggest that the PI3K complex aids in viral replication through formation of DMVs.

To confirm these results, we knocked down a key component of PI3KC3, Beclin. Caco-2 cells were transfected with siRNA for Beclin or a control siRNA at about 70% confluence. After 2 days, cells were infected with HAstV-1. At 24 hpi, cells were collected, and genome copies were measured. Caco-2 cells transfected with siBeclin had at least 50% less Beclin expression and had significantly reduced genome copies of astrovirus compared to siControl (Fig. 3A and B). The experiment was repeated, and cells were fixed at 24 hpi for imaging. Cells treated with siBeclin had significantly less astrovirus capsid and double-stranded RNA at 24 hpi compared to siControl, further supporting a role for the PI3KC3 complex in astrovirus replication (Fig. 3C and D).

LC3 conjugation machinery is not required for astrovirus replication

To determine whether astrovirus-induced DMV formation was accompanied by an upregulation in other autophagy machinery, we utilized a real-time polymerase chain reaction (RT-PCR) array (custom Qiagen RT2 Profiler) of canonical and alternative autophagy-related genes, as well as cell death-related genes, vesicular trafficking genes, and exosome-related genes. At 24 hpi, there was a significant upregulation in autophagy-related genes in HAstV-1 infected cells compared to the 2 hpi time point including ULK1, AMBRA1, UVRAG, SQSTM1, and GABARAPL1, in addition to IDO1. However, MAP1LC3A, ATG5, and ATG7 genes associated with LC3 conjugation machinery were unchanged (Fig. 4A).

Immunoblots of lysates from mock and HAstV-1-infected Caco-2 cells confirmed that ATG5 and ATG7 were not upregulated (Fig. 4B). Given that we did not observe an

upregulation of ATG5 and ATG7, we hypothesized that astrovirus-induced DMVs form independently of LC3 conjugation machinery. To test this, we repeated the siRNA experiment, knocking down Atg5 to disrupt LC3 conjugation machinery. Atg5 was significantly reduced translationally in siATG5 cells compared to siControl, and there was no difference in astrovirus genome copies in siATG5 cells compared to siControl (Fig. 4C; Fig. S2a). In addition, in siATG5-treated Caco-2 cells, there was no difference in capsid or double-stranded RNA at 24 hpi compared to siControl (Fig. 4D; Fig. S2c and d). To validate these results, we utilized Huh-7.5 cells expressing doxycycline-inducible RavZ cysteine protease. RavZ has been shown to cleave LC3, impairing its ability to become conjugated to phosphatidylethanolamine (PE), leading to a reduction in autophagosome formation (36, 37). After validating that induction of RavZ expression decreases LC3 levels, as shown by immunoblot (Fig. S2b), we induced RavZ activity and infected the cells with HAstV-1. After infection with HAstV-1, we collected RNA from cells and supernatants for quantification of HAstV-1 genome copies at 24 hpi. There was no change in genome copies in the absence of LC3 lipidation activity, suggesting that LC3 lipidation machinery and production of LC3-II are not required for astrovirus replication (Fig. 4E)

Transcriptional changes in autophagy machinery occur in astrovirus-infected cells in vitro and in vivo

Finally, to determine if there were changes in autophagy gene expression specifically in astrovirus-infected cells, we performed single-cell RNA sequencing on astrovirus-infected Caco-2 cells at 4, 8, and 24 hpi (Table 1). At 24 hpi, most cells in the HAstV-1-infected Caco-2 sample were infected and clustered together (Fig. 5A). To characterize differences between samples at 24 hpi, we utilized Gene Ontology (GO), Kyoto Encyclopedia of Genes and Genomes (KEGG), and Hallmark pathway analyses to determine differences between gene expression pathways in mock, astrovirus-infected, and bystander cell types (Fig. S3). Next, we explored whether autophagy-related genes were dysregulated in the data set across time points and between infected, bystander, and mock groups. The single cell RNA sequencing (scRNA-seq) data set confirmed that the regulation of PI3KC3-associated genes in HAstV-1-infected samples followed the same pattern as the RT-PCR array, increasing over time (Fig. 5B). In addition, upregulation in upstream autophagy pathway genes occurred only in astrovirus-infected but not bystander cells (Fig. 5C).

Using a single-cell RNA sequencing data set previously collected by our laboratory (13), we found that intestines from murine astrovirus-infected mice had an upregulation in Pik3c3 in Murine Astrovirus (MuAstV)-infected but not bystander cells. This data set showed a downregulation in Map1lc3a and its homologs Gabarap and Gabarapl2, as well as Ulk1, Rb1cc1, Atg7, Atg10, Atg5, and Lamp1 in infected but not bystander cells (Fig. 5D). This suggests that murine astrovirus replication could also utilize the PI3K complex but not the LC3 conjugation machinery, for replication in vivo. Future work will address the involvement of the PI3K complex in murine astrovirus replication and whether PI3K could be a therapeutic target for astrovirus infection spanning different species. These

experiments provide evidence that astrovirus infection upregulates certain, but not all, components of autophagy machinery in vitro and in vivo to facilitate viral replication.

Discussion

Here, we show that astrovirus infection induces formation of DMVs, and this process is replication dependent. Formation of these DMVs also requires some, but not all, canonical autophagy machinery. We demonstrate that astrovirus uses the autophagy-specific PI3KC3 complex for formation of DMVs. The PI3K complex initiates phagophore formation and production of PI3P during canonical autophagy (27, 38, 39). Inhibiting this complex either chemically or through siRNA knockdown of complex component Beclin1 greatly reduces astrovirus replication and infectious virus production, as well as formation of DMVs as seen by electron microscopy. VA1 infection is also significantly reduced upon chemical inhibition of PI3KC3, suggesting a strain-spanning mechanism for astrovirus replication.

Previous studies of positive-sense RNA virus replication have shown that canonical LC3 machinery may not be necessary for RNA virus replication using DMVs (21, 29). The LC3 conjugation system is indispensable for canonical, starvation-induced autophagy. It consists of E1- and E3-like proteins ATG5 and ATG7, which work together to conjugate LC3-I to PE to form LC3-II. This crucial step leads to autophagosome maturation (27, 38). Our work is consistent with previous literature, as we also observed that inhibition of LC3 machinery in multiple cell types does not affect astrovirus replication. These data are consistent with recent studies showing that SARS-CoV-2 and HCV utilize the PI3K complex, but not LC3 conjugation machinery for DMV formation and replication (21, 29). Our work suggests that early parts of autophagy machinery are essential for DMV formation, while LC3 conjugation is not required. This is supported by transcriptional data from single-cell RNA sequencing data sets, showing that astrovirus-infected cells upregulate PI3K-associated genes, while bystander and mock-inoculated cells do not in both human and murine data sets. This suggests a species-spanning mechanism.

Without LC3 involvement in the formation of DMVs, it is possible that an LC3 homolog, such as the significantly upregulated GABARAPL1, could be active in the formation of DMVs during astrovirus replication. Notably, while inhibition of PI3K significantly reduces astrovirus replication, it does not ablate replication entirely. One possible explanation for this is that other phosphatidylinositol kinases are also involved in the formation of these DMV replication organelles, such as PI4K (19, 21, 22, 24). Use of a PI4K inhibitor during astrovirus infection could determine whether this is the case.

While it is clear that formation of DMVs during astrovirus infection is replication-dependent, it is not yet determined which parts of the astrovirus genome are necessary for inducing formation of DMVs. Nonstructural proteins alone from other viruses such as HCV and SARS-CoV-2 are sufficient for induction of DMV formation (40–42). Little is known

about the function of astrovirus nonstructural proteins, and it is likely that they play a role in DMV formation (43, 44).

Altogether, our results indicate that astrovirus replication relies upon the formation of DMVs using early autophagy machinery, including the PI3K complex, but not LC3 conjugation machinery. Future studies will address whether the PI3K complex is necessary for astrovirus infection in brain cells, leading to encephalitis in immunocompromised populations. These results emphasize how distinct positive-strand RNA viruses utilize similar mechanisms of replication. Although SARS-CoV-2, HCV, and HAstV-1 are different, their common use of the PI3K machinery implies the possibility of a conserved therapeutic target for many positive-sense RNA viruses. Understanding these replication mechanisms will help to determine future antiviral therapies.

Materials and Methods

Cells and virus propagation

Caco-2 human intestinal adenocarcinoma cell line was obtained from ATCC (HTB-37). Cells were grown in Corning minimum essential medium containing 20% fetal bovine serum (FBS; HyClone), GlutaMax (Gibco), 1 mM sodium pyruvate (Gibco), and penicillin-streptomycin (Fisher).

The Huh-7.5 RavZ inducible cell line was a generous gift from Brett Lindenbach's lab at the Yale School of Medicine. These cells were grown in Dulbecco's Modified Eagle Medium (DMEM) (ThermoFisher) containing 10% FBS (HyClone) and 3 µg/mL puromycin (Invitrogen).

HAstV-1 and VA1 lab-adapted viral stocks were propagated in Caco-2 cells. Viral titer was quantified using focus-forming unit assay (FFU) as previously described (45). For UV inactivation experiments, a UV cross-linker was utilized to subject HAstV-1 to 100 mJ/cm2, and inactivation was confirmed using FFU assay.

Transmission electron microscopy

Caco-2 cells were plated in a six-well plate (3.5×10^5). After 46 h, appropriate samples were treated with 10 µM PIK-III or DMSO. Two hours later, cells were inoculated with supernatants taken from HAstV-1 (Multiplicity of infection (MOI) 10) or mock-inoculated Caco-2 cells in serum-free media for 1 h. Following virus adsorption, inoculum was replaced with either fresh media, media containing 10 µM PIK-III, or media containing DMSO. At 8, 12, 24, or 36 hpi, cells were fixed in 2.5% glutaraldehyde/2% paraformaldehyde (PFA) in 0.1 M Cacodylate Buffer. Following fixation, samples were post fixed in osmium tetroxide and contrasted with aqueous uranyl acetate. Samples were dehydrated by an ascending series of ethanol to 100% followed by 100% propylene oxide. Samples were infiltrated with EmBed-812 and polymerized at 60°C. Embedded samples were sectioned at 70 nm

on a Leica (Wetzlar, Germany) ultramicrotome and examined in a ThermoFisher Scientific (Hillsboro, OR) TF20 transmission electron microscope at 80 kV. Digital micrographs were captured with an Advanced Microscopy Techniques (Woburn, MA, USA) imaging system. Unless otherwise indicated, all reagents are from Electron Microscopy Sciences (Hatfield, PA, USA).

RT2 profiler

Caco-2 cells were plated in a six-well plate (3.5×10^5). After 48 h, cells were inoculated with supernatants taken from HAstV-1 (MOI 10) or mock-inoculated Caco-2 cells in serum-free media for 1 h. Following virus adsorption, the inoculum was replaced with fresh media. At 2, 8, and 24 hpi, cell supernatants were collected in TRIzol for liquid samples (LS). Cells were collected in TRIzol, and RNA was extracted from all samples per manufacturer's instructions. RNA quality was checked using Thermo Scientific NanoDrop 2000 per manufacturer's instructions. Then, qRT-PCR was performed on supernatant RNA to determine genome copies of HAstV-1 in supernatants, as previously described (46). We confirmed that genome copies of astrovirus increased in HAstV-1-infected cell supernatants over time, and no genome copies were detected in mock-inoculated cell supernatants. Then, RNA from cells was reverse transcribed using the RT2 First Strand Kit from Qiagen (Qiagen 330401). After cDNA was collected, it was utilized with SYBR Green qPCR Mastermix (Qiagen 330500) in a custom-designed real-time RT2 Profiler PCR Array (Qiagen 330171). Cycle threshold (CT) values were collected, and data analysis was performed using Qiagen's data analysis web portal (http://www.qiagen.com/geneglobe). In addition, we have found that astrovirus induces epithelial to mesenchymal transition, reducing epithelial markers on Caco-2 cells later in infection (47). It has also been shown that IDO1 is upregulated during astrovirus infection (48). Thus, IDO1 and EpCAM were included in the panel to verify normal cellular response to astrovirus infection.

Mock and HAstV-1-treated samples were designated as control and test groups, respectively. All samples passed quality checks. Reference genes were included in the RT2 panel, and data were normalized to these genes. The Qiagen data analysis protocol included fold change/regulation calculations based on $\Delta\Delta$CT calculations. Statistical analysis on the Qiagen web portal utilized a Student's t-test to calculate P-values, where parametric, unpaired, two-sample equal variance, two-tailed distribution was utilized.

10x single-cell RNA sequencing sample preparation

Caco-2 cells were plated in a six-well plate (3.5×10^5). Samples were assigned to wells corresponding to 4, 8, or 24 h post-infection. At 48 h post-plating, 24 hpi cell wells were inoculated with supernatants taken from HAstV-1 (MOI 10) or mock-inoculated Caco-2 cells in serum-free media for 1 h. After virus adsorption, the inoculum was replaced with fresh media. At 64 h post-plating, 8 hpi cell wells were inoculated with supernatants taken from HAstV-1 (MOI 10) or mock-inoculated Caco-2 cells in serum-free media for 1 h. After

virus adsorption, the inoculum was replaced with fresh media. At 68 h post-plating, 4 hpi cell wells were inoculated with supernatants taken from HAstV-1 (MOI 10) or mock-inoculated Caco-2 cells in serum-free media for 1 h. After virus adsorption, the inoculum was replaced with fresh media. At 72 h post-plating, all cells were washed with phosphate buffered saline (PBS) and harvested using trypsin. Cells were filtered through at 70 µm cell strainer. Cells were spun down at 1,200 rpm for 10 min at 4°C. Cells were washed in cell wash buffer (1% bovine serum albumin (BSA) in PBS) and spun down again at 1,200 rpm for 10 min at 4°C. Finally, cells were resuspended in 50 µL of cell wash buffer and counted using a hemocytometer. Cells were resuspended in appropriate volume to reach 1,000 cells/µL. Next, 9,000 cells were loaded onto the 10× Genomics Chromium controller for partitioning of single cells into gel beads with a goal of recovering 6,000 cells. Next, using a 10× Genomics 3′ Gene Expression Kit (version 3.1) according to manufacturer's instructions, single-cell transcriptomics libraries were produced. Libraries were sequenced using Illumina NovaSeq 2000 at suggested sequencing lengths and depths.

10x single-cell RNA sequencing analysis

The 10× transcriptomics data were first processed using CellRanger count (version 6.1.1, 10× Genomics). GRCh38 was used as our reference, which was altered to include the human astrovirus 1 genome (accession ID MK059949.1). Samples were aggregated and normalized by the median number of mapped reads per identified cell using CellRanger aggr. Normalized gene expression matrices were then imported into Seurat (version 4.1.1) for downstream analysis and data visualization.

Data were first filtered by excluding any gene that was not present in at least 0.1% of total called cells (23 cells). Cells that exhibited extremes in the total number of transcripts expressed (>6,000), the total number of genes expressed (<400 or >3,000), or mitochondrial gene expression (>8%) were then excluded from downstream analyses. Data were log-normalized using default parameters. We identified the top 2,000 variable features using the variance-stabilizing transformation (VST) method.

The fastMNN algorithm was then utilized to integrate data sets from distinct libraries, effectively minimizing subject- and sample-specific differences in order to identify similar transcriptional subsets. The first 25 fastMNN dimensions were used for Uniform Manifold Approximation and Projection (UMAP) dimensionality reduction and for nearest-neighbor graph construction for identifying transcriptional clusters in Seurat. Markers for each cluster were identified using FindAllMarkers function (min.pct = 0.25, logfc.threshold = 0.25).

We also generated a subset for 24 hpi samples alone. This subset was processed as described above. We split cells in the 24 hpi infected group to two sub-groups: "HAstV1-Infected" included cells that detected at least one astrovirus gene, "HAstV1-Bystander"

included cells that did not detect astrovirus gene. Over-representation analysis was performed using clusterProfiler (function: Function enrichGO, enrichKEGG, and enricher) to explore the biological and molecular functions of each group (49).

Immunofluorescent staining

For PIK-III experiments, Caco-2 cells were plated in a 96-well plate (2.5×10^4). At 46 h post-plating, appropriate wells were treated with 5, 10, or 25 µM PIK-III or DMSO control. At 48 h post-plating, cells were inoculated with supernatants taken from HAstV-1 (MOI 10) or mock-inoculated Caco-2 cells in serum-free media for 1 h. Following virus adsorption, the inoculum was replaced with fresh media or media containing 5, 10, or 25 µM PIK-III or DMSO control. At 24 hpi, cells were fixed in 100% methanol. Cells were washed in PBS and incubated in primary antibody solution containing astrovirus capsid monoclonal antibody 8e7 (Invitrogen MA5-16293) at 1:100 in % normal goat serum (NGS)/PBS for 1 h at room temperature. Cells were washed in PBS. Cells were incubated in secondary antibody solution containing Alexa Fluor 488 goat anti-Mouse (Invitrogen A10680) at 1:1,000 and and Hoechst (ThermoFisher H3569) at 1:2,000 in 1% NGS/PBS for 45 min in the dark. Cells were again washed in PBS. Samples were imaged using the EVOS FL cell imaging system and analyzed using ImageJ 2.9.0/1.53t software. FFU was calculated as previously described (45). The same method was used for supernatants from PIK-III- and DMSO-treated cell supernatants used to infect fresh Caco-2 cells in a 96-well plate.

For siRNA experiments, Caco-2 cells were plated in a 96-well plate (1.5×10^4). At 24 h post-plating, appropriate wells were treated with 15 µM siRNA (Atg5, Beclin, or Control siRNA). Cells were allowed to incubate in the siRNA-containing media for 2 days for optimal knockdown. At 48 h post-treatment with siRNA, cells were inoculated with supernatants taken from HAstV-1-infected (MOI 10) Caco-2 cells in serum-free media for 1 h. Following virus adsorption, the inoculum was replaced with fresh media. At 24 hpi, cells were fixed in 100% methanol. Cells were washed in PBS and incubated in primary antibody solution containing astrovirus capsid monoclonal antibody 8e7 (Invitrogen MA5-16293) at 1:100 in 1% NGS/PBS for 1 h at room temperature. Cells were washed in PBS. Cells were incubated in secondary antibody solution containing Alexa Fluor 488 goat anti-Mouse (Invitrogen A10680) at 1:1,000 and and Hoechst (ThermoFisher H3569) at 1:2,000 in 1% NGS/PBS for 45 min in the dark. Cells were again washed in PBS. Samples were imaged using the EVOS FL cell imaging system and analyzed using ImageJ 2.9.0/1.53t software. FFU was calculated as previously described (45). The same method was used for supernatants from PIK-III- and DMSO-treated cell supernatants used to infect fresh Caco-2 cells in a 96-well plate.

Immunoblotting

Caco-2 cells were plated in a six-well plate (3.5×10^5). At 48 h post-plating, cells were inoculated with supernatants taken from HAstV-1 (MOI 10) or mock-inoculated Caco-2

cells in serum-free media for 1 h. Following virus adsorption, inoculum was replaced with fresh media. At the proper time point, 8 or 24 hpi, cells were collected in 250 µL radioimmunoprecipitation assay (RIPA) lysis buffer (Abcam) containing 1× protease inhibitor cocktail (Pierce) on ice. Samples were vortexed briefly and kept on ice for 30 min. Samples were frozen at –80°C until used. Sample protein concentration was determined using BCA Protein Assay Kit (Pierce). Equal concentrations of protein were prepared under reducing conditions and separated by sodium dodecyl sulfate-polyacrylamide gel electrophoresis (4%–20% tris-glycine 1.0 mm Mini Protein Gels from Invitrogen (XP04200BOX). Gels were transferred to polyvinylidene fluoride (PVDF) membranes using the iBlot 2 transfer stacks (ThermoFisher IB24002). Membranes were probed for protein with respective primary antibodies and IRDye 680RD goat anti-rabbit IgG secondary antibody using the ThermoFisher iBind device according to manufacturer's instructions. Primary antibodies included β-Actin (Cell Signaling 4970S) at 1:1,000, Atg5 (Abcam ab108327) at 1:1,000, and Atg7 (Abcam ab52472) at 1:1,000.

For siRNA experiments, Caco-2 cells were plated in a six-well plate (2.5×10^5). At 24 h post-plating, appropriate wells were treated with 15 µM siRNA (Atg5, Beclin, or Control siRNA). Cells were allowed to incubate in the siRNA-containing media for 2 days for optimal knockdown. At 48 h post-treatment with siRNA, cells were inoculated with supernatants taken from HAstV-1-infected (MOI 10) Caco-2 cells in serum-free media for 1 h. Following virus adsorption, the inoculum was replaced with fresh media. At 24 hpi, cells were collected in 250 µL RIPA lysis buffer (Abcam) containing 1× protease inhibitor cocktail (Pierce) on ice. Samples were vortexed briefly and kept on ice for 30 min. Samples were frozen at –80°C until used. Gels were run using the same protocol as above. Primary antibodies included β-Actin (Cell Signaling 4970S) at 1:1,000, Atg5 (Abcam ab108327) at 1:1,000, and Beclin (Abcam ab207612) at 1:1,000.

For Huh-7.5 immunoblots, Huh-7.5 cells were plated in a six-well plate (3×10^5). After 48 h, cells were treated with 1.5 µM or 6 µM doxycycline to induce RavZ protease activity or DMSO controls. At 24 h post-treatment, cells were inoculated with supernatants taken from HAstV-1-infected (MOI 10) Caco-2 cells in serum-free media for 1 h. Following virus adsorption, the inoculum was replaced with media containing the appropriate concentration of doxycycline or DMSO, as well as 30 µM chloroquine to enable monitor monitoring of LC3-II/LC3-I (50). At 24 hpi, cells were collected in 250 µL RIPA lysis buffer (Abcam) containing 1× protease inhibitor cocktail (Pierce) on ice. Samples were vortexed briefly and kept on ice for 30 min. Samples were frozen at –80°C until used. Sample protein concentration was determined using BCA Protein Assay Kit (Pierce). Immunoblots were performed the same way as described with Caco-2 cell lysates. Membranes were probed for LC3 (Cell Signaling 2775S) at 1:1,000 overnight at 4°C in 5% BSA/tris-buffered saline and Tween 20 (TBST). The following day, membranes were incubated in secondary antibody solution containing IRDye 680RD goat anti-rabbit IgG secondary antibody in 5% BSA/TBST for 1 h at room temperature. Membranes were imaged on the LI-COR Odyssey Fc (software version number 1.0.36). Next, membranes were stained for β-Actin (Cell Signaling 4970S) at

1:1,000 using the ThermoFisher iBind device as described above. All immunoblots were performed in triplicate. Each blot was imaged on the LI-COR Odyssey Fc. Densitometry was measured using Image Studio version 5.2 software.

PIK-III, siRNA, and astrovirus infection RT-PCR

For PIK-III experiments, Caco-2 cells were plated in a 96-well plate (2.5×10^4). At 48 h post-plating, cells were inoculated with supernatants taken from HAstV-1 (MOI 10) or mock-inoculated Caco-2 cells in serum-free media for 1 h. Following virus adsorption, the inoculum was replaced with fresh media or media containing 5, 10, or 25 µM PIK-III or DMSO control. At 24 hpi, supernatants were collected in TRIzol LS, cells were collected in TRIzol, and RNA was extracted per manufacturer's instructions. RNA was then utilized in RT-PCR to determine astrovirus genome copies, as previously described (46).

For siRNA experiments, Caco-2 cells were plated in a six-well plate (2.5×10^5). At 24 h post-plating, appropriate wells were treated with 15 µM siRNA (Atg5, Beclin, or Control siRNA). Cells were allowed to incubate in the siRNA-containing media for 2 days for optimal knockdown. At 48 h post-treatment with siRNA, cells were inoculated with supernatants taken from HAstV-1-infected (MOI 10) Caco-2 cells in serum-free media for 1 h. Following virus adsorption, the inoculum was replaced with fresh media. At 24 hpi, cells were collected in TRIzol, and RNA was extracted per manufacturer's instructions. RNA was then utilized in RT-PCR to determine astrovirus genome copies, as previously described (46).

Huh-7.5 Rav-Z Induction

Huh-7.5 cells were plated in a six-well plate (3×10^5). After 48 h, cells were treated with 3 µM doxycycline to induce RavZ protease activity or DMSO control. At 24 h post-treat treatment, cells were inoculated with supernatants taken from HAstV-1-infected (MOI 10) Caco-2 cells in serum-free media for 1 h. Following virus adsorption, the inoculum was replaced with media containing the appropriate concentration of doxycycline or DMSO. At 24 hpi, supernatants were collected in TRIzol LS, and cells were collected in TRIzol. RNA was extracted from these samples according to the manufacturer's instructions. RNA was then utilized in RT-PCR to determine astrovirus genome copies, as previously described (46).

MuAstV 10x data set

The murine astrovirus 10× single-cell RNA sequencing data set was collected previously, as described (13).

Statistical analysis

Data were analyzed by two-way ANOVA followed by Tukey's multiple comparisons test (western blots, PIK-III genome copies, and PIK-III FFU analysis) or unpaired two-tailed t-test (Huh-7.5 cell genome copies and DMV electron microscopy quantification) quantification)to determine statistical significance using GraphPad Prism version 9. Asterisks show statistical significance as follows: *, $P \leq 0.05$; **, $P \leq 0.01$; ***, $P \leq 0.001$.

Acknowledgments

Electron microscopy images were acquired with the help of Dr. Cam Robinson and Nathan Kurtz using the Electron Microscopy Shared Resource (SJCRH/ALSAC and NCI P30 CA021765). These studies were supported by an NIAID grant 1R03AI166434-01 and funding from ALSAC to S.S.C., K22 AI156116 to V.C., and NIAID grant R21 AI20113 to B.L.

Authorship Contributions

Theresa Bub, Conceptualization, Data curation, Formal analysis, Investigation, Methodology, Supervision, Writing – original draft, Writing – review and editing | Virginia Hargest, Data curation, Methodology, Writing – review and editing | Shaoyuan Tan, Formal analysis, Methodology, Writing – original draft, Writing – review and editing | Maria Smith, Data curation, Methodology, Writing – review and editing | Ana Vazquez-Pagan, Data curation, Methodology, Writing – review and editing | Tim Flerlage, Data curation, Methodology, Writing – review and editing | Pamela Brigleb, Methodology, Writing – review and editing | Victoria Meliopoulos, Methodology, Writing – review and editing | Brett Lindenbach, Methodology | Harish N. Ramanathan, Methodology, Resources | Valerie Cortez, Data curation, Writing – review and editing | Jeremy Chase Crawford, Data curation, Formal analysis, Methodology, Writing – review and editing | Stacey Schultz-Cherry, Conceptualization, Formal analysis, Funding acquisition, Investigation, Methodology, Project administration, Supervision, Writing – original draft, Writing – review and editing

Funding

Data Availability

The scRNA-seq data generated in this work is available at accession ID MK059949.1. Murine scRNA-seq can be accessed in NCBI BioProject with accession code PRJNA573959.

Funder	Grant(s)	Author(s)
HHS | NIH | National Institute of Allergy and Infectious Diseases (NIAID)	1R03AI166434-01	Stacey Schultz-Cherry
American Lebanese Syrian Associated Charities (ALSAC)		Stacey Schultz-Cherry
HHS | NIH | National Institute of Allergy and Infectious Diseases (NIAID)	AI156116	Valerie Cortez

Figure Legends

Figure 1. Astrovirus associates with DMVs during infection. (A) TEM images of mock-inoculated or HAstV-1-infected Caco-2 cells at 12, 24, and 36 hours post-infection (hpi). (B) TEM images of UV-inactive HAstV-1-inoculated Caco-2 cells and HAstV-1-infected Caco-2 cells at 24 hpi. (A & B) Yellow arrows indicate (DMVs).

Figure 2. Inhibition of the PI3K complex reduces astrovirus replication. (A) TEM of PIK-III-treated and DMSO control HAstV-1-infected Caco-2 cells at 24 hpi and quantification of number of DMVs. Arrows indicate DMVs. Statistical analysis was by unpaired two-tailed t test. ***, $P \leq 0.001$. (B) HAstV-1-infected Caco-2 cells were either pre-treated for 2 hours prior to infection or treated 1 hpi with 5, 10, or 25 µM PIK-III or DMSO control. EVOS microscope images represent Caco-2 cells treated at 1 hpi, with astrovirus capsid in green and nucleus (Hoechst) in blue. Quantification shows FFU of samples treated 2 hours before infection and 1 hpi with statistical analysis by two-way ANOVA followed by Tukey's multiple comparison test. (C) Genome copy number of human astrovirus in cell lysate and supernatant at 24 hpi from HAstV-1-infected Caco-2 cells treated with 5, 10, or 25 µM PIK-III or DMSO control at 1hpi with statistical analysis by two-way ANOVA followed by Tukey's multiple comparison test. (D) Supernatants from HAstV-1-infected Caco-2 cells treated with 5, 10, or 25 µM PIK-III or DMSO control were collected and trypsin-treated at 24 hpi. Supernatants were used to infect Caco-2 cells. EVOS images show astrovirus capsid (green) and nucleus (Hoechst, blue). Quantification of FFU fold change to average DMSO control is shown. *, $P \leq 0.05$; **, $P \leq 0.01$; ***, $P \leq 0.001$.

Figure 3. Knockdown of Beclin1 reduces astrovirus replication. (A) Representative immunoblot and quantification of immunoblots for Beclin expression after siBeclin knockdown compared to siControl with statistical analysis by unpaired two-tailed t test. (B) Genome copy number of human astrovirus in cell lysate at 24 hpi from HAstV-1-infected Caco-2 cells treated with either siBeclin or siControl with statistical analysis by unpaired two-tailed t test (C-D) Caco-2 cells were treated with siBeclin or siControl 24 hours after plating, once cells had reached 70% confluency. At 48 hours post-treatment with siRNAs,

Caco-2 cells were infected with HAstV-1. At 24 hpi, Caco-2 cells were fixed. (C) EVOS microscope images show astrovirus capsid in green and nucleus (Hoechst) in blue. Quantification shows FFU with statistical analysis by unpaired two-tailed t test. (D) EVOS microscope images show astrovirus double-stranded RNA (J2) in green and nucleus (Hoechst) in blue. Quantification shows FFU with statistical analysis by unpaired two-tailed t test.

Figure 4. LC3 conjugation machinery is not required for astrovirus replication. (A) Heat map of gene fold regulation from RT2 profiler dataset. (B) Immunoblot showing expression of ATG5 and ATG7 at 8 and 24 hpi in mock-inoculated and HAstV-1-infected Caco-2 cell lysates. Quantification of 8h and 24h time points was performed with statistical analysis by two-way ANOVA followed by Tukey's multiple comparison test. (C) Genome copy number of human astrovirus in cell lysate at 24 hpi from HAstV-1-infected Caco-2 cells treated with either siATG5 or siControl with statistical analysis by unpaired two-tailed t test. (D) Caco-2 cells were treated with siATG5 or siControl 24 hours after plating, once cells had reached 70% confluency. At 48 hours post-treatment with siRNAs, Caco-2 cells were infected with HAstV-1. At 24 hpi, Caco-2 cells were fixed. Quantification shows FFU for astrovirus capsid and double-stranded RNA (J2) with statistical analysis by unpaired two-tailed t test. (E) Genome copies per µL of astrovirus in cell lysate and supernatant RNA collected from HAstV-1-infected Huh-7.5 cells, where cells treated with doxycycline had induced RavZ protease activity. Statistical analysis was by unpaired two-tailed t test.

Figure 5. Changes in autophagy-related genes in astrovirus-infected cells in human and murine single cell RNA sequencing datasets. (A) UMAP showing clustering of HAstV-1 and Mock 4, 8, and 24 hpi samples (B) Dot plot showing percent expression and average expression of autophagy-related genes in HAstV-1-infected Caco-2 cell samples at 4, 8, and 24 hpi from 10X single cell RNA sequencing dataset. (C) Dot plot showing percent expression and average expression of autophagy-related genes in HAstV-1-infected Caco-2 cells, HAstV-1 uninfected (bystander) Caco-2 cells, and mock-inoculated Caco-2 cells at 24 hpi from 10X single cell RNA sequencing dataset. (D) Dot plot showing percent expression and average expression of autophagy-related genes in MuAstV-infected, MuAstV uninfected (bystander), and mock-inoculated cells at 24 hpi from 10X single cell RNA sequencing murine astrovirus dataset (13).

References

1. Bosch A, Pintó RM, Guix S. 2014. Human Astroviruses. Clin Microbiol Rev 27:1048–1074.

2. Cortez V, Meliopoulos VA, Karlsson EA, Hargest V, Johnson C, Schultz-Cherry S. 2017. Astrovirus Biology and Pathogenesis. Annu Rev Virol 4:327–348.

3. Méndez E, Murillo A, Velázquez R, Burnham A, Arias CF. 2012. Replication Cycle of Astroviruses. Astrovirus Res 19–45.

4. Moser L, Schultz-Cherry S. 2008. Astroviruses. Encycl Virol 204–210.

5. Brinker JP, Blacklow NR, Herrmann JE. 2000. Human astrovirus isolation and propagation in multiple cell lines. Arch Virol 145:1847–1856.

6. Guix S, Bosch A, Pintó RM. 2008. Astrovirus Replication: An Overview, p. 571–595. In Structure-Based Study of Viral Replication. WORLD SCIENTIFIC.

7. Vu D-L, Bosch A, Pintó RM, Ribes E, Guix S. 2019. Human Astrovirus MLB Replication In Vitro: Persistence in Extraintestinal Cell Lines. J Virol 93:e00557-19.

8. Hargest V, Davis AE, Tan S, Cortez V, Schultz-Cherry S. 2021. Human Astroviruses: A Tale of Two Strains. Viruses 13:376.

9. Koci MD, Moser LA, Kelley LA, Larsen D, Brown CC, Schultz-Cherry S. 2003. Astrovirus Induces Diarrhea in the Absence of Inflammation and Cell Death. J Virol 77:11798–11808.

10. Marvin SA. 2016. The Immune Response to Astrovirus Infection. Viruses 9:1.

11. Vu D-L, Cordey S, Brito F, Kaiser L. 2016. Novel human astroviruses: Novel human diseases? J Clin Virol Off Publ Pan Am Soc Clin Virol 82:56–63.

12. Vu D-L, Bosch A, Pintó RM, Guix S. 2017. Epidemiology of Classic and Novel Human Astrovirus: Gastroenteritis and Beyond. Viruses 9:33.

13. Cortez V, Boyd DF, Crawford JC, Sharp B, Livingston B, Rowe HM, Davis A, Alsallaq R, Robinson CG, Vogel P, Rosch JW, Margolis E, Thomas PG, Schultz-Cherry S. 2020. Astrovirus infects actively secreting goblet cells and alters the gut mucus barrier. 1. Nat Commun 11:2097.

14. Finkbeiner SR, Holtz LR, Jiang Y, Rajendran P, Franz CJ, Zhao G, Kang G, Wang D. 2009. Human stool contains a previously unrecognized diversity of novel astroviruses. Virol J 6:161.

15. Blanchard E, Roingeard P. 2015. Virus-induced double-membrane vesicles. Cell Microbiol 17:45–50.

16. Hsu N-Y, Ilnytska O, Belov G, Santiana M, Chen Y-H, Takvorian PM, Pau C, van der Schaar H, Kaushik-Basu N, Balla T, Cameron CE, Ehrenfeld E, van Kuppeveld FJM, Altan-Bonnet N. 2010. Viral Reorganization of the Secretory Pathway Generates Distinct Organelles for RNA Replication. Cell 141:799–811.

17. Kirkegaard K, Taylor MP, Jackson WT. 2004. Cellular autophagy: surrender, avoidance and subversion by microorganisms. Nat Rev Microbiol 2:301–314.

18. Limpens RWAL, van der Schaar HM, Kumar D, Koster AJ, Snijder EJ, van Kuppeveld FJM, Bárcena M. 2011. The Transformation of Enterovirus Replication Structures: a Three-Dimensional Study of Single- and Double-Membrane Compartments. mBio 2:e00166-11.

19. Roingeard P, Eymieux S, Burlaud-Gaillard J, Hourioux C, Patient R, Blanchard E. 2022. The double-membrane vesicle (DMV): a virus-induced organelle dedicated to the replication of SARS-CoV-2 and other positive-sense single-stranded RNA viruses. Cell Mol Life Sci 79:425.

20. Suhy DA, Giddings TH, Kirkegaard K. 2000. Remodeling the Endoplasmic Reticulum by Poliovirus Infection and by Individual Viral Proteins: an Autophagy-Like Origin for Virus-Induced Vesicles. J Virol 74:8953–8965.

21. Twu W-I, Lee J-Y, Kim H, Prasad V, Cerikan B, Haselmann U, Tabata K, Bartenschlager R. 2021. Contribution of autophagy machinery factors to HCV and SARS-CoV-2 replication organelle formation. Cell Rep 37.

22. Wolff G, Melia CE, Snijder EJ, Bárcena M. 2020. Double-Membrane Vesicles as Platforms for Viral Replication. Trends Microbiol 28:1022–1033.

23. Choi Y, Bowman JW, Jung JU. 2018. Autophagy during viral infection — a double-edged sword. 6. Nat Rev Microbiol 16:341–354.

24. Kudchodkar SB, Levine B. 2009. Viruses and autophagy. Rev Med Virol 19:359–378.

25. Mao J, Lin E, He L, Yu J, Tan P, Zhou Y. 2019. Autophagy and Viral Infection. Autophagy Regul Innate Immun 1209:55–78.

26. Stolz A, Ernst A, Dikic I. 2014. Cargo recognition and trafficking in selective autophagy. Nat Cell Biol 16:495–501.

27. Codogno P, Mehrpour M, Proikas-Cezanne T. 2012. Canonical and non-canonical autophagy: variations on a common theme of self-eating? 1. Nat Rev Mol Cell Biol 13:7–12.

28. Knoops K, Kikkert M, van den Worm SHE, Zevenhoven-Dobbe JC, van der Meer Y, Koster AJ, Mommaas AM, Snijder EJ. 2008. SARS-Coronavirus Replication Is Supported by a Reticulovesicular Network of Modified Endoplasmic Reticulum. PLoS Biol 6:e226.

29. Fahmy AM, Khabir M, Blanchet M, Labonté P. 2018. LC3B is not recruited along with the autophagy elongation complex (ATG5-12/16L1) at HCV replication site and is dispensable for viral replication. PLoS ONE 13:e0205189.

30. Delorme-Axford E, Morosky S, Bomberger J, Stolz DB, Jackson WT, Coyne CB. 2014. BPIFB3 Regulates Autophagy and Coxsackievirus B Replication through a Noncanonical Pathway Independent of the Core Initiation Machinery. mBio 5:e02147-14.

31. Harris KG, Morosky SA, Drummond C, Patel M, Kim C, Stolz DB, Bergelson JM, Cherry S, Coyne CB. 2015. RIP3 regulates autophagy and promotes Coxsackievirus B3 infection of intestinal epithelial cells. Cell Host Microbe 18:221–232.

32. Mohamud Y, Shi J, Tang H, Xiang P, Xue YC, Liu H, Ng CS, Luo H. 2020. Coxsackievirus infection induces a non-canonical autophagy independent of the ULK and PI3K complexes. 1. Sci Rep 10:19068.

33. Gray EW, Angus KW, Snodgrass DR. 1980. Ultrastructure of the Small Intestine in Astrovirus-infected Lambs. J Gen Virol 49:71–82.

34. Tange S, Zhou Y, Nagakui-Noguchi Y, Imai T, Nakanishi A. 2013. Initiation of human astrovirus type 1 infection was blocked by inhibitors of phosphoinositide 3-kinase. Virol J 10:153.

35. Yu X, Long YC, Shen H-M. 2015. Differential regulatory functions of three classes of phosphatidylinositol and phosphoinositide 3-kinases in autophagy. Autophagy 11:1711–1728.

36. Choy A, Dancourt J, Mugo B, O'Connor TJ, Isberg RR, Melia TJ, Roy CR. 2012. The Legionella effector RavZ inhibits host autophagy through irreversible Atg8 deconjugation. Science 338:1072–1076.

37. Sherwood RK, Roy CR. 2016. Autophagy Evasion and Endoplasmic Reticulum Subversion: The Yin and Yang of Legionella Intracellular Infection. Annu Rev Microbiol 70:413–433.

38. Lamb CA, Yoshimori T, Tooze SA. 2013. The autophagosome: origins unknown, biogenesis complex. Nat Rev Mol Cell Biol 14:759–774.

39. Corona Velazquez AF, Jackson WT. 2018. So Many Roads: the Multifaceted Regulation of Autophagy Induction. Mol Cell Biol 38:e00303-18.

40. Oudshoorn D, Rijs K, Limpens RWAL, Groen K, Koster AJ, Snijder EJ, Kikkert M, Bárcena M. 2017. Expression and Cleavage of Middle East Respiratory Syndrome Coronavirus nsp3-4 Polyprotein Induce the Formation of Double-Membrane Vesicles That Mimic Those Associated with Coronaviral RNA Replication. mBio 8:e01658-17.

41. Romero-Brey I, Merz A, Chiramel A, Lee J-Y, Chlanda P, Haselman U, Santarella-Mellwig R, Habermann A, Hoppe S, Kallis S, Walther P, Antony C, Krijnse-Locker J, Bartenschlager R. 2012. Three-Dimensional Architecture and Biogenesis of Membrane Structures Associated with Hepatitis C Virus Replication. PLoS Pathog 8:e1003056.

42. Romero-Brey I, Berger C, Kallis S, Kolovou A, Paul D, Lohmann V, Bartenschlager R. 2015. NS5A Domain 1 and Polyprotein Cleavage Kinetics Are Critical for Induction of Double-Membrane Vesicles Associated with Hepatitis C Virus Replication. mBio 6:e00759-15.

43. Guix S, Caballero S, Bosch A, Pintó RM. 2004. C-Terminal nsP1a Protein of Human Astrovirus Colocalizes with the Endoplasmic Reticulum and Viral RNA. J Virol 78:13627–13636.

44. Méndez E, Aguirre-Crespo G, Zavala G, Arias CF. 2007. Association of the Astrovirus Structural Protein VP90 with Membranes Plays a Role in Virus Morphogenesis. J Virol 81:10649–10658.

45. Marvin S, Meliopoulos V, Schultz-Cherry S. 2014. Human Astrovirus Propagation, Purification and Quantification. BIO-Protoc 4.

46. Gu Z, Zhu H, Rodriguez A, Mhaissen M, Schultz-Cherry S, Adderson E, Hayden RT. 2015. Comparative Evaluation of Broad-Panel PCR Assays for the Detection of Gastrointestinal Pathogens in Pediatric Oncology Patients. J Mol Diagn 17:715–721.

47. Hargest V, Bub T, Neale G, Schultz-Cherry S. 2022. Astrovirus-induced epithelial-mesenchymal transition via activated TGF-β increases viral replication. PLoS Pathog 18:e1009716.

48. Cortez V, Livingston B, Sharp B, Hargest V, Papizan JB, Pedicino N, Lanning S, Jordan SV, Gulman J, Vogel P, DuBois RM, Crawford JC, Boyd DF, Pruett-Miller SM, Thomas PG, Schultz-Cherry S. 2023. Indoleamine 2,3-dioxygenase 1 regulates cell permissivity to astrovirus infection. Mucosal Immunol S1933-0219(23)00042–9.

49. Wu T, Hu E, Xu S, Chen M, Guo P, Dai Z, Feng T, Zhou L, Tang W, Zhan L, Fu X, Liu S, Bo X, Yu G. 2021. clusterProfiler 4.0: A universal enrichment tool for interpreting omics data. Innov Camb Mass 2:100141.

50. Klionsky DJ, Abdalla FC, Abeliovich H, Abraham RT, Acevedo-Arozena A, Adeli K, Agholme L, Agnello M, Agostinis P, Aguirre-Ghiso JA, Ahn HJ, Ait-Mohamed O, Ait-Si-Ali S, Akematsu T, Akira S, Al-Younes HM, Al-Zeer MA, Albert ML, Albin RL, Alegre-Abarrategui J, Aleo MF, Alirezaei M, Almasan A, Almonte-Becerril M, Amano A, Amaravadi RK, Amarnath S, Amer AO, Andrieu-Abadie N, Anantharam V, Ann DK, Anoopkumar-Dukie S, Aoki H, Apostolova N, Arancia G, Aris JP, Asanuma K, Asare NYO, Ashida H, Askanas V, Askew DS, Auberger P, Baba M, Backues SK, Baehrecke EH, Bahr BA, Bai X-Y, Bailly Y, Baiocchi R, Baldini G, Balduini W, Ballabio A, Bamber BA, Bampton ETW, Juhász G, Bartholomew CR, Bassham DC, Bast RC, Batoko H, Bay B-H, Beau I, Béchet DM, Begley TJ, Behl C, Behrends C, Bekri S, Bellaire B, Bendall LJ, Benetti L, Berliocchi L, Bernardi H, Bernassola F, Besteiro S, Bhatia-Kissova I, Bi X, Biard-Piechaczyk M, Blum JS, Boise LH, Bonaldo P, Boone DL, Bornhauser BC, Bortoluci KR, Bossis I, Bost F, Bourquin J-P, Boya P, Boyer-Guittaut M, Bozhkov PV, Brady NR, Brancolini C, Brech A, Brenman JE, Brennand A, Bresnick EH, Brest P, Bridges D, Bristol ML, Brookes PS, Brown EJ, Brumell JH, Brunetti-Pierri N, Brunk UT, Bulman DE, Bultman SJ, Bultynck G, Burbulla LF, Bursch W, Butchar JP, Buzgariu W, Bydlowski SP, Cadwell K, Cahová M, Cai D, Cai J, Cai Q, Calabretta B, Calvo-Garrido J, Camougrand N, Campanella M, Campos-Salinas J, Candi E, Cao L, Caplan AB, Carding SR, Cardoso SM, Carew JS, Carlin CR, Carmignac V, Carneiro LAM, Carra S, Caruso RA, Casari G, Casas C, Castino R, Cebollero E, Cecconi F, Celli J, Chaachouay H, Chae H-J, Chai C-Y, Chan DC, Chan EY, Chang RC-C, Che C-M, Chen C-C, Chen G-C, Chen G-Q, Chen M, Chen Q, Chen SS-L, Chen W, Chen X, Chen X, Chen X,

Chen Y-G, Chen Y, Chen Y, Chen Y-J, Chen Z, Cheng A, Cheng CHK, Cheng Y, Cheong H, Cheong J-H, Cherry S, Chess-Williams R, Cheung ZH, Chevet E, Chiang H-L, Chiarelli R, Chiba T, Chin L-S, Chiou S-H, Chisari FV, Cho CH, Cho D-H, Choi AMK, Choi D, Choi KS, Choi ME, Chouaib S, Choubey D, Choubey V, Chu CT, Chuang T-H, Chueh S-H, Chun T, Chwae Y-J, Chye M-L, Ciarcia R, Ciriolo MR, Clague MJ, Clark RSB, Clarke PGH, Clarke R, Codogno P, Coller HA, Colombo MI, Comincini S, Condello M, Condorelli F, Cookson MR, Coombs GH, Coppens I, Corbalan R, Cossart P, Costelli P, Costes S, Coto-Montes A, Couve E, Coxon FP, Cregg JM, Crespo JL, Cronjé MJ, Cuervo AM, Cullen JJ, Czaja MJ, D'Amelio M, Darfeuille-Michaud A, Davids LM, Davies FE, De Felici M, de Groot JF, de Haan CAM, De Martino L, De Milito A, De Tata V, Debnath J, Degterev A, Dehay B, Delbridge LMD, Demarchi F, Deng YZ, Dengjel J, Dent P, Denton D, Deretic V, Desai SD, Devenish RJ, Di Gioacchino M, Di Paolo G, Di Pietro C, Díaz-Araya G, Díaz-Laviada I, Diaz-Meco MT, Diaz-Nido J, Dikic I, Dinesh-Kumar SP, Ding W-X, Distelhorst CW, Diwan A, Djavaheri-Mergny M, Dokudovskaya S, Dong Z, Dorsey FC, Dosenko V, Dowling JJ, Doxsey S, Dreux M, Drew ME, Duan Q, Duchosal MA, Duff KE, Dugail I, Durbeej M, Duszenko M, Edelstein CL, Edinger AL, Egea G, Eichinger L, Eissa NT, Ekmekcioglu S, El-Deiry WS, Elazar Z, Elgendy M, Ellerby LM, Eng KE, Engelbrecht A-M, Engelender S, Erenpreisa J, Escalante R, Esclatine A, Eskelinen E-L, Espert L, Espina V, Fan H, Fan J, Fan Q-W, Fan Z, Fang S, Fang Y, Fanto M, Fanzani A, Farkas T, Farre J-C, Faure M, Fechheimer M, Feng CG, Feng J, Feng Q, Feng Y, Fésüs L, Feuer R, Figueiredo-Pereira ME, Fimia GM, Fingar DC, Finkbeiner S, Finkel T, Finley KD, Fiorito F, Fisher EA, Fisher PB, Flajolet M, Florez-McClure ML, Florio S, Fon EA, Fornai F, Fortunato F, Fotedar R, Fowler DH, Fox HS, Franco R, Frankel LB, Fransen M, Fuentes JM, Fueyo J, Fujii J, Fujisaki K, Fujita E, Fukuda M, Furukawa RH, Gaestel M, Gailly P, Gajewska M, Galliot B, Galy V, Ganesh S, Ganetzky B, Ganley IG, Gao F-B, Gao GF, Gao J, Garcia L, Garcia-Manero G, Garcia-Marcos M, Garmyn M, Gartel AL, Gatti E, Gautel M, Gawriluk TR, Gegg ME, Geng J, Germain M, Gestwicki JE, Gewirtz DA, Ghavami S, Ghosh P, Giammarioli AM, Giatromanolaki AN, Gibson SB, Gilkerson RW, Ginger ML, Ginsberg HN, Golab J, Goligorsky MS, Golstein P, Gomez-Manzano C, Goncu E, Gongora C, Gonzalez CD, Gonzalez R, González-Estévez C, González-Polo RA, Gonzalez-Rey E, Gorbunov NV, Gorski S, Goruppi S, Gottlieb RA, Gozuacik D, Granato GE, Grant GD, Green KN, Gregorc A, Gros F, Grose C, Grunt TW, Gual P, Guan J-L, Guan K-L, Guichard SM, Gukovskaya AS, Gukovsky I, Gunst J, Gustafsson ÅB, Halayko AJ, Hale AN, Halonen SK, Hamasaki M, Han F, Han T, Hancock MK, Hansen M, Harada H, Harada M, Hardt SE, Harper JW, Harris AL, Harris J, Harris SD, Hashimoto M, Haspel JA, Hayashi S, Hazelhurst LA, He C, He Y-W, Hébert M-J, Heidenreich KA, Helfrich MH, Helgason GV, Henske EP, Herman B, Herman PK, Hetz C, Hilfiker S, Hill JA, Hocking LJ, Hofman P, Hofmann TG, Höhfeld J, Holyoake TL, Hong M-H, Hood DA, Hotamisligil GS, Houwerzijl EJ, Høyer-Hansen M, Hu B, Hu CA, Hu H-M, Hua Y, Huang C, Huang J, Huang S, Huang W-P, Huber TB, Huh W-K, Hung T-H, Hupp TR, Hur GM, Hurley JB, Hussain SNA, Hussey PJ, Hwang JJ, Hwang S, Ichihara A, Ilkhanizadeh S, Inoki K, Into T, Iovane V, Iovanna JL, Ip NY, Isaka Y, Ishida H, Isidoro C, Isobe K, Iwasaki A, Izquierdo M, Izumi Y, Jaakkola PM, Jäättelä M, Jackson GR, Jackson WT, Janji B, Jendrach M, Jeon

J-H, Jeung E-B, Jiang H, Jiang H, Jiang JX, Jiang M, Jiang Q, Jiang X, Jiang X, Jiménez A, Jin M, Jin SV, Joe CO, Johansen T, Johnson DE, Johnson GVW, Jones NL, Joseph B, Joseph SK, Joubert AM, Juhász G, Juillerat-Jeanneret L, Jung CH, Jung Y-K, Kaarniranta K, Kaasik A, Kabuta T, Kadowaki M, Kågedal K, Kamada Y, Kaminskyy VO, Kampinga HH, Kanamori H, Kang C, Kang KB, Kang KI, Kang R, Kang Y-A, Kanki T, Kanneganti T-D, Kanno H, Kanthasamy AG, Kanthasamy A, Karantza V, Kaushal GP, Kaushik S, Kawazoe Y, Ke P-Y, Kehrl JH, Kelekar A, Kerkhoff C, Kessel DH, Khalil H, Kiel JAKW, Kiger AA, Kihara A, Kim DR, Kim D-H, Kim D-H, Kim E-K, Kim H-R, Kim J-S, Kim JH, Kim JC, Kim JK, Kim PK, Kim SW, Kim Y-S, Kim Y, Kimchi A, Kimmelman AC, King JS, Kinsella TJ, Kirkin V, Kirshenbaum LA, Kitamoto K, Kitazato K, Klein L, Klimecki WT, Klucken J, Knecht E, Ko BCB, Koch JC, Koga H, Koh J-Y, Koh YH, Koike M, Komatsu M, Kominami E, Kong HJ, Kong W-J, Korolchuk VI, Kotake Y, Koukourakis MI, Flores JBK, Kovács AL, Kraft C, Krainc D, Krämer H, Kretz-Remy C, Krichevsky AM, Kroemer G, Krüger R, Krut O, Ktistakis NT, Kuan C-Y, Kucharczyk R, Kumar A, Kumar R, Kumar S, Kundu M, Kung H-J, Kurz T, Kwon HJ, La Spada AR, Lafont F, Lamark T, Landry J, Lane JD, Lapaquette P, Laporte JF, László L, Lavandero S, Lavoie JN, Layfield R, Lazo PA, Le W, Le Cam L, Ledbetter DJ, Lee AJX, Lee B-W, Lee GM, Lee J, lee J, Lee M, Lee M-S, Lee SH, Leeuwenburgh C, Legembre P, Legouis R, Lehmann M, Lei H-Y, Lei Q-Y, Leib DA, Leiro J, Lemasters JJ, Lemoine A, Lesniak MS, Lev D, Levenson VV, Levine B, Levy E, Li F, Li J-L, Li L, Li S, Li W, Li X-J, Li Y-B, Li Y-P, Liang C, Liang Q, Liao Y-F, Liberski PP, Lieberman A, Lim HJ, Lim K-L, Lim K, Lin C-F, Lin F-C, Lin J, Lin JD, Lin K, Lin W-W, Lin W-C, Lin Y-L, Linden R, Lingor P, Lippincott-Schwartz J, Lisanti MP, Liton PB, Liu B, Liu C-F, Liu K, Liu L, Liu QA, Liu W, Liu Y-C, Liu Y, Lockshin RA, Lok C-N, Lonial S, Loos B, Lopez-Berestein G, López-Otín C, Lossi L, Lotze MT, Low P, Lu B, Lu B, Lu B, Lu Z, Luciano F, Lukacs NW, Lund AH, Lynch-Day MA, Ma Y, Macian F, MacKeigan JP, Macleod KF, Madeo F, Maiuri L, Maiuri MC, Malagoli D, Malicdan MCV, Malorni W, Man N, Mandelkow E-M, Manon S, Manov I, Mao K, Mao X, Mao Z, Marambaud P, Marazziti D, Marcel YL, Marchbank K, Marchetti P, Marciniak SJ, Marcondes M, Mardi M, Marfe G, Mariño G, Markaki M, Marten MR, Martin SJ, Martinand-Mari C, Martinet W, Martinez-Vicente M, Masini M, Matarrese P, Matsuo S, Matteoni R, Mayer A, Mazure NM, McConkey DJ, McConnell MJ, McDermott C, McDonald C, McInerney GM, McKenna SL, McLaughlin B, McLean PJ, McMaster CR, McQuibban GA, Meijer AJ, Meisler MH, Meléndez A, Melia TJ, Melino G, Mena MA, Menendez JA, Menna-Barreto RFS, Menon MB, Menzies FM, Mercer CA, Merighi A, Merry DE, Meschini S, Meyer CG, Meyer TF, Miao C-Y, Miao J-Y, Michels PAM, Michiels C, Mijaljica D, Milojkovic A, Minucci S, Miracco C, Miranti CK, Mitroulis I, Miyazawa K, Mizushima N, Mograbi B, Mohseni S, Molero X, Mollereau B, Mollinedo F, Momoi T, Monastyrska I, Monick MM, Monteiro MJ, Moore MN, Mora R, Moreau K, Moreira PI, Moriyasu Y, Moscat J, Mostowy S, Mottram JC, Motyl T, Moussa CE-H, Müller S, Muller S, Münger K, Münz C, Murphy LO, Murphy ME, Musarò A, Mysorekar I, Nagata E, Nagata K, Nahimana A, Nair U, Nakagawa T, Nakahira K, Nakano H, Nakatogawa H, Nanjundan M, Naqvi NI, Narendra DP, Narita M, Navarro M, Nawrocki ST, Nazarko TY, Nemchenko A, Netea MG, Neufeld TP, Ney PA, Nezis IP, Nguyen HP, Nie D, Nishino I, Nislow C, Nixon RA, Noda T, Noegel AA, Nogalska

A, Noguchi S, Notterpek L, Novak I, Nozaki T, Nukina N, Nürnberger T, Nyfeler B, Obara K, Oberley TD, Oddo S, Ogawa M, Ohashi T, Okamoto K, Oleinick NL, Oliver FJ, Olsen LJ, Olsson S, Opota O, Osborne TF, Ostrander GK, Otsu K, Ou JJ, Ouimet M, Overholtzer M, Ozpolat B, Paganetti P, Pagnini U, Pallet N, Palmer GE, Palumbo C, Pan T, Panaretakis T, Pandey UB, Papackova Z, Papassideri I, Paris I, Park J, Park OK, Parys JB, Parzych KR, Patschan S, Patterson C, Pattingre S, Pawelek JM, Peng J, Perlmutter DH, Perrotta I, Perry G, Pervaiz S, Peter M, Peters GJ, Petersen M, Petrovski G, Phang JM, Piacentini M, Pierre P, Pierrefite-Carle V, Pierron G, Pinkas-Kramarski R, Piras A, Piri N, Platanias LC, Pöggeler S, Poirot M, Poletti A, Poüs C, Pozuelo-Rubio M, Prætorius-Ibba M, Prasad A, Prescott M, Priault M, Produit-Zengaffinen N, Progulske-Fox A, Proikas-Cezanne T, Przedborski S, Przyklenk K, Puertollano R, Puyal J, Qian S-B, Qin L, Qin Z-H, Quaggin SE, Raben N, Rabinowich H, Rabkin SW, Rahman I, Rami A, Ramm G, Randall G, Randow F, Rao VA, Rathmell JC, Ravikumar B, Ray SK, Reed BH, Reed JC, Reggiori F, Régnier-Vigouroux A, Reichert AS, Reiners JJ, Reiter RJ, Ren J, Revuelta JL, Rhodes CJ, Ritis K, Rizzo E, Robbins J, Roberge M, Roca H, Roccheri MC, Rocchi S, Rodemann HP, Rodríguez de Córdoba S, Rohrer B, Roninson IB, Rosen K, Rost-Roszkowska MM, Rouis M, Rouschop KMA, Rovetta F, Rubin BP, Rubinsztein DC, Ruckdeschel K, Rucker EB, Rudich A, Rudolf E, Ruiz-Opazo N, Russo R, Rusten TE, Ryan KM, Ryter SW, Sabatini DM, Sadoshima J, Saha T, Saitoh T, Sakagami H, Sakai Y, Salekdeh GH, Salomoni P, Salvaterra PM, Salvesen G, Salvioli R, Sanchez AMJ, Sánchez-Alcázar JA, Sánchez-Prieto R, Sandri M, Sankar U, Sansanwal P, Santambrogio L, Saran S, Sarkar S, Sarwal M, Sasakawa C, Sasnauskiene A, Sass M, Sato K, Sato M, Schapira AHV, Scharl M, Schätzl HM, Scheper W, Schiaffino S, Schneider C, Schneider ME, Schneider-Stock R, Schoenlein PV, Schorderet DF, Schüller C, Schwartz GK, Scorrano L, Sealy L, Seglen PO, Segura-Aguilar J, Seiliez I, Seleverstov O, Sell C, Seo JB, Separovic D, Setaluri V, Setoguchi T, Settembre C, Shacka JJ, Shanmugam M, Shapiro IM, Shaulian E, Shaw RJ, Shelhamer JH, Shen H-M, Shen W-C, Sheng Z-H, Shi Y, Shibuya K, Shidoji Y, Shieh J-J, Shih C-M, Shimada Y, Shimizu S, Shintani T, Shirihai OS, Shore GC, Sibirny AA, Sidhu SB, Sikorska B, Silva-Zacarin ECM, Simmons A, Simon AK, Simon H-U, Simone C, Simonsen A, Sinclair DA, Singh R, Sinha D, Sinicrope FA, Sirko A, Siu PM, Sivridis E, Skop V, Skulachev VP, Slack RS, Smaili SS, Smith DR, Soengas MS, Soldati T, Song X, Sood AK, Soong TW, Sotgia F, Spector SA, Spies CD, Springer W, Srinivasula SM, Stefanis L, Steffan JS, Stendel R, Stenmark H, Stephanou A, Stern ST, Sternberg C, Stork B, Strålfors P, Subauste CS, Sui X, Sulzer D, Sun J, Sun S-Y, Sun Z-J, Sung JJY, Suzuki K, Suzuki T, Swanson MS, Swanton C, Sweeney ST, Sy L-K, Szabadkai G, Tabas I, Taegtmeyer H, Tafani M, Takács-Vellai K, Takano Y, Takegawa K, Takemura G, Takeshita F, Talbot NJ, Tan KSW, Tanaka K, Tanaka K, Tang D, Tang D, Tanida I, Tannous BA, Tavernarakis N, Taylor GS, Taylor GA, Taylor JP, Terada LS, Terman A, Tettamanti G, Thevissen K, Thompson CB, Thorburn A, Thumm M, Tian F, Tian Y, Tocchini-Valentini G, Tolkovsky AM, Tomino Y, Tönges L, Tooze SA, Tournier C, Tower J, Towns R, Trajkovic V, Travassos LH, Tsai T-F, Tschan MP, Tsubata T, Tsung A, Turk B, Turner LS, Tyagi SC, Uchiyama Y, Ueno T, Umekawa M, Umemiya-Shirafuji R, Unni VK, Vaccaro MI, Valente EM, Van den Berghe G, van der Klei IJ, van Doorn WG, van Dyk LF, van Egmond M, van Grunsven LA, Vandenabeele P,

Vandenberghe WP, Vanhorebeek I, Vaquero EC, Velasco G, Vellai T, Vicencio JM, Vierstra RD, Vila M, Vindis C, Viola G, Viscomi MT, Voitsekhovskaja OV, von Haefen C, Votruba M, Wada K, Wade-Martins R, Walker CL, Walsh CM, Walter J, Wan X-B, Wang A, Wang C, Wang D, Wang F, Wang F, Wang G, Wang H, Wang H-G, Wang H-D, Wang J, Wang K, Wang M, Wang RC, Wang X, Wang XJ, Wang Y-J, Wang Y, Wang Z-B, Wang ZC, Wang Z, Wansink DG, Ward DM, Watada H, Waters SL, Webster P, Wei L, Weihl CC, Weiss WA, Welford SM, Wen L-P, Whitehouse CA, Whitton JL, Whitworth AJ, Wileman T, Wiley JW, Wilkinson S, Willbold D, Williams RL, Williamson PR, Wouters BG, Wu C, Wu D-C, Wu WKK, Wyttenbach A, Xavier RJ, Xi Z, Xia P, Xiao G, Xie Z, Xie Z, Xu D, Xu J, Xu L, Xu X, Yamamoto A, Yamamoto A, Yamashina S, Yamashita M, Yan X, Yanagida M, Yang D-S, Yang E, Yang J-M, Yang SY, Yang W, Yang WY, Yang Z, Yao M-C, Yao T-P, Yeganeh B, Yen W-L, Yin J-J, Yin X-M, Yoo O-J, Yoon G, Yoon S-Y, Yorimitsu T, Yoshikawa Y, Yoshimori T, Yoshimoto K, You HJ, Youle RJ, Younes A, Yu L, Yu L, Yu S-W, Yu WH, Yuan Z-M, Yue Z, Yun C-H, Yuzaki M, Zabirnyk O, Silva-Zacarin E, Zacks D, Zacksenhaus E, Zaffaroni N, Zakeri Z, Zeh, III HJ, Zeitlin SO, Zhang H, Zhang H-L, Zhang J, Zhang J-P, Zhang L, Zhang L, Zhang M-Y, Zhang XD, Zhao M, Zhao Y-F, Zhao Y, Zhao ZJ, Zheng X, Zhivotovsky B, Zhong Q, Zhou C-Z, Zhu C, Zhu W-G, Zhu X-F, Zhu X, Zhu Y, Zoladek T, Zong W-X, Zorzano A, Zschocke J, Zuckerbraun B. 2012. Guidelines for the use and interpretation of assays for monitoring autophagy. Autophagy 8:445–544.

Supplemental Material

Supplementary Figure 1. Inhibition of the PI3K complex reduces astrovirus replication for multiple human strains (A) HAstV-1-infected Caco-2 cells were either pre-treated for 2 hours prior to infection or treated 1 hpi with 5, 10, or 25 µM PIK-III or DMSO control. EVOS microscope images represent Caco-2 cells treated at 1 hpi, with astrovirus dsRNA (J2) in green and nucleus (Hoechst) in blue. Quantification shows FFU of samples treated 2 hours before infection and 1 hpi with statistical analysis by two-way ANOVA followed by Tukey's multiple comparison test. (B) VA1-infected Caco-2 cells were treated at 1 hpi with 5 or 10 µM PIK-III or DMSO control. EVOS microscope images show VA1 in green and nucleus (Hoechst) in blue. Quantification shows FFU fold change to average DMSO control with statistical analysis by two-way ANOVA followed by Tukey's multiple comparison test.

Supplementary Figure 2. siATG5 knockdown and Huh-7.5 validation. (A) Representative immunoblot and quantification of immunoblots for ATG5 expression after siATG5 knockdown compared to siControl with statistical analysis by unpaired two-tailed t test. (B) Validation of Huh-7.5 LC3 dysregulation upon doxycycline treatment. Immunoblot and quantification of LC3-II/LC3-I expression in cell lysates from Huh-7.5 cells treated with 1.5 or 6 µM doxycycline or DMSO control. (C-D) Caco-2 cells were treated with siATG5 or siControl 24 hours after plating, once cells had reached 70% confluency. At 48 hours post-treatment with siRNAs, Caco-2 cells were infected with HAstV-1. At 24 hpi, Caco-2 cells were fixed. (C) EVOS microscope images show astrovirus capsid in green and nucleus

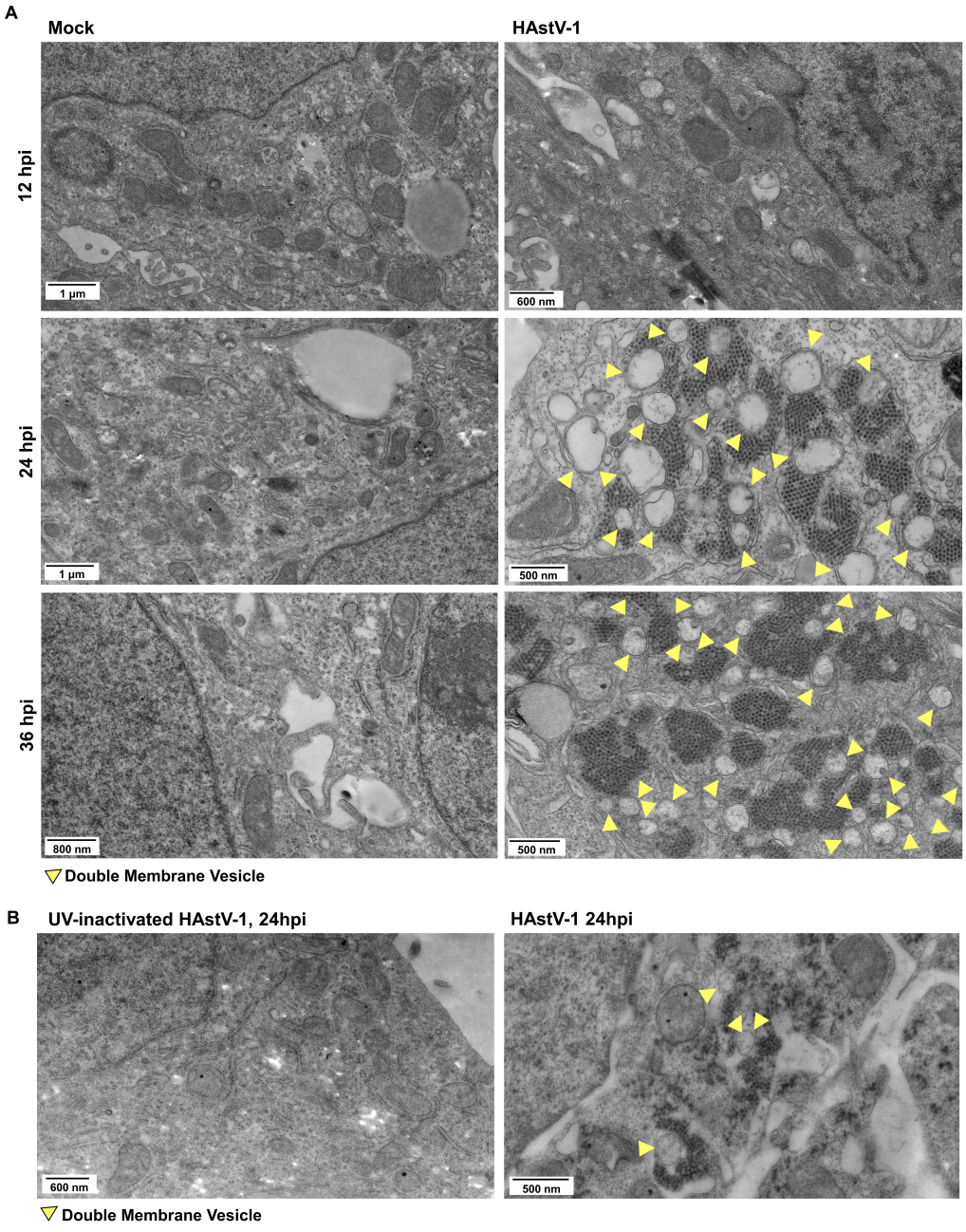
A
Mock
HAstV-1
12 hpi
24 hpi
36 hpi
1 µm
600 nm
1 µm
500 nm
800 nm
500 nm
Double Membrane Vesicle
B
UV-inactivated HAstV-1, 24hpi
HAstV-1 24hpi
600 nm
500 nm
Double Membrane Vesicle

Figure 1

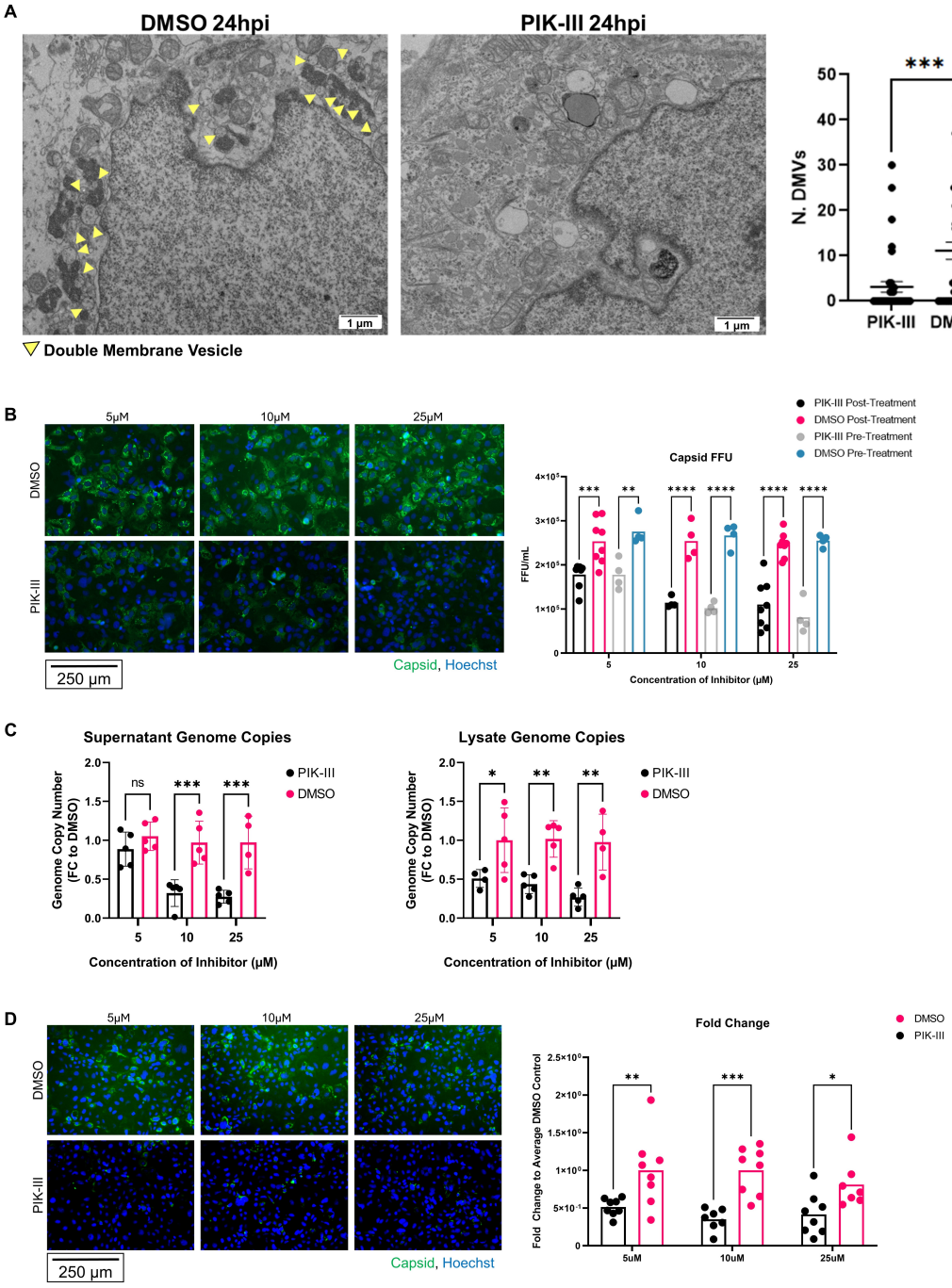
A
DMSO 24hpi
PIK-III 24hpi
1 µm
1 µm
Double Membrane Vesicle
N. DMVs
PIK-III
DMSO
B
5µM
10µM
25µM
DMSO
PIK-III
250 µm
Capsid, Hoechst
PIK-III Post-Treatment
DMSO Post-Treatment
PIK-III Pre-Treatment
DMSO Pre-Treatment
Capsid FFU
FFU/mL
Concentration of Inhibitor (µM)
C
Supernatant Genome Copies
Lysate Genome Copies
Genome Copy Number (FC to DMSO)
PIK-III
DMSO
Concentration of Inhibitor (µM)
D
5µM
10µM
25µM
DMSO
PIK-III
250 µm
Capsid, Hoechst
Fold Change
Fold Change to Average DMSO Control
5uM
10uM
25uM

Figure 2

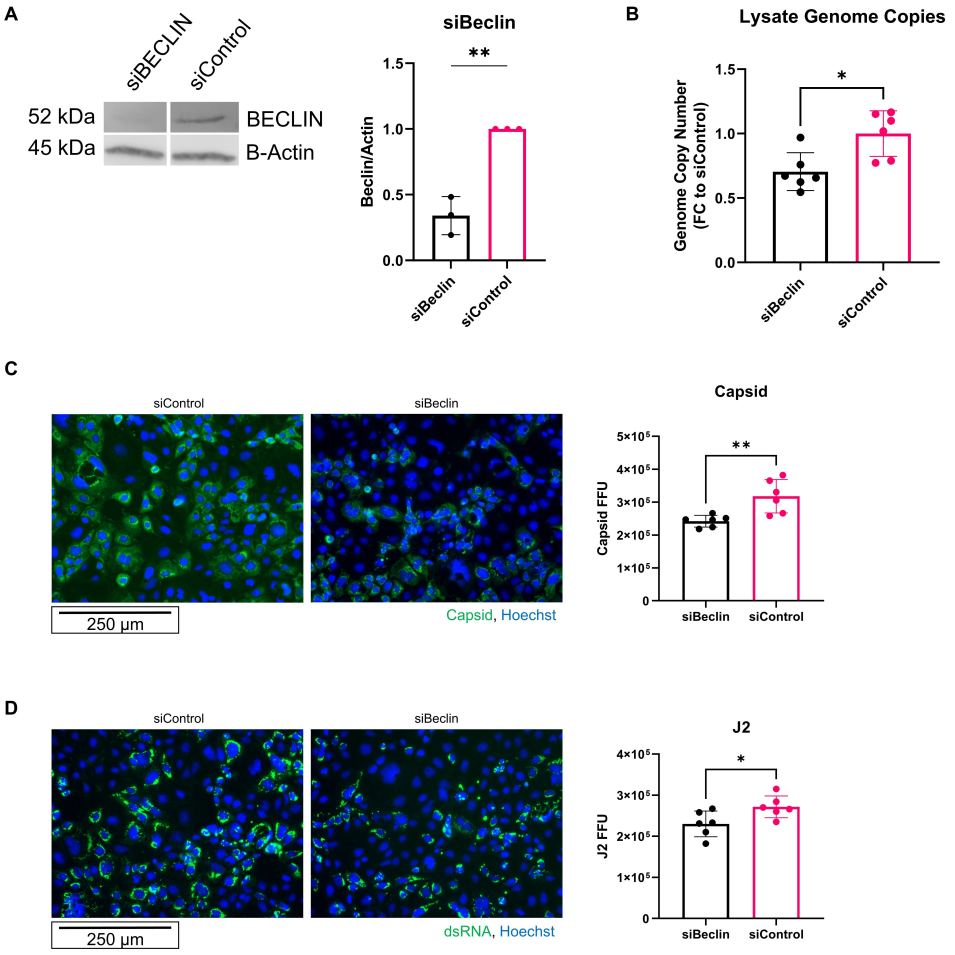
A
siBECLIN
siControl
52 kDa
45 kDa
BECLIN
B-Actin
siBeclin
Beclin/Actin
**
siBeclin
siControl
B
Lysate Genome Copies
Genome Copy Number (FC to siControl)
*
siBeclin
siControl
C
siControl
siBeclin
250 µm
Capsid, Hoechst
Capsid
Capsid FFU
**
siBeclin
siControl
D
siControl
siBeclin
250 µm
dsRNA, Hoechst
J2
J2 FFU
*
siBeclin
siControl

Figure 3

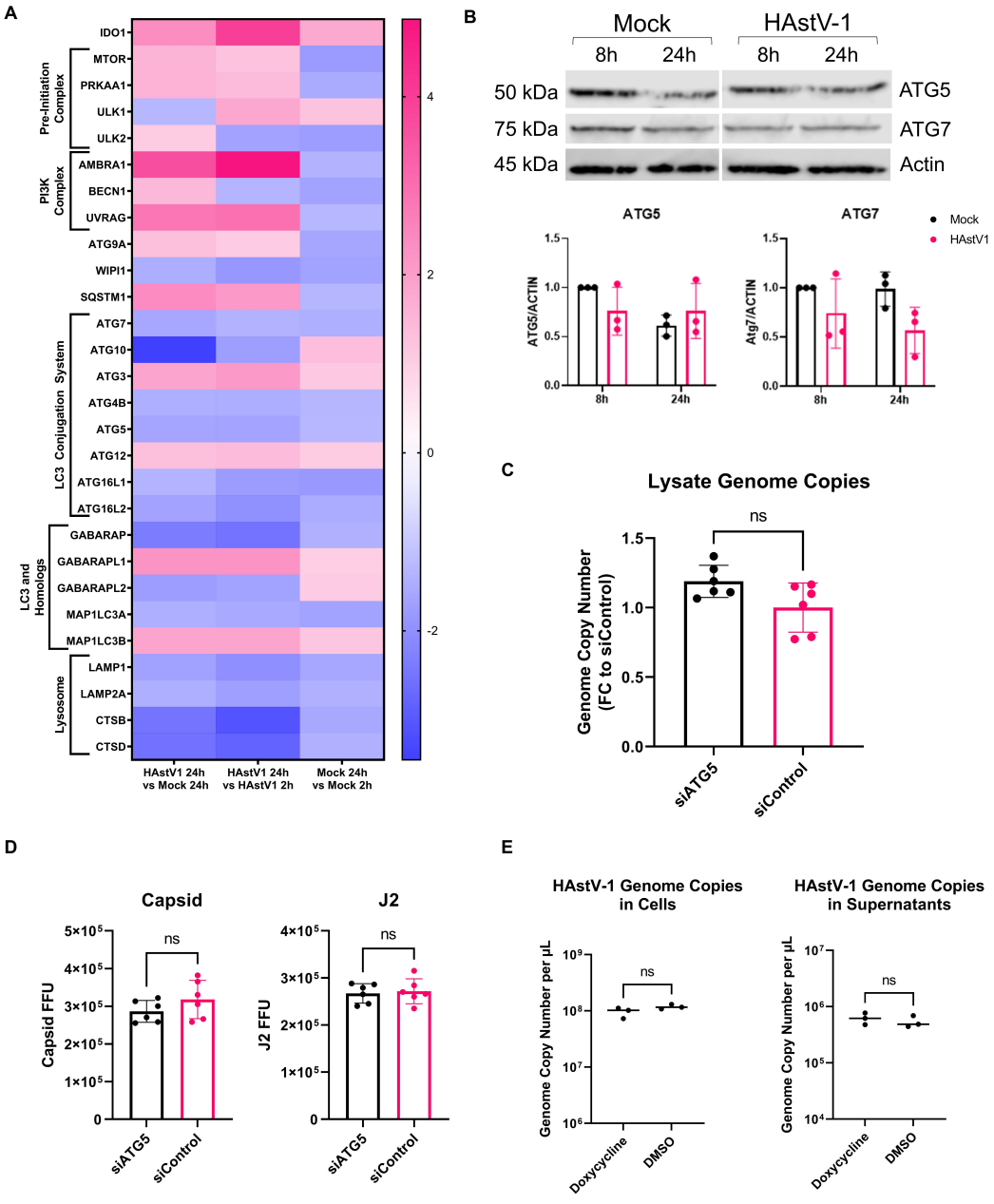
A
IDO1
MTOR
PRKAA1
ULK1
ULK2
Pre-Initiation Complex
AMBRA1
BECN1
UVRAG
PI3K Complex
ATG9A
WIPI1
SQSTM1
ATG7
ATG10
ATG3
ATG4B
ATG5
ATG12
ATG16L1
ATG16L2
LC3 Conjugation System
GABARAP
GABARAPL1
GABARAPL2
MAP1LC3A
MAP1LC3B
LC3 and Homologs
LAMP1
LAMP2A
CTSB
CTSD
Lysosome
HAstV1 24h vs Mock 24h
HAstV1 24h vs HAstV1 2h
Mock 24h vs Mock 2h
4
2
0
-2
B
Mock
HAstV-1
8h
24h
8h
24h
50 kDa
75 kDa
45 kDa
ATG5
ATG7
Actin
ATG5
ATG7
Mock
HAstV1
ATG5/ACTIN
Atg7/ACTIN
1.5
1.0
0.5
0.0
8h
24h
C
Lysate Genome Copies
ns
Genome Copy Number (FC to siControl)
siATG5
siControl
D
Capsid
J2
ns
Capsid FFU
J2 FFU
siATG5
siControl
E
HAstV-1 Genome Copies in Cells
HAstV-1 Genome Copies in Supernatants
Genome Copy Number per µL
ns
Doxycycline
DMSO

Figure 4

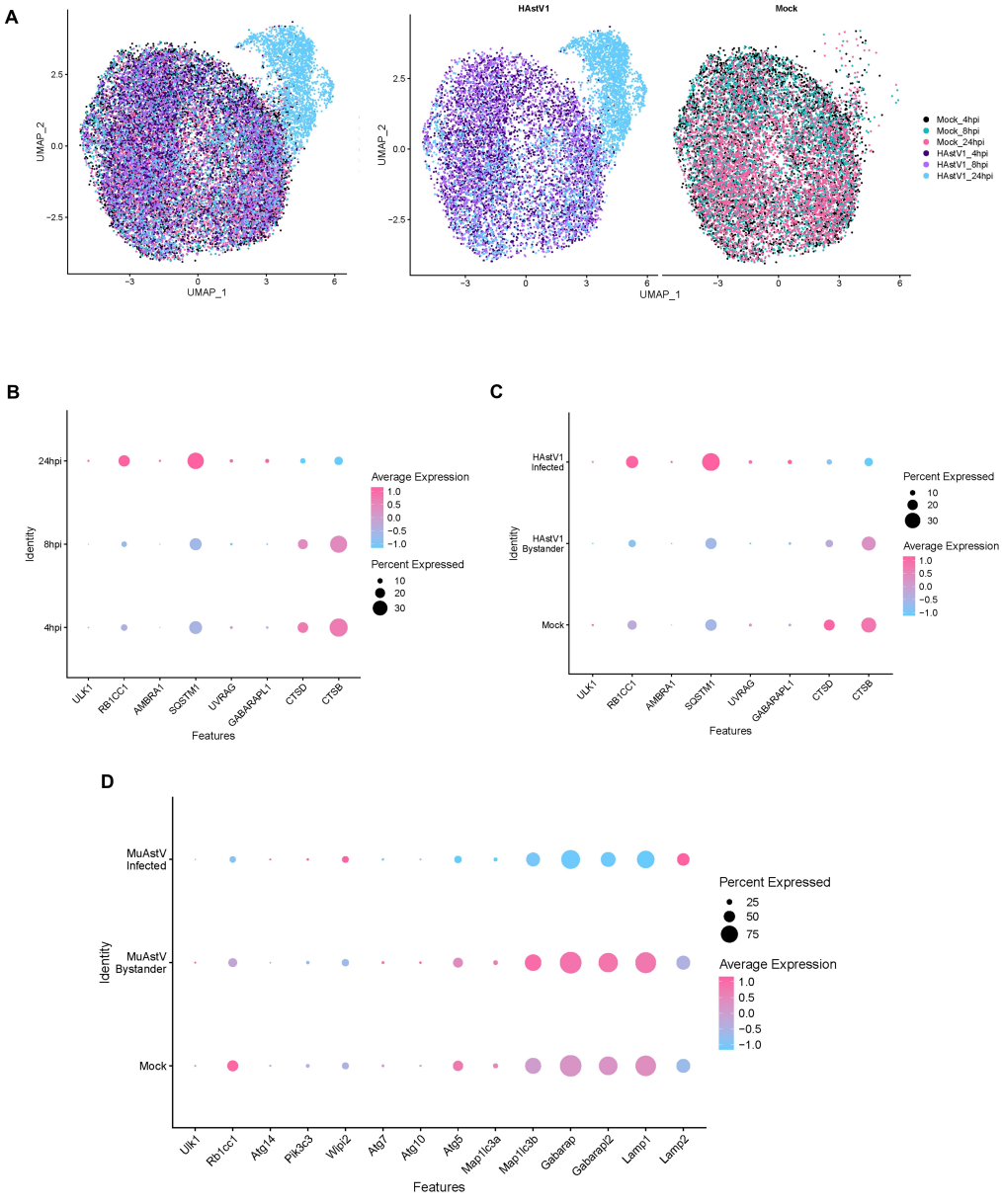
A
HAstV1
Mock
UMAP_2
UMAP_1
Mock_4hpi
Mock_8hpi
Mock_24hpi
HAstV1_4hpi
HAstV1_8hpi
HAstV1_24hpi
B
C
Identity
24hpi
8hpi
4hpi
HAstV1 Infected
HAstV1 Bystander
Mock
Features
ULK1
RB1CC1
AMBRA1
SQSTM1
UVRAG
GABARAPL1
CTSD
CTSB
Average Expression
Percent Expressed
D
MuAstV Infected
MuAstV Bystander
Ulk1
Rb1cc1
Atg14
Plk3c3
Wipi2
Atg7
Atg10
Atg5
Map1lc3a
Map1lc3b
Gabarap
Gabarapl2
Lamp1
Lamp2

Figure 5

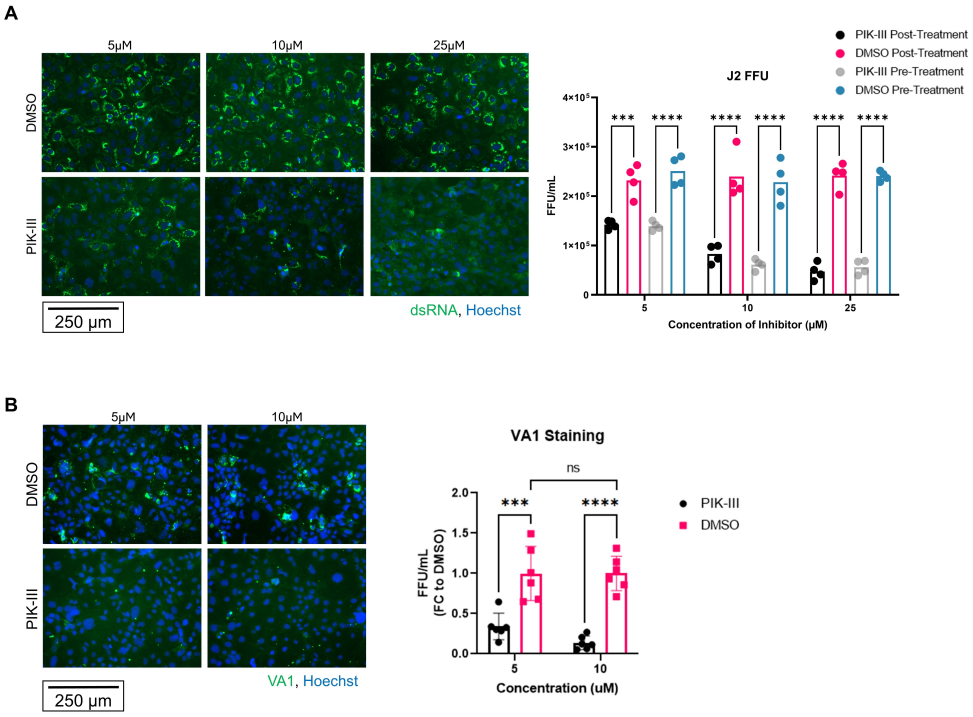
A
5μM
10μM
25μM
DMSO
PIK-III
250 μm
dsRNA, Hoechst
J2 FFU
PIK-III Post-Treatment
DMSO Post-Treatment
PIK-III Pre-Treatment
DMSO Pre-Treatment
FFU/mL
Concentration of Inhibitor (μM)
B
VA1 Staining
ns
FFU/mL (FC to DMSO)
Concentration (uM)
VA1, Hoechst

Figure S1

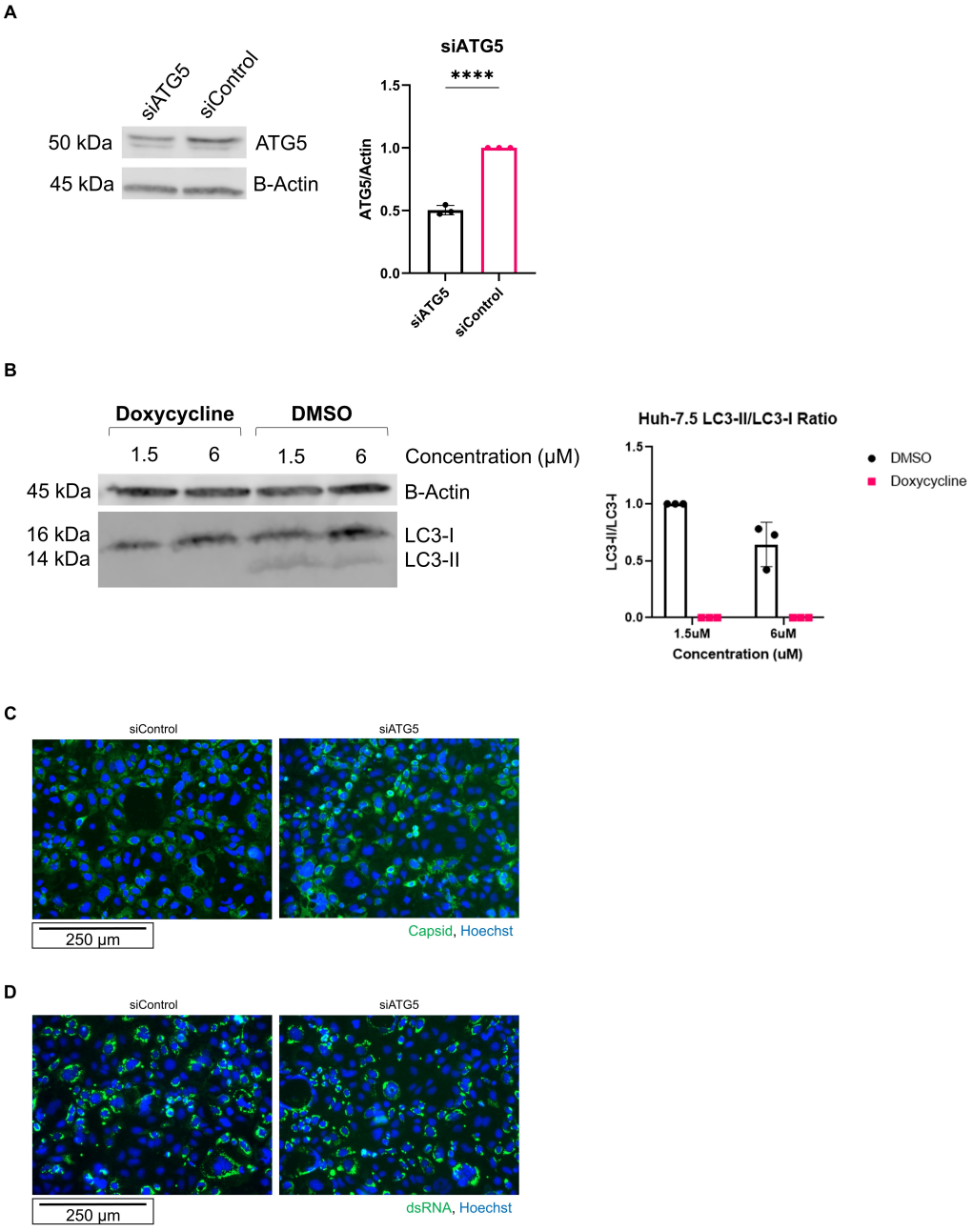
A
siATG5
siControl
50 kDa
ATG5
45 kDa
B-Actin
siATG5
****
ATG5/Actin
1.5
1.0
0.5
0.0
siATG5
siControl
B
Doxycycline
DMSO
1.5
6
1.5
6
Concentration (μM)
45 kDa
B-Actin
16 kDa
14 kDa
LC3-I
LC3-II
Huh-7.5 LC3-II/LC3-I Ratio
DMSO
Doxycycline
LC3-II/LC3-I
1.5
1.0
0.5
0.0
1.5uM
6uM
Concentration (uM)
C
siControl
siATG5
250 μm
Capsid, Hoechst
D
siControl
siATG5
250 μm
dsRNA, Hoechst

Figure S2

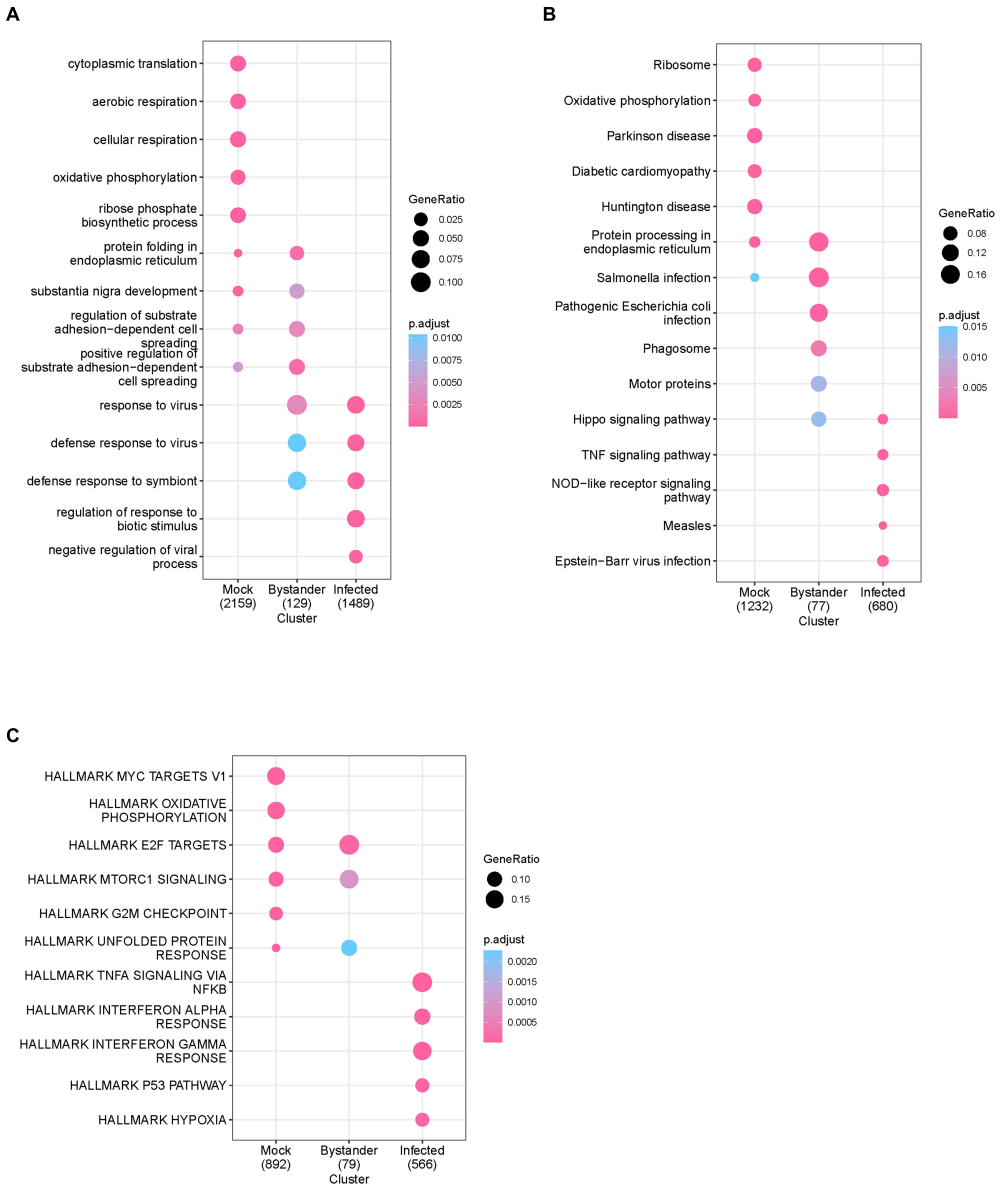
A
cytoplasmic translation
aerobic respiration
cellular respiration
oxidative phosphorylation
ribose phosphate biosynthetic process
protein folding in endoplasmic reticulum
substantia nigra development
regulation of substrate adhesion−dependent cell spreading
positive regulation of substrate adhesion−dependent cell spreading
response to virus
defense response to virus
defense response to symbiont
regulation of response to biotic stimulus
negative regulation of viral process
Mock (2159)
Bystander (129)
Infected (1489)
Cluster
GeneRatio
0.025
0.050
0.075
0.100
p.adjust
0.0100
0.0075
0.0050
0.0025
B
Ribosome
Oxidative phosphorylation
Parkinson disease
Diabetic cardiomyopathy
Huntington disease
Protein processing in endoplasmic reticulum
Salmonella infection
Pathogenic Escherichia coli infection
Phagosome
Motor proteins
Hippo signaling pathway
TNF signaling pathway
NOD−like receptor signaling pathway
Measles
Epstein−Barr virus infection
Mock (1232)
Bystander (77)
Infected (680)
Cluster
GeneRatio
0.08
0.12
0.16
p.adjust
0.015
0.010
0.005
C
HALLMARK MYC TARGETS V1
HALLMARK OXIDATIVE PHOSPHORYLATION
HALLMARK E2F TARGETS
HALLMARK MTORC1 SIGNALING
HALLMARK G2M CHECKPOINT
HALLMARK UNFOLDED PROTEIN RESPONSE
HALLMARK TNFA SIGNALING VIA NFKB
HALLMARK INTERFERON ALPHA RESPONSE
HALLMARK INTERFERON GAMMA RESPONSE
HALLMARK P53 PATHWAY
HALLMARK HYPOXIA
Mock (892)
Bystander (79)
Infected (566)
Cluster
GeneRatio
0.10
0.15
p.adjust
0.0020
0.0015
0.0010
0.0005

Figure S3

Gene	Cluster	avg_log2FC	pct.1	pct.2	p_val_adj
ITM2B	Mock	0.656933	0.785	0.428	0
RPL17	Mock	0.529021	0.943	0.716	0
S100A10	Mock	0.52348	0.916	0.681	0
CD99	Mock	0.5072	0.972	0.786	0
H2AFZ	Mock	0.701308	0.649	0.268	8.89E−265
EPCAM	Mock	0.635118	0.698	0.345	1.78E−252
MIF	Mock	0.636467	0.625	0.27	2.30E − 220
SCD	Mock	0.563748	0.689	0.377	8.00E−201
PTMA	Mock	0.548704	0.725	0.397	1.02E−186
NME2	Mock	0.536384	0.663	0.357	1.60E−171
CST3	Mock	0.544066	0.678	0.387	3.19E−171
TUBA1B	Mock	0.565624	0.604	0.28	6.11E−167
PDIA6	Mock	0.534388	0.433	0.15	8.62E−149
PFN1	Mock	0.526555	0.53	0.247	9.26E−148
TPI1	Mock	0.510377	0.522	0.244	1.72E−138
HAstV1	Infected	2.749525	1	0	0
ZC3HAV1	Infected	1.110522	0.792	0.255	0
IFIT3	Infected	1.061962	0.517	0.039	0
IRF1	Infected	0.981695	0.523	0.041	0
IFI6	Infected	0.981588	0.784	0.3	0
DTX3L	Infected	0.967167	0.776	0.276	0
KLF6	Infected	0.93654	0.687	0.229	0
APOL2	Infected	0.933543	0.558	0.129	0
HELZ2	Infected	0.92706	0.509	0.04	0
DDX58	Infected	0.89635	0.464	0.041	0
PARP14	Infected	0.877263	0.722	0.276	0
ISG15	Infected	0.87406	0.495	0.058	0
TFAP2C	Infected	0.859227	0.731	0.335	0
IFIT2	Infected	0.856451	0.342	0.012	0
STAT2	Infected	0.849258	0.8	0.407	0
HMGB1	Bystander	0.315939	0.894	0.735	4.06E−19
HMGN2	Bystander	0.336253	0.82	0.657	3.40E−18
TUBA1B	Bystander	0.427122	0.707	0.439	6.20E−18
SSR3	Bystander	0.329197	0.749	0.6	9.21E−17
EBP	Bystander	0.31393	0.848	0.688	1.71E−15
PARP14	Bystander	0.405334	0.71	0.46	5.39E−15
SYNC	Bystander	0.401247	0.587	0.372	3.74E−14
AC091607.2	Bystander	0.349163	0.668	0.496	2.80E−12
TUBB	Bystander	0.381438	0.541	0.337	4.94E−12
PTMA	Bystander	0.315548	0.731	0.562	2.88E−11
RRM2	Bystander	0.407369	0.516	0.304	2.98E−11
PA2G4	Bystander	0.339074	0.65	0.439	5.45E−11
IFI6	Bystander	0.367067	0.746	0.501	1.96E−10
IFIT1	Bystander	0.327753	0.325	0.154	2.79E−10
MYADM	Bystander	0.347887	0.583	0.412	4.98E−09

Table 1

(Hoechst) in blue. (D) EVOS microscope images show astrovirus double-stranded RNA (J2) in green and nucleus (Hoechst) in blue.

Supplementary Figure 3. Single cell RNA sequencing pathway analysis. (A) GO Pathway analysis comparing mock, infected, and bystander groups at 24 hpi. (B) KEGG Pathway analysis comparing mock, infected, and bystander groups at 24 hpi. (C) HALLMARK Pathway analysis comparing mock, infected, and bystander groups at 24 hpi.

Table 1. Top 15 upregulated genes in mock, infected, and bystander clusters for the HAstV-1 Caco-2 single cell RNA sequencing dataset at 24 hpi

List of References

Aizawa, Shu et al. (2016). "Lysosomal putative RNA transporter SIDT2 mediates direct uptake of RNA by lysosomes". In: *Autophagy* 12.3, pp. 565–578.

Anding, Allyson L and Eric H Baehrecke (2017). "Cleaning house: selective autophagy of organelles". In: *Developmental cell* 41.1, pp. 10–22.

Arias, Carlos F and Rebecca M DuBois (2017). "The astrovirus capsid: a review". In: *Viruses* 9.1, p. 15.

Axe, Elizabeth L et al. (2008). "Autophagosome formation from membrane compartments enriched in phosphatidylinositol 3-phosphate and dynamically connected to the endoplasmic reticulum". In: *The Journal of cell biology* 182.4, pp. 685–701.

Baez-Navarro, Carlos et al. (2022). "The Association of Human Astrovirus with Extracellular Vesicles Facilitates Cell Infection and Protects the Virus from Neutralizing Antibodies". In: *Journal of Virology* 96.14, e00848–22.

Bagga, Sumedha and Michael J Bouchard (2014). "Cell cycle regulation during viral infection". In: *Cell Cycle Control: Mechanisms and Protocols*, pp. 165–227.

Balla, Andras and Tamas Balla (2006). "Phosphatidylinositol 4-kinases: old enzymes with emerging functions". In: *Trends in cell biology* 16.7, pp. 351–361.

Bami, Sakshi et al. (2022). "Human astrovirus VA1 encephalitis in pediatric patients with cancer: report of 2 cases and review of the literature". In: *Journal of the Pediatric Infectious Diseases Society* 11.9, pp. 408–412.

Barnum, Kevin J and Matthew J O'Connell (2014). "Cell cycle regulation by checkpoints". In: *Cell cycle control: mechanisms and protocols*, pp. 29–40.

Bas, Levent et al. (2018). "Reconstitution reveals Ykt6 as the autophagosomal SNARE in autophagosome–vacuole fusion". In: *Journal of Cell Biology* 217.10, pp. 3656–3669.

Belliot, Gaël, Henri Laveran, and Stephan S Monroe (1997). "Outbreak of gastroenteritis in military recruits associated with serotype 3 astrovirus infection". In: *Journal of medical virology* 51.2, pp. 101–106.

Bellot, Grégory et al. (2009). "Hypoxia-induced autophagy is mediated through hypoxia-inducible factor induction of BNIP3 and BNIP3L via their BH3 domains". In: *Molecular and cellular biology* 29.10, pp. 2570–2581.

Bertolotti, Anne et al. (2001). "Increased sensitivity to dextran sodium sulfate colitis in IRE1β-deficient mice". In: *The Journal of clinical investigation* 107.5, pp. 585–593.

Björkholm, Magnus et al. (1995). "Successful intravenous immunoglobulin therapy for severe and persistent astrovirus gastroenteritis after fludarabine treatment in a patient with Waldenström's macroglobulinemia." In: *International journal of hematology* 62.2, pp. 117–120.

Bogdanoff, Walter A et al. (2018). "Structural basis for escape of human astrovirus from antibody neutralization: broad implications for rational vaccine design". In: *Journal of virology* 92.1, e01546–17.

Bojjireddy, Naveen et al. (2014). "Pharmacological and genetic targeting of the PI4KA enzyme reveals its important role in maintaining plasma membrane phosphatidylinositol 4-phosphate and phosphatidylinositol 4, 5-bisphosphate levels". In: *Journal of Biological Chemistry* 289.9, pp. 6120–6132.

Bonaparte, Rheba S et al. (2008). "Human astrovirus coat protein inhibits serum complement activation via C1, the first component of the classical pathway". In: *Journal of virology* 82.2, pp. 817–827.

Bouzalas, Ilias G et al. (2014). "Neurotropic astrovirus in cattle with nonsuppurative encephalitis in Europe". In: *Journal of clinical microbiology* 52.9, pp. 3318–3324.

Brinker, JP, NR Blacklow, and JE Herrmann (2000). "Human astrovirus isolation and propagation in multiple cell lines". In: *Archives of virology* 145, pp. 1847–1856.

Bub, Theresa et al. (2023). "Astrovirus replication is dependent on induction of double membrane vesicles through a PI3K-dependent, LC3-independent pathway". In: *Journal of Virology*. DOI: 10.1128/jvi.01025-23. URL: https://journals.asm.org/doi/10.1128/jvi.01025-23.

Calfon, Marcella et al. (2002). "IRE1 couples endoplasmic reticulum load to secretory capacity by processing the XBP-1 mRNA". In: *Nature* 415.6867, pp. 92–96.

Castillo, Jonathan P and Timothy F Kowalik (2004). "HCMV infection: modulating the cell cycle and cell death". In: *International reviews of immunology* 23.1-2, pp. 113–139.

Castillo, Karen et al. (2011). "BAX inhibitor-1 regulates autophagy by controlling the IRE1α branch of the unfolded protein response". In: *The EMBO journal* 30.21, pp. 4465–4478.

Cayrol, C and EK Flemington (1996). "The Epstein-Barr virus bZIP transcription factor Zta causes G0/G1 cell cycle arrest through induction of cyclin-dependent kinase inhibitors." In: *The EMBO Journal* 15.11, pp. 2748–2759.

Chan, Ching-Ping et al. (2006). "Modulation of the unfolded protein response by the severe acute respiratory syndrome coronavirus spike protein". In: *Journal of virology* 80.18, pp. 9279–9287.

Chen, Chun-Jen and Shinji Makino (2004). "Murine coronavirus replication induces cell cycle arrest in G0/G1 phase". In: *Journal of virology* 78.11, pp. 5658–5669.

Chen, Chun-Jen, Kazuo Sugiyama, et al. (2004). "Murine coronavirus nonstructural protein p28 arrests cell cycle in G0/G1 phase". In: *Journal of virology* 78.19, pp. 10410–10419.

Choi, Ji-Ae and Chang-Hwa Song (2020). "Insights into the role of endoplasmic reticulum stress in infectious diseases". In: *Frontiers in immunology* 10, p. 3147.

Choi, Younho, James W Bowman, and Jae U Jung (2018). "Autophagy during viral infection—a double-edged sword". In: *Nature Reviews Microbiology* 16.6, pp. 341–354.

Colli, Maikel L et al. (2019). "Coxsackievirus B tailors the unfolded protein response to favour viral amplification in pancreatic β cells". In: *Journal of innate immunity* 11.4, pp. 375–390.

Compton, Susan R, Carmen J Booth, and James D Macy (2017). "Murine astrovirus infection and transmission in neonatal CD1 mice". In: *Journal of the American Association for Laboratory Animal Science* 56.4, pp. 402–411.

Cortese, Mirko et al. (2020). "Integrative imaging reveals SARS-CoV-2-induced reshaping of subcellular morphologies". In: *Cell host & microbe* 28.6, pp. 853–866.

Cortez, Valerie, Pamela Freiden, et al. (2017). "Persistent infections with diverse co-circulating astroviruses in pediatric oncology patients, Memphis, Tennessee, USA". In: *Emerging infectious diseases* 23.2, p. 288.

Cortez, Valerie, Brandi Livingston, et al. (2023). "Indoleamine 2, 3-dioxygenase 1 regulates cell permissivity to astrovirus infection". In: *Mucosal Immunology*.

Cortez, Valerie, Victoria A Meliopoulos, et al. (2017). "Astrovirus biology and pathogenesis". In: *Annual review of virology* 4, pp. 327–348.

Cortez, Valerie, Bridgett Sharp, et al. (2019). "Characterizing a murine model for astrovirus using viral isolates from persistently infected immunocompromised mice". In: *Journal of Virology* 93.13, pp. 10–1128.

Cottam, Eleanor M et al. (2011). "Coronavirus nsp6 proteins generate autophagosomes from the endoplasmic reticulum via an omegasome intermediate". In: *Autophagy* 7.11, pp. 1335–1347.

Cufí, Sílvia et al. (2011). "Autophagy positively regulates the CD44+ CD24-/low breast cancer stem-like phenotype". In: *Cell cycle* 10.22, pp. 3871–3885.

Datan, E et al. (2016). "Dengue-induced autophagy, virus replication and protection from cell death require ER stress (PERK) pathway activation". In: *Cell death & disease* 7.3, e2127–e2127.

De Bondt, Hendrik L et al. (1993). "Crystal structure of cyclin-dependent kinase 2". In: *Nature* 363.6430, pp. 595–602.

De Duve, Christian (1963). "Ciba Foundation Symposium". In.

De Duve, Christian et al. (1955). "Tissue fractionation studies. 6. Intracellular distribution patterns of enzymes in rat-liver tissue". In: *Biochemical Journal* 60.4, p. 604.

De Grazia, S et al. (2011). "Surveillance of human astrovirus circulation in Italy 2002-2005: emergence of lineage 2c strains". In: *Clinical microbiology and infection* 17.1, pp. 97–101.

Del Rocío Banos-Lara, Ma and Ernesto Méndez (2010). "Role of individual caspases induced by astrovirus on the processing of its structural protein and its release from the cell through a non-lytic mechanism". In: *Virology* 401.2, pp. 322–332.

Di Bartolomeo, Sabrina et al. (2010). "The dynamic interaction of AMBRA1 with the dynein motor complex regulates mammalian autophagy". In: *Journal of Cell Biology* 191.1, pp. 155–168.

Ding, Binbin et al. (2014). "Phosphoprotein of human parainfluenza virus type 3 blocks autophagosome-lysosome fusion to increase virus production". In: *Cell host & microbe* 15.5, pp. 564–577.

Diwan, Prerna, Jonathan J Lacasse, and Luis M Schang (2004). "Roscovitine inhibits activation of promoters in herpes simplex virus type 1 genomes independently of promoter-specific factors". In: *Journal of virology* 78.17, pp. 9352–9365.

Doerflinger, Sylvie Y et al. (2017). "Membrane alterations induced by nonstructural proteins of human norovirus". In: *PLoS pathogens* 13.10, e1006705.

Donato, Celeste and Dhanasekaran Vijaykrishna (2017). "The broad host range and genetic diversity of mammalian and avian astroviruses". In: *Viruses* 9.5, p. 102.

Donelli, Gianfranco et al. (1992). "Mechanism of astrovirus entry into Graham 293 cells". In: *Journal of medical virology* 38.4, pp. 271–277.

Dove, Brian et al. (2006). "Cell cycle perturbations induced by infection with the coronavirus infectious bronchitis virus and their effect on virus replication". In: *Journal of virology* 80.8, pp. 4147–4156.

Dreux, Marlène et al. (2009). "The autophagy machinery is required to initiate hepatitis C virus replication". In: *Proceedings of the National Academy of Sciences* 106.33, pp. 14046–14051.

Duan, Linna (2016). "Janeway's immunobiology". In: *The Yale Journal of Biology and Medicine* 89.3, p. 424.

Durand, Lizette Olga and Bernard Roizman (2008). "Role of cdk9 in the optimization of expression of the genes regulated by ICP22 of herpes simplex virus 1". In: *Journal of virology* 82.21, pp. 10591–10599.

Egan, Daniel F et al. (2011). "Phosphorylation of ULK1 (hATG1) by AMP-activated protein kinase connects energy sensing to mitophagy". In: *Science* 331.6016, pp. 456–461.

Engeland, Kurt (2022). "Cell cycle regulation: p53-p21-RB signaling". In: *Cell Death & Differentiation* 29.5, pp. 946–960.

English, Luc et al. (2009). "Autophagy enhances the presentation of endogenous viral antigens on MHC class I molecules during HSV-1 infection". In: *Nature immunology* 10.5, pp. 480–487.

Fahmy, Ahmed M and Patrick Labonté (2017). "The autophagy elongation complex (ATG5-12/16L1) positively regulates HCV replication and is required for wild-type membranous web formation". In: *Scientific reports* 7.1, p. 40351.

Feng, Zhike et al. (2019). "Recruitment of Vps34 PI3K and enrichment of PI3P phosphoinositide in the viral replication compartment is crucial for replication of a positive-strand RNA virus". In: *PLOS pathogens* 15.1, e1007530.

Fraser, Jane et al. (2019). "Targeting of early endosomes by autophagy facilitates EGFR recycling and signalling". In: *EMBO reports* 20.10, e47734.

Fuentes, Cristina et al. (2011). "The C-terminal nsP1a protein of human astrovirus is a phosphoprotein that interacts with the viral polymerase". In: *Journal of virology* 85.9, pp. 4470–4479.

Fujita, Naonobu et al. (2008). "An Atg4B mutant hampers the lipidation of LC3 paralogues and causes defects in autophagosome closure". In: *Molecular biology of the cell* 19.11, pp. 4651–4659.

Fujiwara, Yuuki, Akiko Furuta, et al. (2013). "Discovery of a novel type of autophagy targeting RNA". In: *Autophagy* 9.3, pp. 403–409.

Fujiwara, Yuuki, Katsunori Hase, et al. (2015). "An RNautophagy/DNautophagy receptor, LAMP2C, possesses an arginine-rich motif that mediates RNA/DNA-binding". In: *Biochemical and biophysical research communications* 460.2, pp. 281–286.

Funderburk, Sarah F, Qing Jun Wang, and Zhenyu Yue (2010). "The Beclin 1–VPS34 complex–at the crossroads of autophagy and beyond". In: *Trends in cell biology* 20.6, pp. 355–362.

Fung, To Sing and Ding Xiang Liu (2019). "The ER stress sensor IRE1 and MAP kinase ERK modulate autophagy induction in cells infected with coronavirus infectious bronchitis virus". In: *Virology* 533, pp. 34–44.

Gabbay, Yvone B et al. (2007). "Molecular epidemiology of astrovirus type 1 in Belem, Brazil, as an agent of infantile gastroenteritis, over a period of 18 years (1982–2000): identification of two possible new lineages". In: *Virus research* 129.2, pp. 166–174.

Gaggero, Aldo et al. (1998). "Prevalence of astrovirus infection among Chilean children with acute gastroenteritis". In: *Journal of clinical microbiology* 36.12, pp. 3691–3693.

Gao, Jieqiong, Fulvio Reggiori, and Christian Ungermann (2018). "A novel in vitro assay reveals SNARE topology and the role of Ykt6 in autophagosome fusion with vacuoles". In: *Journal of Cell Biology* 217.10, pp. 3670–3682.

Ge, Liang et al. (2013). "The ER–Golgi intermediate compartment is a key membrane source for the LC3 lipidation step of autophagosome biogenesis". In: *elife* 2, e00947.

Geigenmüller, Ute et al. (2002). "Processing of nonstructural protein 1a of human astrovirus". In: *Journal of virology* 76.4, pp. 2003–2008.

Giono, Luciana E and James J Manfredi (2006). "The p53 tumor suppressor participates in multiple cell cycle checkpoints". In: *Journal of cellular physiology* 209.1, pp. 13–20.

Gotoh, Tomomi et al. (2002). "Nitric oxide-induced apoptosis in RAW 264.7 macrophages is mediated by endoplasmic reticulum stress pathway involving ATF6 and CHOP". In: *Journal of Biological Chemistry* 277.14, pp. 12343–12350.

Gray, EW, KW Angus, and DR Snodgrass (1980). "Ultrastructure of the small intestine in astrovirus-infected lambs". In: *Journal of General Virology* 49.1, pp. 71–82.

Gray, JJ et al. (1987). "An outbreak of gastroenteritis in a home for the elderly associated with astrovirus type 1 and human calicivirus". In: *Journal of medical virology* 23.4, pp. 377–381.

Guerrero, M Lourdes et al. (1998). "A prospective study of astrovirus diarrhea of infancy in Mexico City". In: *The Pediatric infectious disease journal* 17.8, pp. 723–727.

Guévin, Carl et al. (2010). "Autophagy protein ATG5 interacts transiently with the hepatitis C virus RNA polymerase (NS5B) early during infection". In: *Virology* 405.1, pp. 1–7.

Guix, Susana, Albert Bosch, and Rosa M Pintó (2013). "Astrovirus taxonomy". In: *Astrovirus research: essential ideas, everyday impacts, future directions*, pp. 97–118.

Guix, Susana, Santiago Caballero, Albert Bosch, et al. (2004). "C-terminal nsP1a protein of human astrovirus colocalizes with the endoplasmic reticulum and viral RNA". In: *Journal of virology* 78.24, pp. 13627–13636.

– (2005). "Human astrovirus C-terminal nsP1a protein is involved in RNA replication". In: *Virology* 333.1, pp. 124–131.

Guix, Susana, Santiago Caballero, Cristina Villena, et al. (2002). "Molecular epidemiology of astrovirus infection in Barcelona, Spain". In: *Journal of clinical microbiology* 40.1, pp. 133–139.

Guix, Susana, Anna Pérez-Bosque, et al. (2015). "Type I interferon response is delayed in human astrovirus infections". In: *PLoS One* 10.4, e0123087.

Guy, James S and H John Barnes (1991). "Partial characterization of a turkey enterovirus-like virus". In: *Avian diseases*, pp. 197–203.

Haga, Kei et al. (2022). "Neonatal Fc receptor is a functional receptor for human astrovirus". In: *bioRxiv*, pp. 2022–11.

Hailey, Dale W et al. (2010). "Mitochondria supply membranes for autophagosome biogenesis during starvation". In: *Cell* 141.4, pp. 656–667.

Hair, Pamela S et al. (2010). "Human astrovirus coat protein binds C1q and MBL and inhibits the classical and lectin pathways of complement activation". In: *Molecular immunology* 47.4, pp. 792–798.

Harding, Heather P et al. (2000). "Regulated translation initiation controls stress-induced gene expression in mammalian cells". In: *Molecular cell* 6.5, pp. 1099–1108.

Hargest, Virginia, Theresa Bub, et al. (2022). "Astrovirus-induced epithelial-mesenchymal transition via activated TGF-β increases viral replication". In: *PLoS Pathogens* 18.4, e1009716.

Hargest, Virginia, Amy E Davis, et al. (2021). "Human astroviruses: A tale of two strains". In: *Viruses* 13.3, p. 376.

Hargest, Virginia, Bridgett Sharp, et al. (2020). "Astrovirus replication is inhibited by nitazoxanide in vitro and in vivo". In: *Journal of virology* 94.5, pp. 10–1128.

Hase, Katsunori et al. (2015). "RNautophagy/DNautophagy possesses selectivity for RNA/DNA substrates". In: *Nucleic acids research* 43.13, pp. 6439–6449.

Hayashi-Nishino, Mitsuko et al. (2009). "A subdomain of the endoplasmic reticulum forms a cradle for autophagosome formation". In: *Nature cell biology* 11.12, pp. 1433–1437.

Hayes, C Nelson et al. (2022). "Road to elimination of HCV: Clinical challenges in HCV management". In: *Liver international* 42.9, pp. 1935–1944.

Hayn, Manuel et al. (2021). "Systematic functional analysis of SARS-CoV-2 proteins uncovers viral innate immune antagonists and remaining vulnerabilities". In: *Cell reports* 35.7.

He, Yuan et al. (2010). "Influenza A virus replication induces cell cycle arrest in G0/G1 phase". In: *Journal of virology* 84.24, pp. 12832–12840.

Heaton, Nicholas S and Glenn Randall (2010). "Dengue virus-induced autophagy regulates lipid metabolism". In: *Cell host & microbe* 8.5, pp. 422–432.

Hegedűs, Krisztina et al. (2016). "The Ccz1-Mon1-Rab7 module and Rab5 control distinct steps of autophagy". In: *Molecular biology of the cell* 27.20, pp. 3132–3142.

Hoffmann, H-Heinrich et al. (2021). "Functional interrogation of a SARS-CoV-2 host protein interactome identifies unique and shared coronavirus host factors". In: *Cell Host & Microbe* 29.2, pp. 267–280.

Holtz, Lori R et al. (2014). "Seroepidemiology of astrovirus MLB1". In: *Clinical and Vaccine Immunology* 21.6, pp. 908–911.

Isobe, Tomoyasu et al. (2019). "Upregulation of CHOP participates in caspase activation and virus release in human astrovirus-infected cells". In: *Journal of General Virology* 100.5, pp. 778–792.

Itakura, Eisuke, Chieko Kishi, et al. (2008). "Beclin 1 forms two distinct phosphatidylinositol 3-kinase complexes with mammalian Atg14 and UVRAG". In: *Molecular biology of the cell* 19.12, pp. 5360–5372.

Itakura, Eisuke, Chieko Kishi-Itakura, and Noboru Mizushima (2012). "The hairpin-type tail-anchored SNARE syntaxin 17 targets to autophagosomes for fusion with endosomes/lysosomes". In: *Cell* 151.6, pp. 1256–1269.

Jackson, William T et al. (2005). "Subversion of cellular autophagosomal machinery by RNA viruses". In: *PLoS biology* 3.5, e156.

Jang, So Young et al. (2010). "Detection of replicating negative-sense RNAs in CaCo-2 cells infected with human astrovirus". In: *Archives of virology* 155, pp. 1383–1389.

Jarchow-Macdonald, Anna A et al. (2015). "First report of an astrovirus type 5 gastroenteritis outbreak in a residential elderly care home identified by sequencing". In: *Journal of Clinical Virology* 73, pp. 115–119.

Järviluoma, Annika and Päivi M Ojala (2006). "Cell signaling pathways engaged by KSHV". In: *Biochimica et Biophysica Acta (BBA)-Reviews on Cancer* 1766.1, pp. 140–158.

Jeffrey, Philip D et al. (1995). "Mechanism of CDK activation revealed by the structure of a cyclinA-CDK2 complex". In: *Nature* 376.6538, pp. 313–320.

Jiang, Hao-Yuan, Li Jiang, and Ronald C Wek (2007). "The eukaryotic initiation factor-2 kinase pathway facilitates differential GADD45a expression in response to environmental stress". In: *Journal of Biological Chemistry* 282.6, pp. 3755–3765.

Jiao, Lin et al. (2018). "Regulation of glycolytic metabolism by autophagy in liver cancer involves selective autophagic degradation of HK2 (hexokinase 2)". In: *Autophagy* 14.4, pp. 671–684.

Johansson, Marie et al. (2007). "Activation of endosomal dynein motors by stepwise assembly of Rab7–RILP–p150Glued, ORP1L, and the receptor βlll spectrin". In: *The Journal of cell biology* 176.4, pp. 459–471.

Jordan, Robert et al. (2002). "Replication of a cytopathic strain of bovine viral diarrhea virus activates PERK and induces endoplasmic reticulum stress-mediated apoptosis of MDBK cells". In: *Journal of virology* 76.19, pp. 9588–9599.

Jordens, Ingrid et al. (2001). "The Rab7 effector protein RILP controls lysosomal transport by inducing the recruitment of dynein-dynactin motors". In: *Current Biology* 11.21, pp. 1680–1685.

Judith, Delphine et al. (2013). "Species-specific impact of the autophagy machinery on Chikungunya virus infection". In: *EMBO reports* 14.6, pp. 534–544.

Jung, Chang Hwa et al. (2009). "ULK-Atg13-FIP200 complexes mediate mTOR signaling to the autophagy machinery". In: *Molecular biology of the cell* 20.7, pp. 1992–2003.

Kalies, Kai-Uwe and Karin Römisch (2015). "Inhibitors of protein translocation across the ER membrane". In: *Traffic* 16.10, pp. 1027–1038.

Karagöz, G Elif et al. (2017). "An unfolded protein-induced conformational switch activates mammalian IRE1". In: *Elife* 6, e30700.

Kast, David J and Roberto Dominguez (2015). "WHAMM links actin assembly via the Arp2/3 complex to autophagy". In: *Autophagy* 11.9, pp. 1702–1704.

Kayisoglu, Özge, Nicolas Schlegel, and Sina Bartfeld (2021). "Gastrointestinal epithelial innate immunity—regionalization and organoids as new model". In: *Journal of Molecular Medicine* 99.4, pp. 517–530.

Khamrin, Pattara et al. (2016). "Multiple astrovirus MLB1, MLB2, VA2 clades, and classic human astrovirus in children with acute gastroenteritis in Japan". In: *Journal of medical virology* 88.2, pp. 356–360.

Killander, D and A Zetterberg (1965a). "A quantitative cytochemical investigation of the relationship between cell mass and initiation of DNA synthesis in mouse fibroblasts in vitro". In: *Experimental cell research* 40.1, pp. 12–20.

– (1965b). "Quantitative cytochemical studies on interphase growth: I. Determination of DNA, RNA and mass content of age determined mouse fibroblasts in vitro and of intercellular variation in generation time". In: *Experimental cell research* 38.2, pp. 272–284.

Kim, Joungmok et al. (2011). "AMPK and mTOR regulate autophagy through direct phosphorylation of Ulk1". In: *Nature cell biology* 13.2, pp. 132–141.

Kimura, Shunsuke, Takeshi Noda, and Tamotsu Yoshimori (2008). "Dynein-dependent movement of autophagosomes mediates efficient encounters with lysosomes". In: *Cell structure and function* 33.1, pp. 109–122.

Kjeldsberg, Elisabeth and Annelise Hem (1985). "Detection of astroviruses in gut contents of nude and normal mice". In: *Archives of virology* 84, pp. 135–140.

Klionsky, Daniel J et al. (2021). "Guidelines for the use and interpretation of assays for monitoring autophagy". In: *autophagy* 17.1, pp. 1–382.

Knoops, Kèvin, Montserrat Bárcena, et al. (2012). "Ultrastructural characterization of arterivirus replication structures: reshaping the endoplasmic reticulum to accommodate viral RNA synthesis". In: *Journal of virology* 86.5, pp. 2474–2487.

Knoops, Kèvin, Marjolein Kikkert, et al. (2008). "SARS-coronavirus replication is supported by a reticulovesicular network of modified endoplasmic reticulum". In: *PLoS biology* 6.9, e226.

Koci, Matthew D, Laura A Kelley, et al. (2004). "Astrovirus-induced synthesis of nitric oxide contributes to virus control during infection". In: *Journal of virology* 78.3, pp. 1564–1574.

Koci, Matthew D, Lindsey A Moser, et al. (2003). "Astrovirus induces diarrhea in the absence of inflammation and cell death". In: *Journal of virology* 77.21, pp. 11798–11808.

Koci, Matthew D and Schultz-Cherry (2002). "Avian astroviruses". In: *Avian pathology* 31.3, pp. 213–227.

Koci, Matthew D, Bruce S Seal, and Schultz-Cherry (2000). "Molecular characterization of an avian astrovirus". In: *Journal of Virology* 74.13, pp. 6173–6177.

Kolawole, Abimbola O et al. (2019). "Astrovirus replication in human intestinal enteroids reveals multi-cellular tropism and an intricate host innate immune landscape". In: *PLoS pathogens* 15.10, e1008057.

Kuma, Akiko, Masaaki Komatsu, and Noboru Mizushima (2017). "Autophagy-monitoring and autophagy-deficient mice". In: *Autophagy* 13.10, pp. 1619–1628.

Kuma, Akiko, Noboru Mizushima, et al. (2002). "Formation of the 350-kDa Apg12-Apg5· Apg16 multimeric complex, mediated by Apg16 oligomerization, is essential for autophagy in yeast". In: *Journal of Biological Chemistry* 277.21, pp. 18619–18625.

Kurtz and Lee (1978). "Astrovirus gastroenteritis age distribution of antibody". In: *Medical microbiology and immunology* 166, pp. 227–230.

Kurtz, Lee, et al. (1979). "Astrovirus infection in volunteers". In: *Journal of medical virology* 3.3, pp. 221–230.

Lechauve, Christophe et al. (2019). "The autophagy-activating kinase ULK1 mediates clearance of free α-globin in β-thalassemia". In: *Science translational medicine* 11.506, eaav4881.

Lee, Jong Woo et al. (2010). "The association of AMPK with ULK1 regulates autophagy". In: *PloS one* 5.11, e15394.

Lee, Jong-Soo et al. (2009). "FLIP-mediated autophagy regulation in cell death control". In: *Nature cell biology* 11.11, pp. 1355–1362.

Lee, You-Kyung and Jin-A Lee (2016). "Role of the mammalian ATG8/LC3 family in autophagy: differential and compensatory roles in the spatiotemporal regulation of autophagy". In: *BMB reports* 49.8, p. 424.

Lemasters, John J (2005). "Selective mitochondrial autophagy, or mitophagy, as a targeted defense against oxidative stress, mitochondrial dysfunction, and aging". In: *Rejuvenation research* 8.1, pp. 3–5.

Levine, Beth and Guido Kroemer (2008). "Autophagy in the pathogenesis of disease". In: *Cell* 132.1, pp. 27–42.

Li, Shanshan, Lingbao Kong, and Xilan Yu (2015). "The expanding roles of endoplasmic reticulum stress in virus replication and pathogenesis". In: *Critical reviews in microbiology* 41.2, pp. 150–164.

Liang, Chengyu et al. (2008). "Beclin1-binding UVRAG targets the class C Vps complex to coordinate autophagosome maturation and endocytic trafficking". In: *Nature cell biology* 10.7, pp. 776–787.

Liang, Qiming et al. (2014). "Crosstalk between the cGAS DNA sensor and Beclin-1 autophagy protein shapes innate antimicrobial immune responses". In: *Cell host & microbe* 15.2, pp. 228–238.

Lin, Jonathan H, Peter Walter, and TS Benedict Yen (2008). "Endoplasmic reticulum stress in disease pathogenesis". In: *Annu. Rev. Pathol. Mech. Dis.* 3, pp. 399–425.

Lindl, KA et al. (2007). "Expression of the endoplasmic reticulum stress response marker, BiP, in the central nervous system of HIV-positive individuals". In: *Neuropathology and applied neurobiology* 33.6, pp. 658–669.

Liu, Ying, Eckard Wimmer, and Aniko V Paul (2009). "Cis-acting RNA elements in human and animal plus-strand RNA viruses". In: *Biochimica et Biophysica Acta (BBA)-Gene Regulatory Mechanisms* 1789.9-10, pp. 495–517.

Liu et al. (2002). "Human immunodeficiency virus type 1 enters brain microvascular endothelia by macropinocytosis dependent on lipid rafts and the mitogen-activated protein kinase signaling pathway". In: *Journal of virology* 76.13, pp. 6689–6700.

Lu, Guang et al. (2022). "Autophagy in health and disease: From molecular mechanisms to therapeutic target". In: *MedComm* 3.3, e150.

Lu, Lijuan et al. (2021). "Molecular and epidemiological characterization of human adenovirus and classic human astrovirus in children with acute diarrhea in Shanghai, 2017–2018". In: *BMC infectious diseases* 21, pp. 1–10.

Łukasik, Paweł, Michał Załuski, and Izabela Gutowska (2021). "Cyclin-dependent kinases (CDK) and their role in diseases development–review". In: *International journal of molecular sciences* 22.6, p. 2935.

Lulla, Valeria and Andrew E Firth (2020). "A hidden gene in astroviruses encodes a viroporin". In: *Nature communications* 11.1, p. 4070.

Lv, Zhengtong, Yuan Chu, and Yong Wang (2015). "HIV protease inhibitors: a review of molecular selectivity and toxicity". In: *HIV/AIDS-Research and palliative care*, pp. 95–104.

Mareninova, Olga A et al. (2022). "Rab9 mediates pancreatic autophagy switch from canonical to noncanonical, aggravating experimental pancreatitis". In: *Cellular and molecular gastroenterology and hepatology* 13.2, pp. 599–622.

Maria Fimia, Gian et al. (2007). "Ambra1 regulates autophagy and development of the nervous system". In: *Nature* 447.7148, pp. 1121–1125.

Marshall, JA et al. (2007). "Molecular features of astrovirus associated with a gastroenteritis outbreak in an aged-care centre". In: *European Journal of Clinical Microbiology & Infectious Diseases* 26, pp. 67–71.

Martella, Vito et al. (2011). "Detection and characterization of canine astroviruses". In: *Journal of general virology* 92.8, pp. 1880–1887.

Marvin, Shauna, Victoria Meliopoulos, and Stacey Schultz-Cherry (2014). "Human astrovirus propagation, purification and quantification". In: *Bio-protocol* 4.6, e1078–e1078.

Marvin, Shauna A et al. (2016). "Type I interferon response limits astrovirus replication and protects against increased barrier permeability in vitro and in vivo". In: *Journal of virology* 90.4, pp. 1988–1996.

Matsuda, Noriyuki et al. (2010). "PINK1 stabilized by mitochondrial depolarization recruits Parkin to damaged mitochondria and activates latent Parkin for mitophagy". In: *Journal of Cell Biology* 189.2, pp. 211–221.

Matsunaga, Kohichi et al. (2009). "Two Beclin 1-binding proteins, Atg14L and Rubicon, reciprocally regulate autophagy at different stages". In: *Nature cell biology* 11.4, pp. 385–396.

Maximova, Olga A et al. (2022). "Imbalanced immune response and dysregulation of neural functions underline fatal opportunistic encephalitis caused by astrovirus". In: *bioRxiv*, pp. 2022–08.

McEwan, David G et al. (2015). "PLEKHM1 regulates autophagosome-lysosome fusion through HOPS complex and LC3/GABARAP proteins". In: *Molecular cell* 57.1, pp. 39–54.
McLean, Janel R et al. (2011). "State of the APC/C: organization, function, and structure". In: *Critical reviews in biochemistry and molecular biology* 46.2, pp. 118–136.
Mead, Paul S et al. (1999). "Food-related illness and death in the United States." In: *Emerging infectious diseases* 5.5, p. 607.
Melia, Charlotte E et al. (2019). "Origins of enterovirus replication organelles established by whole-cell electron microscopy". In: *MBio* 10.3, pp. 10–1128.
Meliopoulos, Victoria A et al. (2016). "Oral administration of astrovirus capsid protein is sufficient to induce acute diarrhea in vivo". In: *MBio* 7.6, pp. 10–1128.
Méndez, Ernesto, Gabriela Aguirre-Crespo, et al. (2007). "Association of the astrovirus structural protein VP90 with membranes plays a role in virus morphogenesis". In: *Journal of virology* 81.19, pp. 10649–10658.
Méndez, Ernesto, Teresa Fernández-Luna, et al. (2002). "Proteolytic processing of a serotype 8 human astrovirus ORF2 polyprotein". In: *Journal of virology* 76.16, pp. 7996–8002.
Méndez, Ernesto, Claudia Muñoz-Yañez, et al. (2014). "Characterization of human astrovirus cell entry". In: *Journal of virology* 88.5, pp. 2452–2460.
Méndez, Ernesto, Andrea Murillo, et al. (2013). "Replication cycle of astroviruses". In: *Astrovirus research: essential ideas, everyday impacts, future directions*, pp. 19–45.
Méndez, Ernesto, Elizabeth Salas-Ocampo, and Carlos F Arias (2004). "Caspases mediate processing of the capsid precursor and cell release of human astroviruses". In: *Journal of virology* 78.16, pp. 8601–8608.
Miao, Guangyan et al. (2021). "ORF3a of the COVID-19 virus SARS-CoV-2 blocks HOPS complex-mediated assembly of the SNARE complex required for autolysosome formation". In: *Developmental cell* 56.4, pp. 427–442.
Mihelc, Elaine M, Susan C Baker, and Jason K Lanman (2021). "Coronavirus infection induces progressive restructuring of the endoplasmic reticulum involving the formation and degradation of double membrane vesicles". In: *Virology* 556, pp. 9–22.
Misiewicz, Michael et al. (2013). "Identification of a novel endoplasmic reticulum stress response element regulated by XBP1". In: *Journal of Biological Chemistry* 288.28, pp. 20378–20391.
Mizushima, Noboru, Beth Levine, et al. (2008). "Autophagy fights disease through cellular self-digestion". In: *nature* 451.7182, pp. 1069–1075.
Mizushima, Noboru, Takeshi Noda, and Yoshinori Ohsumi (1999). "Apg16p is required for the function of the Apg12p–Apg5p conjugate in the yeast autophagy pathway". In: *The EMBO journal* 18.14, pp. 3888–3896.
Mizushima, Noboru, Takeshi Noda, Tamotsu Yoshimori, et al. (1998). "A protein conjugation system essential for autophagy". In: *Nature* 395.6700, pp. 395–398.
Mizushima, Noboru, Akitsugu Yamamoto, et al. (2004). "In vivo analysis of autophagy in response to nutrient starvation using transgenic mice expressing a fluorescent autophagosome marker". In: *Molecular biology of the cell* 15.3, pp. 1101–1111.

Mohamud, Yasir et al. (2020). "Coxsackievirus infection induces a non-canonical autophagy independent of the ULK and PI3K complexes". In: *Scientific Reports* 10.1, p. 19068.
Molberg, Øyvind et al. (1998). "CD4+ T cells with specific reactivity against astrovirus isolated from normal human small intestine". In: *Gastroenterology* 114.1, pp. 115–122.
Monastyrska, Iryna et al. (2009). "Multiple roles of the cytoskeleton in autophagy". In: *Biological Reviews* 84.3, pp. 431–448.
Monroe, Stephan S et al. (1993). "Subgenomic RNA sequence of human astrovirus supports classification of Astroviridae as a new family of RNA viruses". In: *Journal of virology* 67.6, pp. 3611–3614.
Moradpour, Darius et al. (2004). "Membrane association of the RNA-dependent RNA polymerase is essential for hepatitis C virus RNA replication". In: *Journal of virology* 78.23, pp. 13278–13284.
Morita, Hanako et al. (2021). "Pathogenesis of murine astrovirus in experimentally infected mice". In: *Experimental Animals* 70.3, pp. 355–363.
Moser, Lindsey A, Michael Carter, and Stacey Schultz-Cherry (2007). "Astrovirus increases epithelial barrier permeability independently of viral replication". In: *Journal of virology* 81.21, pp. 11937–11945.
Moser and Schultz-Cherry (2008a). "Astroviruses". In: *Encyclopedia of Virology*, p. 204.
– (2008b). "Suppression of astrovirus replication by an ERK1/2 inhibitor". In: *Journal of virology* 82.15, pp. 7475–7482.
Mosser, Anne G, Lawrence A Caliguiri, and Igor Tamm (1972). "Incorporation of lipid precursors into cytoplasmic membranes of poliovirus-infected HeLa cells". In: *Virology* 47.1, pp. 39–47.
Mouna, Lina et al. (2016). "Analysis of the role of autophagy inhibition by two complementary human cytomegalovirus BECN1/Beclin 1-binding proteins". In: *Autophagy* 12.2, pp. 327–342.
Munakata, Tsubasa et al. (2007). "Hepatitis C virus induces E6AP-dependent degradation of the retinoblastoma protein". In: *PLoS pathogens* 3.9, e139.
Murillo, Andrea et al. (2015). "Identification of host cell factors associated with astrovirus replication in Caco-2 cells". In: *Journal of virology* 89.20, pp. 10359–10370.
Mustafa, Huseyin, Enzo A Palombo, and Ruth F Bishop (2000). "Epidemiology of astrovirus infection in young children hospitalized with acute gastroenteritis in Melbourne, Australia, over a period of four consecutive years, 1995 to 1998". In: *Journal of clinical microbiology* 38.3, pp. 1058–1062.
Nakanishi, Keiko, Tatsuhiko Sudo, and Nobuhiro Morishima (2005). "Endoplasmic reticulum stress signaling transmitted by ATF6 mediates apoptosis during muscle development". In: *The Journal of cell biology* 169.4, pp. 555–560.
Narendra, Derek et al. (2008). "Parkin is recruited selectively to impaired mitochondria and promotes their autophagy". In: *The Journal of cell biology* 183.5, pp. 795–803.
Narendra, Derek P et al. (2010). "PINK1 is selectively stabilized on impaired mitochondria to activate Parkin". In: *PLoS biology* 8.1, e1000298.

Nelemans, Tessa and Marjolein Kikkert (2019). "Viral innate immune evasion and the pathogenesis of emerging RNA virus infections". In: *Viruses* 11.10, p. 961.

Niendorf, Sandra et al. (2022). "Diversity of human astroviruses in Germany 2018 and 2019". In: *Virology journal* 19.1, p. 221.

Nishida, Yuya et al. (2009). "Discovery of Atg5/Atg7-independent alternative macroautophagy". In: *Nature* 461.7264, pp. 654–658.

Nishitani, Hideo and Z Lygerou (2004). "DNA replication licensing". In: *Frontiers in Bioscience-Landmark* 9.3, pp. 2115–2132.

O'Donnell, Vivian et al. (2011). "Foot-and-mouth disease virus utilizes an autophagic pathway during viral replication". In: *Virology* 410.1, pp. 142–150.

Obara, Keisuke et al. (2008). "Transport of phosphatidylinositol 3-phosphate into the vacuole via autophagic membranes in Saccharomyces cerevisiae". In: *Genes to Cells* 13.6, pp. 537–547.

Oh, Ji Eun and Heung Kyu Lee (2014). "Pattern recognition receptors and autophagy". In: *Frontiers in immunology* 5, p. 300.

Oishi, Isao et al. (1994). "A large outbreak of acute gastroenteritis associated with astrovirus among students and teachers in Osaka, Japan". In: *Journal of infectious diseases* 170.2, pp. 439–443.

Okitsu, Shoko et al. (2023). "Molecular Epidemiology of Classic, MLB, and VA Astroviruses in Children with Acute Gastroenteritis, 2014–2021: Emergence of MLB3 Strain in Japan". In: *Microbiology Spectrum*, e00700–23.

Orvedahl, Anthony, Sarah MacPherson, et al. (2010). "Autophagy protects against Sindbis virus infection of the central nervous system". In: *Cell host & microbe* 7.2, pp. 115–127.

Orvedahl, Anthony, Rhea Sumpter Jr, et al. (2011). "Image-based genome-wide siRNA screen identifies selective autophagy factors". In: *Nature* 480.7375, pp. 113–117.

Otsuka, Motoyuki et al. (2000). "Hepatitis C virus core protein enhances p53 function through augmentation of DNA binding affinity and transcriptional ability". In: *Journal of Biological Chemistry* 275.44, pp. 34122–34130.

Pager, Cara T and AD Steele (2002). "Astrovirus-associated diarrhea in South African adults". In: *Clinical infectious diseases* 35.11, pp. 1452–1453.

Palombo, Enzo A and Ruth F Bishop (1996). "Annual incidence, serotype distribution, and genetic diversity of human astrovirus isolates from hospitalized children in Melbourne, Australia." In: *Journal of Clinical Microbiology* 34.7, p. 1750.

Paludan, Casper et al. (2005). "Endogenous MHC class II processing of a viral nuclear antigen after autophagy". In: *Science* 307.5709, pp. 593–596.

Pang, X-L and T Vesikari (1999). "Human astrovirus-associated gastroenteritis in children under 2 years of age followed prospectively during a rotavirus vaccine trial". In: *Acta Paediatrica* 88.5, pp. 532–536.

Pantin-Jackwood, MJ et al. (2011). "Molecular characterization of avian astroviruses". In: *Archives of virology* 156, pp. 235–244.

Pattingre, Sophie et al. (2005). "Bcl-2 antiapoptotic proteins inhibit Beclin 1-dependent autophagy". In: *Cell* 122.6, pp. 927–939.

Paul, David et al. (2013). "Morphological and biochemical characterization of the membranous hepatitis C virus replication compartment". In: *Journal of virology* 87.19, pp. 10612–10627.

Pavletich, Nikola P (1999). "Mechanisms of cyclin-dependent kinase regulation: structures of Cdks, their cyclin activators, and Cip and INK4 inhibitors". In: *Journal of molecular biology* 287.5, pp. 821–828.

Payne, Susan (2017). "Family astroviridae". In: *Viruses*, p. 125.

Petiot, Anne et al. (2000). "Distinct classes of phosphatidylinositol 3'-kinases are involved in signaling pathways that control macroautophagy in HT-29 cells". In: *Journal of Biological Chemistry* 275.2, pp. 992–998.

Pfaff, F et al. (2017). "A novel astrovirus associated with encephalitis and ganglionitis in domestic sheep". In: *Transboundary and emerging diseases* 64.3, pp. 677–682.

Poggioli, George J, Terence S Dermody, and Kenneth L Tyler (2001). "Reovirus-induced ς1s-dependent G2/M phase cell cycle arrest is associated with inhibition of p34cdc2". In: *Journal of Virology* 75.16, pp. 7429–7434.

Pogue, GP, CC Huntley, and TC Hall (1994). "Common replication strategies emerging from the study of diverse groups of positive-strand RNA viruses". In: *Positive-Strand RNA Viruses*, pp. 181–194.

Pons-Salort, Margarita et al. (2018). "The seasonality of nonpolio enteroviruses in the United States: Patterns and drivers". In: *Proceedings of the National Academy of Sciences* 115.12, pp. 3078–3083.

Prasad, Vibhu and Urs F Greber (2021). "The endoplasmic reticulum unfolded protein response–homeostasis, cell death and evolution in virus infections". In: *FEMS microbiology reviews* 45.5, fuab016.

Prentice, Erik et al. (2004). "Coronavirus replication complex formation utilizes components of cellular autophagy". In: *Journal of Biological Chemistry* 279.11, pp. 10136–10141.

Pu, Jing et al. (2016). "Mechanisms and functions of lysosome positioning". In: *Journal of cell science* 129.23, pp. 4329–4339.

Qiao, Haiping et al. (1999). "Viral diarrhea in children in Beijing, China". In: *Journal of medical virology* 57.4, pp. 390–396.

Qu, Yafei et al. (2021). "ORF3a-mediated incomplete autophagy facilitates severe acute respiratory syndrome coronavirus-2 replication". In: *Frontiers in cell and developmental biology* 9, p. 716208.

Ra, Eun A et al. (2016). "TRIM31 promotes Atg5/Atg7-independent autophagy in intestinal cells". In: *Nature communications* 7.1, p. 11726.

Rathore, Abhay PS, Mah-Lee Ng, and Subhash G Vasudevan (2013). "Differential unfolded protein response during Chikungunya and Sindbis virus infection: CHIKV nsP4 suppresses eIF2α phosphorylation". In: *Virology journal* 10.1, pp. 1–15.

Ravikumar, Brinda et al. (2005). "Dynein mutations impair autophagic clearance of aggregate-prone proteins". In: *Nature genetics* 37.7, pp. 771–776.

Reither, Klaus et al. (2007). "Acute childhood diarrhoea in northern Ghana: epidemiological, clinical and microbiological characteristics". In: *BMC infectious diseases* 7, pp. 1–8.

Resque, Hugo Reis et al. (2007). "Molecular characterization of astrovirus in stool samples from children in Sao Paulo, Brazil". In: *Memórias do Instituto Oswaldo Cruz* 102, pp. 969–974.

Reynolds, DL, YM Saif, and KW Theil (1987). "A survey of enteric viruses of turkey poults". In: *Avian Diseases*, pp. 89–98.

Roingeard, Philippe et al. (2022). "The double-membrane vesicle (DMV): a virus-induced organelle dedicated to the replication of SARS-CoV-2 and other positive-sense single-stranded RNA viruses". In: *Cellular and Molecular Life Sciences* 79.8, p. 425.

Romero-Brey, Inés et al. (2012). "Three-dimensional architecture and biogenesis of membrane structures associated with hepatitis C virus replication". In: *PLoS pathogens* 8.12, e1003056.

Ruggieri, A et al. (2003). "Cell cycle perturbation in a human hepatoblastoma cell line constitutively expressing Hepatitis C virus core protein". In: *Archives of virology* 149, pp. 61–74.

Saleeb, Rebecca S et al. (2019). "A VPS33A-binding motif on syntaxin 17 controls autophagy completion in mammalian cells". In: *Journal of Biological Chemistry* 294.11, pp. 4188–4201.

Schafer, KA (1998). "The cell cycle: a review". In: *Veterinary pathology* 35.6, pp. 461–478.

Schang, Luis M, Joanna Phillips, and Priscilla A Schaffer (1998). "Requirement for cellular cyclin-dependent kinases in herpes simplex virus replication and transcription". In: *Journal of virology* 72.7, pp. 5626–5637.

Schroder, BA et al. (n.d.). "The proteome of lysosomes. 986 Proteomics 10: 4053-4076, 2010. 987 43. Sharma AK, Ye L, Baer CE, Shanmugasundaram K, Alber T, Alper SL, and Rigby AC. 988 Solution Structure of the Guanine Nucleotide-binding STAS Domain of SLC26-related SulP 989 Protein Rv1739c from Mycobacterium tuberculosis". In: *J Biol Chem* 286 (), pp. 8534–8544.

Schuck, Sebastian, Ciara M Gallagher, and Peter Walter (2014). "ER-phagy mediates selective degradation of endoplasmic reticulum independently of the core autophagy machinery". In: *Journal of cell science* 127.18, pp. 4078–4088.

Shaban, Mohammed Samer et al. (2021). "Multi-level inhibition of coronavirus replication by chemical ER stress". In: *Nature communications* 12.1, p. 5536.

Shang, Libin et al. (2011). "Nutrient starvation elicits an acute autophagic response mediated by Ulk1 dephosphorylation and its subsequent dissociation from AMPK". In: *Proceedings of the National Academy of Sciences* 108.12, pp. 4788–4793.

Shelly, Spencer et al. (2009). "Autophagy is an essential component of Drosophila immunity against vesicular stomatitis virus". In: *Immunity* 30.4, pp. 588–598.

Shimizu, M et al. (1990). "Cytopathic astrovirus isolated from porcine acute gastroenteritis in an established cell line derived from porcine embryonic kidney". In: *Journal of clinical microbiology* 28.2, pp. 201–206.

Sinclair, John et al. (2000). "Human cytomegalovirus mediates cell cycle progression through G1 into early S phase in terminally differentiated cells". In: *Journal of General Virology* 81.6, pp. 1553–1565.

Snijder, Eric J et al. (2020). "A unifying structural and functional model of the coronavirus replication organelle: Tracking down RNA synthesis". In: *PLoS biology* 18.6, e3000715.

Snodgrass, DR and Gray (1977). "Detection and transmission of 30 nm virus particles (astroviruses) in faeces of lambs with diarrhoea". In: *Archives of virology* 55, pp. 287–291.

Staring, Jacqueline et al. (2017). "PLA2G16 represents a switch between entry and clearance of Picornaviridae". In: *Nature* 541.7637, pp. 412–416.

Stark, George R and William R Taylor (2006). "Control of the G 2/M transition". In: *Molecular biotechnology* 32, pp. 227–248.

Stuempfig, ND and J Seroy (2018). "Gastroenteritis, viral". In: *StatPearls [Internet]. StatPearls Publishing*.

Su, Hong-Lin, Ching-Len Liao, and Yi-Ling Lin (2002). "Japanese encephalitis virus infection initiates endoplasmic reticulum stress and an unfolded protein response". In: *Journal of virology* 76.9, pp. 4162–4171.

Sui, Liyan et al. (2023). "Host cell cycle checkpoint as antiviral target for SARS-CoV-2 revealed by integrative transcriptome and proteome analyses". In: *Signal Transduction and Targeted Therapy* 8.1, p. 21.

Sung, Shu-Chiun et al. (2009). "The 8ab protein of SARS-CoV is a luminal ER membrane-associated protein and induces the activation of ATF6". In: *Virology* 387.2, pp. 402–413.

Takáts, Szabolcs et al. (2013). "Autophagosomal Syntaxin17-dependent lysosomal degradation maintains neuronal function in Drosophila". In: *Journal of Cell Biology* 201.4, pp. 531–539.

Takeshige, Kazuhiko et al. (1992). "Autophagy in yeast demonstrated with proteinase-deficient mutants and conditions for its induction." In: *The Journal of cell biology* 119.2, pp. 301–311.

Tallóczy, Zsolt et al. (2002). "Regulation of starvation-and virus-induced autophagy by the eIF2α kinase signaling pathway". In: *Proceedings of the National Academy of Sciences* 99.1, pp. 190–195.

Tange, Shoichiro et al. (2013). "Initiation of human astrovirus type 1 infection was blocked by inhibitors of phosphoinositide 3-kinase". In: *Virology journal* 10.1, pp. 1–13.

Tardif, Keith D, Gulam Waris, and Aleem Siddiqui (2005). "Hepatitis C virus, ER stress, and oxidative stress". In: *Trends in microbiology* 13.4, pp. 159–163.

Torii, Satoru et al. (2020). "Identification of a phosphorylation site on Ulk1 required for genotoxic stress-induced alternative autophagy". In: *Nature communications* 11.1, p. 1754.

Triana, Sergio et al. (2021). "Single-cell transcriptomics reveals immune response of intestinal cell types to viral infection". In: *Molecular systems biology* 17.7, e9833.

Tsuboyama, Kotaro et al. (2016). "The ATG conjugation systems are important for degradation of the inner autophagosomal membrane". In: *Science* 354.6315, pp. 1036–1041.

Tsukada, Miki and Yoshinori Ohsumi (1993). "Isolation and characterization of autophagy-defective mutants of Saccharomyces cerevisiae". In: *FEBS letters* 333.1-2, pp. 169–174.

Tumbarello, David A et al. (2015). "The autophagy receptor TAX1BP1 and the molecular motor myosin VI are required for clearance of salmonella typhimurium by autophagy". In: *PLoS pathogens* 11.10, e1005174.

Twu, Woan-Ing et al. (2021). "Contribution of autophagy machinery factors to HCV and SARS-CoV-2 replication organelle formation". In: *Cell reports* 37.8.

Umareddy, Indira et al. (2007). "Dengue virus serotype infection specifies the activation of the unfolded protein response". In: *Virology journal* 4.1, pp. 1–10.

Unicomb, Leanne E et al. (1998). "Astrovirus infection in association with acute, persistent and nosocomial diarrhea in Bangladesh". In: *The Pediatric infectious disease journal* 17.7, pp. 611–614.

Valera, María-Soledad et al. (2015). "The HDAC6/APOBEC3G complex regulates HIV-1 infectiveness by inducing Vif autophagic degradation". In: *Retrovirology* 12, pp. 1–26.

Vancamelbeke, Maaike and Séverine Vermeire (2017). "The intestinal barrier: a fundamental role in health and disease". In: *Expert review of gastroenterology & hepatology* 11.9, pp. 821–834.

Venkataraman, Sangita, Burra VLS Prasad, and Ramasamy Selvarajan (2018). "RNA dependent RNA polymerases: insights from structure, function and evolution". In: *Viruses* 10.2, p. 76.

Vives-Bauza, Cristofol et al. (2010). "PINK1-dependent recruitment of Parkin to mitochondria in mitophagy". In: *Proceedings of the National Academy of Sciences* 107.1, pp. 378–383.

Wang, Hanzhi et al. (2015). "GABARAPs regulate PI4P-dependent autophagosome: lysosome fusion". In: *Proceedings of the National Academy of Sciences* 112.22, pp. 7015–7020.

Wek, RC, H-Y Jiang, and TG Anthony (2006). "Coping with stress: eIF2 kinases and translational control". In: *Biochemical Society Transactions* 34.1, pp. 7–11.

White, Timothy M and Felicia D Goodrum (2023). *Viruses trick bystander cells into lowering their defences*.

Wild, Philipp et al. (2011). "Phosphorylation of the autophagy receptor optineurin restricts Salmonella growth". In: *Science* 333.6039, pp. 228–233.

Wolff, Georg et al. (2020). "A molecular pore spans the double membrane of the coronavirus replication organelle". In: *Science* 369.6509, pp. 1395–1398.

Wong, Jerry et al. (2008). "Autophagosome supports coxsackievirus B3 replication in host cells". In: *Journal of virology* 82.18, pp. 9143–9153.

Wong, Karen, Rachel Meyers, and Lewis C Cantley (1997). "Subcellular locations of phosphatidylinositol 4-kinase isoforms". In: *Journal of Biological Chemistry* 272.20, pp. 13236–13241.

Wood, DJ et al. (1988). "Chronic enteric virus infection in two T-cell immunodeficient children". In: *Journal of medical virology* 24.4, pp. 435–444.

Woode, GN et al. (1985). "Serotypes of bovine astrovirus". In: *Journal of clinical microbiology* 22.4, pp. 668–670.

Xing, Weijia et al. (2014). "Epidemiological characteristics of hand-foot-and-mouth disease in China, 2008-2012". In: *The Lancet infectious diseases* 14.4, p. 308.

Xiong, Jian and Michael X Zhu (2016). "Regulation of lysosomal ion homeostasis by channels and transporters". In: *Science China Life Sciences* 59, pp. 777–791.

Xu, Linhua et al. (2023). "Infection and innate immune mechanism of goose astrovirus". In: *Frontiers in Microbiology* 14, p. 1121763.

Yamaguchi, Hirofumi et al. (2020). "Wipi3 is essential for alternative autophagy and its loss causes neurodegeneration". In: *Nature Communications* 11.1, p. 5311.

Yang, Xiao-Jun et al. (2006). "HCV NS2 protein inhibits cell proliferation and induces cell cycle arrest in the S-phase in mammalian cells through down-regulation of cyclin A expression". In: *Virus research* 121.2, pp. 134–143.

Ye, Jin et al. (2000). "ER stress induces cleavage of membrane-bound ATF6 by the same proteases that process SREBPs". In: *Molecular cell* 6.6, pp. 1355–1364.

Yeo, Kok-Siong, Taznim Begam Mohd Mohidin, and Ching-Ching Ng (2012). "Epstein-Barr virus-encoded latent membrane protein-1 upregulates 14-3-3σ and Reprimo to confer G_2/M phase cell cycle arrest". In.

Yeo, Syn Kok et al. (2016). "Autophagy differentially regulates distinct breast cancer stem-like cells in murine models via EGFR/Stat3 and Tgfβ/Smad signaling". In: *Cancer research* 76.11, pp. 3397–3410.

Yokoyama, Christine C et al. (2012). "Adaptive immunity restricts replication of novel murine astroviruses". In: *Journal of virology* 86.22, pp. 12262–12270.

Yoshida, Hiderou et al. (2001). "XBP1 mRNA is induced by ATF6 and spliced by IRE1 in response to ER stress to produce a highly active transcription factor". In: *Cell* 107.7, pp. 881–891.

Yu, Chia-Yi et al. (2006). "Flavivirus infection activates the XBP1 pathway of the unfolded protein response to cope with endoplasmic reticulum stress". In: *Journal of virology* 80.23, pp. 11868–11880.

Yu, Xinlei, Yun Chau Long, and Han-Ming Shen (2015). "Differential regulatory functions of three classes of phosphatidylinositol and phosphoinositide 3-kinases in autophagy". In: *Autophagy* 11.10, pp. 1711–1728.

Yuan, Xiaoling, Yajun Shan, et al. (2005). "G0/G1 arrest and apoptosis induced by SARS-CoV 3b protein in transfected cells". In: *Virology journal* 2, pp. 1–5.

Yuan, Xiaoling, Jie Wu, et al. (2006). "SARS coronavirus 7a protein blocks cell cycle progression at G0/G1 phase via the cyclin D3/pRb pathway". In: *Virology* 346.1, pp. 74–85.

Zhang, Ji et al. (2009). "Mitochondrial clearance is regulated by Atg7-dependent and-independent mechanisms during reticulocyte maturation". In: *Blood, The Journal of the American Society of Hematology* 114.1, pp. 157–164.

Zhang, Yabin et al. (2021). "The SARS-CoV-2 protein ORF3a inhibits fusion of autophagosomes with lysosomes". In: *Cell discovery* 7.1, p. 31.

Zheng, Yiyu T et al. (2009). "The adaptor protein p62/SQSTM1 targets invading bacteria to the autophagy pathway". In: *The Journal of Immunology* 183.9, pp. 5909–5916.

Zhong, Yu et al. (2014). "Nrbf2 protein suppresses autophagy by modulating Atg14L protein-containing Beclin 1-Vps34 complex architecture and reducing intracellular phosphatidylinositol-3 phosphate levels". In: *Journal of Biological Chemistry* 289.38, pp. 26021–26037.

Zhong, Yun et al. (2009). "Distinct regulation of autophagic activity by Atg14L and Rubicon associated with Beclin 1–phosphatidylinositol-3-kinase complex". In: *Nature cell biology* 11.4, pp. 468–476.

Zhou, Yuting, Edmund B Rucker III, and Binhua P Zhou (2016). "Autophagy regulation in the development and treatment of breast cancer". In: *Acta biochimica et biophysica Sinica* 48.1, pp. 60–74.

Zientara-Rytter, Katarzyna and Suresh Subramani (2016). "Autophagic degradation of peroxisomes in mammals". In: *Biochemical Society Transactions* 44.2, pp. 431–440.

Vita

Theresa Taggart Bub was born in Westchester, New York in 1996. She attended Shaker High School in Albany, New York and graduated in the top 5% of her class in 2014 with an Advanced Regents Diploma. She then obtained a Bachelor of Science in Biochemistry with honors, as well as a minor in Data Science in 2018 from Houghton College. For the next year, she worked for Regeneron Pharmaceuticals in Albany, NY as a Quality Control Analytical Specialist, developing analytical biochemistry and chemistry methods. She then joined the Integrated Program in Biomedical Sciences (IPBS) within the Microbiology, Immunology, and Biochemistry (MIB) track at the University of Tennessee Health Science Center for doctoral studies in August of 2019 in Memphis, TN. After completing her initial training and qualifying exam in the Kundu Lab from March 2020 to July 2021, she joined the Schultz-Cherry lab in the Department of Infectious Diseases at St. Jude Children's Research Hospital in August of 2021. During her time in the IPBS program, she achieved a 4.0 GPA, was awarded with Outstanding Graduate Student in the MIB track in 2022, and received multiple other awards for her work as a graduate student and to fund travel to academic conferences to share her work. She successfully defended her dissertation and expects to receive her doctorate in October 2023.